YOUNG MULTIS 2023

Multiscale Phenomena in Condensed Matter online conference for young researchers

Kraków, 3 – 5 July 2023

Institute of Nuclear Physics
Polish Academy of Sciences

ORGANIZERS

Chairperson

Magdalena Fitta

Co-chairperson

Małgorzata Jasiurkowska-Delaporte

Scientific Committee

Naveen Kumar Chogondahalli Muniraju

Mirosław Gałązka

Paweł Horodek

Ewa Juszyńska-Gałązka

Piotr Konieczny

Michał Krupiński

Natalia Osiecka-Drewniak

Robert Pełka

Andrzej Ptok

Oleksandr Tomchuk

Local Committee

Paweł Sobieszczyk

Juliusz Chojenka

Dominik Czernia

Aleksandra Deptuch

Anna Drzewicz

Jędrzej Kobylarczyk

Aleksandra Pacanowska

Marcin Piwowarczyk

Oliwia Polit

Wojciech Sas

Monika Synowska-Kałuża

Contents

PROGRAM OF THE CONFERENCE

Monday, 03 July 2023

09:45	**Opening of the Conference** — The Henryk Niewodniczański Institute of Nuclear Phisics Polish Academy of Sciences	
10:00	**Opening lecture** — **Mark Johnson** (France) Addressing the global health challenge: neutrons to study multiscale phenomena	p.8

Session I: Soft matter and glass-formers

11:00	**Joana Silva** (Portugal) Relaxation pathways from amorphous to crystals: thermal and kinetic stability of ranolazine/tryptophan high-energy solid forms	p. 10
11:15	**Amanda De Almeida** (Brazil) Synthesis and characterization of nimesulide dual-drug co-amorphous systems	p. 11
11:30	**Anna Drzewicz** (Poland) Thin films of liquid crystals obtained via organic molecular beam deposition methods	p. 12
11:45	**Alfred Błażytko** (Poland) Reorientation dynamics of structural isomers of sizeable glass-forming liquids revealed in dielectric studies at ambient and elevated pressure	p. 13
12:00	**Taoufik Lamrani** (Poland) The influence of the various amorphisation processes on the molecular-scale structure of ritonavir active pharmaceutical ingredient	p. 14
12:15	LUNCH BREAK	

Session II: Molecular magnets and nanomagnets

13:30	**David Gracia** (Spain) A $Gd_{12}Na_6$ Molecular Quadruple-Wheel with a Record Magnetocaloric Effect at Low Magnetic Fields and Temperatures	p. 16
13:45	**Xiaochun Li** (Belgium) Synthesis, Crystal Structure, and Spin Crossover Behavior in an Iron(II) Complex Based on Tris(4,4'-bis-1,2,4-triazole) Ligand	p. 17
14:00	**Petro Danylchenko** (Slovakia) A spin 1/2 Quasi-Two-Dimensional antiferromagnet $Cu(en)(H_2O)_2SO_4$ encapsulated into mesoporous silica SBA-15	p. 18
14:15	**Anna Nykiel** (Poland) Influence of the electrodeposition parameters on the properties of FeCoNiCu nanowires	p. 19
14:30	**Dominik Czernia** (Poland) Plasma irradiation: a promising technique for modifying magnetic properties in molecular magnets	p. 20
14:45	**Pavlo Baloh** (Slovakia) Experimental study of low-temperature magnetic properties of Dy-doped phosphate glass	p. 21
15:15	BREAK	

Session III: Computational physics

16:00	**Iuliia Voroshylova** (Portugal) Computational study of the influence of temperature on $EMImBF_4$ – graphene interface: explanation in the framework of bilayer model	p. 23
16:15	**Surajit Basak** (Poland) A first principle study of the materials hosting chiral phonons	p. 24
16:30	**Jacek Gatlik** (Poland) Thermal Effects on the Dynamic of Kink in Heterogeneous Energy Landscapes	p. 25

Tuesday, 04 July 2023

09:00	**Poster session**	10:15

Session IV: Multifunctional materials

10:30	**Luming Zhang** (Japan) Thermal Conductivity Measurement System for Wide-Temperature Range for Single Crystals of Molecular Compounds	p. 27
10:45	**Qingping Wang** (xxxx) Pyroelectric materials for thermal sensing and harvesting	p. 28
11:00	**Sara El Houbbadi** (Poland) Experimental and Theoretical XAFS studies of the atomic structure of Copper functionalized SBA-15 mesoporous matrix	p. 29
11:15	**Veronika Mukharovska** (Ukraine) Optical properties of opal-based photonic crystal films and heterostructures	p. 30
11:30	**Mateusz Gala** (Poland) Evolution of the Verwey transition in magnetite observed through electronic transport studies under uniaxial stress	p. 31
11:45	**Bahjou Yousra** (Morocco) A new environmentally safe hybrid material aimed at removing heavy metals from contaminated water, magnetic studies of the iron(II) complex	p. 32
12:00	**Juliusz Chojenka** (Poland) Manipulating Electrical Properties of Nanopatterned Double-Barrier Schottky Junctions in Ti/TiO$_x$/Fe Systems	p. 33
12:15	Lunch break	

Session V: Soft matter and glass-formers

13:30	**Marcin Piwowarczyk** (Poland) Thermochromism of mesogenic mixtures containing liquid-crystalline azo and chiral compounds	p. 35
13:45	**Aleksandra Deptuch** (Poland) Crystallization kinetics vs. fluorosubstitution of the molecular core - the study of four chiral compounds forming the smectic phases	p. 36
14:00	**Valeria Morales Alvarez** (Poland) Effect of alkyl chain length on phase transitions and ion dynamics of phosphonium ionic liquids at ambient and elevated pressure	p. 37
14:15	**Beibei Yao** (Poland) Liquid-liquid phase transition promotes the decoupling of ion diffusion from structural dynamics in aprotic ionic liquids	p. 38
15:00	Break	

Session VI: Multiferroic

15:00	**Franco Di Rino** (France) Surface tension assisted polar phases in one-dimensional ferroelectrics	p. 40
15:15	**Anna Szeremeta** (Poland) The electrical properties of bismuth manganite -– lead titanate – epoxy composite	p. 41
15:30	**Tina Tasheva** (Bulgaria) Structural characterization and magnetic properties of glass-ceramics with high iron oxide concentration	p. 42
15:45	**Leo Boron** (France) Topological polar phases in ferroelectric nanowires	p. 43

WENDESDAY, 05 JULY 2023

	Session VII: Spectroscopic and diffraction methods	
09:00	**Rikumaru Saito** (Japan) ^{13}C NMR study on π-d interaction system, λ-$(BEST)_2\mathrm{FeCl}_4$	p. 45
09:15	**N. S. Dhami** (Croatia) High-Pressure studies on non-centrosymmetric EuTGe$_3$ (T= Co, Rh and Ir) Materials	p. 46
09:30	**Oleksandr Tomchuk** (Poland) Neutron scattering study of LC ordering in cylindrical mesopores	p. 47
09:45	**Tsunehisa Kihara** (Japan) Low Temperature Crystal Structure of $\beta" - (BEDT-TTF)_2Hg(SCN)_2Cl$	p. 48
10:00	**Aleksandr Bamburov** (Portugal) Intolerance of Ruddlesden-Popper $La_2NiO_{4\pm\delta}$ structure to A-site cation deficiency	p. 49
10:15	**Andrius Pakalniškis** (Lithuania) Temperature Induced Magnetic and Crystal Structure Transition in Novel Sc doped Lutetium ferrite	p. 50
10:30	**Kinga Łucak** (Poland) The supramolecular structures in propanol and its halogen derivatives	p. 51
10:45	BREAK	
	Session VIII: Miscellany	
11:15	**Mohammad Sadegh Shakeri** (Poland) Synthesis of CuFe$_2$O$_4$-Cu$_2$O composite using pulsed laser irradiation of cupric-magnetite-ethanol suspension for photocatalysis application, experimental and DFT calculation approaches	p. 53
11:30	**Samuel Diaz Escribano** (Israel) Semiconductor-Superconductor-Ferromagnetic Heterostructure as a Platform for Topological Superconductivity	p. 54
11:45	**Dimitrios Tzitzilis** (Greece) Wenzel-to-Cassie transition on lubricant-impregnated surfaces	p. 55
12:00	**Yousra El Fannassi** (France) Microencapsulation of a water-soluble ruthenium (II) complex derived from limonene as an effective tool against pathogenic bacterial biofilms	p. 56
12:15	**Rui Pinto** (Portugal) Characterization and Performance Evaluation of PrVO$_y$-CaVO$_y$ Oxides for Solid Oxide Fuel Cells	p. 57
12:30	**Michał Adamek** (Poland) Synthesis and structural characterization of spherical silica nanoparticles with different diameters	p. 58
12:45	VOTING	**13:00**
13:15	CLOSING REMARKS	

OPENING LECTURE

Opening lecture, Mon./10:00

Addressing the global health challenge: neutrons to study multiscale phenomena

M. Johnson[1]

[1] *Institut Laue Langevin, Grenoble, France*

email: `johnson@ill.eu`

A healthy population is a major global challenge. Increased life expectancy has caused a surge in age-related conditions, chronic disease and disability. Developing countries still suffer the burden of HIV/AIDS, malaria and tuberculosis. As the COVID-19 pandemic has clearly demonstrated, it is extremely difficult to contain highly contagious diseases in our global mobile society. In this context, it is essential to understand soft and biological materials and processes at the atomic and molecular level.

Neutron techniques cover many orders of magnitude in time and length scales, which can be extended even further by combining real and reciprocal, time and space techniques – neutrons are therefore perfectly suited to studying multiscale phenomena in soft and biological systems. This talk will use a range of examples, from fundamental studies to applications for COVID-19 and cancer, to illustrate the unique insight provided by neutron techniques. New instrumentation and scientific services at ILL will be presented as the basis for the next generation of experiments in soft matter and biology.

SESSION I: SOFT MATTER AND GLASS-FORMERS

11:00	**Joana Silva** (Portugal) Relaxation pathways from amorphous to crystals: thermal and kinetic stability of ranolazine/tryptophan high-energy solid forms	p. 10
11:15	**Amanda De Almeida** (Brazil) Synthesis and characterization of nimesulide dual-drug co-amorphous systems	p. 11
11:30	**Anna Drzewicz** (Poland) Thin films of liquid crystals obtained via organic molecular beam deposition methods	p. 12
11:45	**Alfred Błażytko** (Poland) Reorientation dynamics of structural isomers of sizeable glass-forming liquids revealed in dielectric studies at ambient and elevated pressure	p. 13
12:00	**Taoufik Lamrani** (Poland) The influence of the various amorphisation processes on the molecular-scale structure of ritonavir active pharmaceutical ingredient	p. 14

Contributed talk, Mon./11:00

Relaxation pathways from amorphous to crystals: thermal and kinetic stability of ranolazine/tryptophan high-energy solid forms

J. F. C. Silva[1], P. S. Pereira[2], M. R. Silva[2], E. Fantechi[3], L. Chelazzi[3], S. Ciattini[3], M. E. S. Eusébio[1], and M. T. S. Rosado[1]

[1] *CQC-ICM, Centro de Química de Coimbra-Instituto de Ciências Moleculares, Departamento de Química, Universidade de Coimbra, 3004-535 Coimbra, Portugal*
[2] *CFisUC, Departamento de Física, Universidade de Coimbra, 3000-370, Coimbra, Portugal*
[3] *CRIST, Centro di Cristallografia Strutturale, Università degli Studi di Firenze, 50019, Sesto Fiorentino, Firenze, Italy*

email: `joana.silva@qui.uc.pt`

Most active pharmaceutical ingredients are administered orally in crystalline solid forms with low aqueous solubility, and amorphization has been recognized as one of the most promising approaches to improve bioavailability. However, amorphous solids, being metastable forms, are prone to relax into crystals. To overcome this, co-amorphization with small-molecule co-formers has been recently proposed as an alternative to enhance the kinetical stability of the high-energy disordered phases [1, 2].

In this work, ranolazine-tryptophan co-amorphous solid phases were prepared by cryo-milling and their stability evaluated by thermal analysis, X-ray diffraction and FTIR-ATR spectroscopy. The intimate molecular association extended the amorphous stability of ranolazine at room temperature from less than a couple of hours to at least 2 months. The molar ratio corresponding to the higher glass transition determined by DSC was selected for ranolazine aqueous solubility determination, showing significant improvement.

The thermal behavior and phase stability of the co-amorphous systems was compared with the corresponding amorphous pure components. The latter exhibited crystallization into metastable polymorphs when subjected to thermal stress. For tryptophan in particular, the influence of DSC experimental conditions in the relaxation paths and outcome was recognized. Heating runs starting from amorphous tryptophan revealed phase transitions between its different polymorphs and the serendipitous production of the neutral form of this amino acid in the pure solid phase.

Acknowledgements: CQC-IMS and CFisUC are funded by Fundação para a Ciência e Tecnologia (FCT) projects UIDB/00313/2020 and UID/FIS/04564/2020, respectively. Access to TAIL-UC facility, funded under QREN-Mais Centro Project ICT/2009/02/012/1890, is gratefully acknowledged. Joana F. C. Silva acknowledges FCT for the SFRH/BD/146809/2019 Ph.D. scholarship.

[1] J. Liu *et al.*, Pharmaceutics, 13 (2021) 389
[2] J. Han, *et al.*, Expert Opin. Drug Delivery, 17 (2020) 1411

CONTRIBUTED TALK, MON./11:15

Synthesis and characterization of nimesulide dual-drug co-amorphous systems

A. C. de Almeida[1,2], P. O. Ferreira[1], R. A. E. Castro[2,3], J. Canotilho[2,3], M. E. S. Eusébio[2], and F. J. Caires[1]

[1]*School of Sciences, São Paulo State University (UNESP), Bauru, Brazil*
[2]*CQC/IMS, Chemistry Department, University of Coimbra, Coimbra, Portugal*
[3]*Faculty of Pharmacy, University of Coimbra, Coimbra, Portugal*

email: `amanda.cosmo@unesp.br`

The conversion of a crystalline active pharmaceutical ingredient (API) to its amorphous phase could achieve an increased solubility and dissolution rate. Besides amorphous drugs present higher energy and entropy due to the lack of long-range order, the solid tend to be more unstable and crystallizes over time [1]. Polymer-based solid dispersions are widely employed to stabilize the amorphous material, however, many polymeric excipients increase the higroscopicity and leads to a higher dosage formulation [2].

Alternatively to polymers, co-amorphous systems mix smaller coformers to the API preventing the drug molecules aggregation. In a simple description, co-amorphous systems are homogeneous multicomponent solids with no long-range order, that can be classified into four categories, depending on the nature of the coformer [3]. In the case of drug-drug co-amorphization, at least two APIs form the amorphous material leading to a combination of pharmaceutical properties, in addition to the modification of physicochemical properties, like solubility and dissolution rate [4].

Considering the low aqueous solubility of nimesulide (NMS), a widely used and prescribed anti-inflammatory non-steroidal drug [4]. the present work aimed the synthesis and characterization of drug-drug co-amorphous systems of NMS.

The NMS dual-drug co-amorphous were prepared through quench cooling and/or cryomilling, and the parameters for choosing the other API were the compatible functional groups and/or the desired combination of therapeutic action with nimesulide. Samples were characterized by Differential Scanning Calorimetry (DSC), X-ray powder diffraction (XRPD) and infrared spectroscopy (FTIR).

Drug-drug co-amorphous systems were identified, produced both by quench cooling and by cryomilling. Quench cooling, that is more prone to promoting total crystallinity breakdown, produced co-amorphous materials with higher physical stability than those obtained by cryomilling, as observed for the nimesulide-bicalutamide system (Fig. 1) [1].

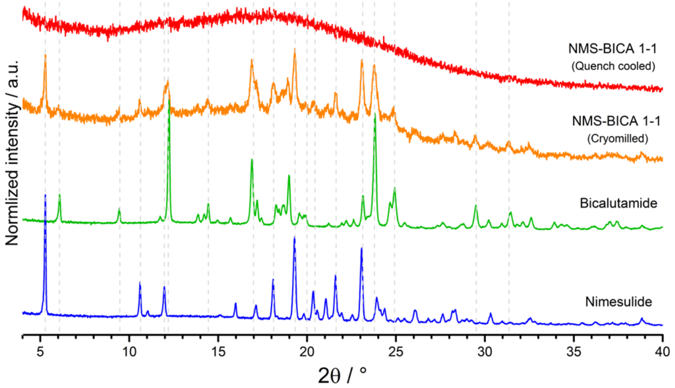

Figure 1: XRPD diffractograms of Nimesulide-bicalutamide system prepared through quench cooling and cryomilling.

Acknowledgements: A.C.A. thanks Brazilian CAPES-PrInt Program (mobility number 88887.684961/2022-00) for financial support. CQC-IMS is funded by national funds through FCT, project UIDB/00313/2020. Thanks are due to UCQFarma for the use of XRPD and dissolution experiments facility.

[1] Q. Shi, Acta Pharm. Sin. B., 9 (2019) 19
[2] J. F. C. Silva *et al.*, J. Mol. Struct., 1242 (2021) 130709
[3] J. Zhang *et al.*, Int. J. Pharm., 610 (2021) 121235
[4] M. Wang *et al.*, Eur. J. Pharm. Sci., 147 (2020) 1

CONTRIBUTED TALK, MON./11:30

Thin films of liquid crystals obtained via organic molecular beam deposition methods

A. Drzewicz[1], M. Wübbenhorst[2], and P. Kula[3]

[1]*Department of Soft Matter Research, Institute of Nuclear Physics Polish Academy of Sciences, Kraków, Poland*
[2]*Laboratory for Soft Matter and Biophysics, Catholic University of Leuven, Belgium*
[3]*Institute of Chemistry, Military University of Technology, Warszawa, Poland*

email: `anna.drzewicz@ifj.edu.pl`

Liquid crystals have a variety of applications in a range of areas, including medicine, pharmacy and sensing, but still their widespread use is in displays and electrically driven optical switches. Even though the climax of liquid crystals applications for large area displays is gone, they are still an irreplaceable material in the technology of small pocket device. The miniaturization of devices causes an increase in scientists' interest in the possibility of creating thin layers of liquid crystals and their properties. One of the methods of formation thin films is organic molecular beam deposition (OMBD), which allows the production of organic thin layers in ultra-high vacuum by evaporating the material whose the molecules impinge on a cold substrate [1]. However, the OMBD method has so far not been used for liquid crystals, but for other organic compounds, such as glycerol [2].

In this paper, we have verified the possibility to create thin films of liquid crystal below the glass transition temperature by the OMBD method. We have also investigated the effect of OMBD measurement parameters on the layer thickness and the α-relaxation dynamics of compound under study. Thin films represent an alternative geometry to investigate molecular dynamics. Some striking differences in relaxation dynamics related with glassy state of thin films compared to the sample in the bulk form [3, 4] have been observed.

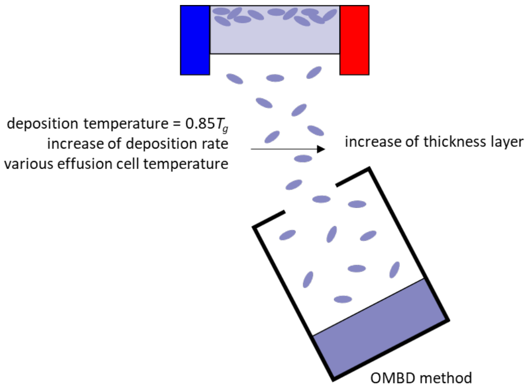

Figure 1: Scheme of the organic molecular beam deposition method.

Acknowledgements: A. Drzewicz acknowledged the National Science Centre (Grant MINIATURA 5: UMO-2021-05/X/ST3/00888) for financial support.

[1] M. Wübbenhorst *et al.*, Eur. Phys. J. Spec. Top., 189 (2010) 181
[2] S. Capponi *et al.*, Nat. Commun., 3 (2012) 1233
[3] A. Drzewicz *et al.*, Phys. Chem. Chem. Phys., 24 (2022) 4595
[4] A. Drzewicz *et al.*, CrystEngComm, 24 (2022) 3074

CONTRIBUTED TALK, MON./11:45

Reorientation dynamics of structural isomers of sizeable glass-forming liquids revealed in dielectric studies at ambient and elevated pressure

A. Błażytko[1], M. Rams-Baron[1], and M. Paluch[1]

[1]*Institute of Physics, University of Silesia, Chorzów, Poland*

email: `alfred.blazytko@us.edu.pl`

The study of molecular mobility is important in many areas of science and engineering, including materials science,physics, and chemical engineering. It can provide insight into the physical and chemical properties of materials and can help to design and optimize materials for specific applications. Broadband dielectric spectroscopy (BDS) is one of the most widely used techniques for observing molecular dynamics. It allows observation of the movements of molecules over a wide range of frequencies and under varying temperatures and pressures.

We used dielectric spectroscopy to study the reorientation dynamics of three newly-synthesized structural isomers of sizeable molecules [1, 2] at ambient and elevated pressure. Thermal properties were assessed using a differential scanning calorimeter (DSC). Investigated materials had the same atomic composition and molar mass. Their non-polar rigid and sizeable molecular core was identical. The differences concerned the position of polar group in the ortho, meta, or para position. We obtained a number of compounds whose systematic dielectric investigations allowed us to uncover structure-dynamics relationships, in particular, we addressed the question about the impact of molecular features (such as large size, anisotropy, and dipole moment properties) on dielectric behavior at ambient and elevated pressure.

During the presentation, it will be discussed to what extent the differences in structure and related molecular properties affect the thermal properties and the molecular reorientation dynamics investigated using dielectric method. Based on calorimetric and dielectric studies, we will show that investigated isomers differ in their glass transition temperature, melting point and tendency to crystallize in the supercooled liquid phase. We observed very high values of the pressure coefficient of glass transition temperature dT_g/dP and activation volume $\Delta V^{\#}$. We found a strong correlation between the activation volume and the length of the molecule along the long axis. In contrast, the activation volume correlates weakly with the value of the dipole moment. Our results may contribute to a better understanding of the link between the structure of molecules and their dynamics, which is desirable in the context of designing new materials for selected applications.

Acknowledgements: This research was funded by National Science Centre, Poland (Grant No. 2021/41/B/ST5/00992).

[1] M. Rams-Baron *et al.*, J. Phys. Chem. Lett., 12 (2021) 11303
[2] A. Jedrzejowska *et al.*, Phys. Rev. E, 101 (2020) 010603

CONTRIBUTED TALK, MON./12:00

The influence of the various amorphisation processes on the molecular-scale structure of ritonavir active pharmaceutical ingredient

T. Lamrani[1], P. Jesionek[2,3], D. Heczko[4], K. Kamiński[1], E. Kamińska[3], and K. Jurkiewicz[1]

[1]*Institute of Physics, University of Silesia in Katowice, 75 Pułku Piechoty 1, 41-506 Chorzów, Poland*
[2]*Institute of Chemistry, University of Silesia in Katowice, ul. Szkolna 9, 40-007 Katowice, Poland*
[3]*Department of Pharmacognosy and Phytochemistry, Faculty of Pharmaceutical Sciences in Sosnowiec, Medical University of Silesia in Katowice, Jagiellońska 4, 41-200 Sosnowiec, Poland*
[4]*Department of Statistics, Department of Instrumental Analysis, Faculty of Pharmaceutical Sciences in Sosnowiec, Medical University of Silesia in Katowice, ul. Ostrogórska 30, 41-200 Sosnowiec, Poland*

email: `taoufik.lamrani@us.edu.pl`

The low aqueous solubility of crystalline active pharmaceutical ingredients (APIs) poses a significant challenge in drug development. To enhance the dissolution of poorly water-soluble drugs, various approaches are available. Among them, the amorphisation process is an effective method to achieve better drug dissolution than in the case of their crystalline counterparts [1].

Amorphisation can be induced by various methods, such as quench cooling, spray drying, or mechanical treatment (milling, shearing, compression, etc.). The techniques mentioned above can alter the molecular-scale structure of pharmaceuticals and lead to subtle differences in the amorphous-like organization of molecules. Quench-cooling or pressurisation under proper thermodynamic conditions can tune the degree of intermolecular order as well as the intramolecular conformation.

This contribution will present the results of the structural characterisation of ritonavir glasses produced by conventional vitrification and pressure densification. We used X-ray diffraction, pair distribution function, and molecular dynamics simulations. The results of the simulations allowed us to understand the effect of pressurization on the formation of the amorphous state and hydrogen bond network in this API. It is worth to mention that ritonavir has recently revolutionised the HIV treatment.

This work is a continuation of our recent investigations on ritonavir, which revealed the variation in the local ordering, H-bonding pattern and molecular dynamics in the pressure-densified glass [2]. Dielectric studies indicated the narrowing of α-dispersion with compression, reported so far only for a few van der Waals compounds. To understand such peculiar behaviour more thorough analysis of the molecular-scale structure is needed.

Acknowledgements: Authors acknowledge financial support from the National Science Centre (Poland), grant number: Opus 21 No. 2021/41/B/NZ7/01654.

[1] B. C. Hancock and M. Parks, Pharm. Res., 17 (2000) 397
[2] D. Heczko *et al.*, J. Mol. Liq., 351 (2022) 118666

SESSION II: MOLECULAR MAGNETS AND NANOMAGNETS

13:30	**David Gracia** (Spain) A $Gd_{12}Na_6$ Molecular Quadruple-Wheel with a Record Magnetocaloric Effect at Low Magnetic Fields and Temperatures	p. 16
13:45	**Xiaochun Li** (Belgium) Synthesis, Crystal Structure, and Spin Crossover Behavior in an Iron(II) Complex Based on Tris(4,4'-bis-1,2,4-triazole) Ligand	p. 17
14:00	**Petro Danylchenko** (Slovakia) A spin 1/2 Quasi-Two-Dimensional antiferromagnet $Cu(en)(H_2O)_2SO_4$ encapsulated into mesoporous silica SBA-15	p. 18
14:15	**Anna Nykiel** (Poland) Influence of the electrodeposition parameters on the properties of FeCoNiCu nanowires	p. 19
14:30	**Dominik Czernia** (Poland) Plasma irradiation: a promising technique for modifying magnetic properties in molecular magnets	p. 20
14:45	**Pavlo Baloh** (Slovakia) Experimental study of low-temperature magnetic properties of Dy-doped phosphate glass	p. 21

Contributed talk, Mon./13:30

A $Gd_{12}Na_6$ Molecular Quadruple-Wheel with a Record Magnetocaloric Effect at Low Magnetic Fields and Temperatures

D. Gracia[1], T. G. Tziotzi[2], S. J. Dalgarno[3], J. Schnack[4], M. Evangelisti[1], E. K. Brenchin[5], and C. J. Milios[2]

[1] *Instituto de Nanociencia y Materiales de Aragón, CSIC & Universidad de Zaragoza, Spain*
[2] *Department of Chemistry, University of Crete, Herakleion, Greece*
[3] *Institute of Chemical Sciences, Heriot-Watt University, Edinburgh, United Kingdom*
[4] *Fakultät für Physik, Universität Bielefeld, Germany*
[5] *EaStCHEM School of Chemistry, The University of Edinburgh, United Kingdom*

email: `davidg@unizar.es`

Adiabatic demagnetization was the first method used to reach temperatures well below 1 K [1]. The principle of operation is based on the magnetocaloric effect (MCE), i.e., the reversible thermal change that occurs in a susceptible material following a variation of the applied magnetic field. During the last decades, ^{3}He-^{4}He dilution refrigeration has routinely replaced magnetic refrigeration because of the advantage of continuous vs. single-shot cooling, respectively. However, modern multi-stage adiabatic demagnetization refrigerators (ADRs) can bypass this limitation. For example, the LiteBIRD space observatory will include two ADR for the cooling module between 0.3 K and 1.8 K, one transiting between these two temperatures and one providing continuous cooling at 0.3 K [2]. Magnetocaloric materials that can be operated at this base temperature are therefore sought after.

Here, we present our recent results on a novel Gd_{12} molecular nanomagnet [3]. Each molecular unit can be described as a quadruple wheel that comprises two Gd_6 and two Na_3 rings held together by a combination of acetate, formate and carbonate ligands (Figure 1). Magnetization and heat capacity measurements reveal the presence of very weak antiferromagnetic interactions and a negligible anisotropy. No phase transition is detected, at least down to the minimum accessed temperature of ca. 0.3 K.

Regarding its MCE, large values of the magnetic entropy change ($-\Delta S_m = 46.0$ J kg^{-1} K^{-1}) and the adiabatic temperature change ($\Delta T_{ad} = 11.3$ K) are found for $T < 2$ K and the maximum field variation $\Delta B = 7$ T (Figure 1). The low field region is even more extraordinary since, for instance, an unprecedently large $-\Delta S_m = 29.3$ J kg^{-1} K^{-1} is attained for $\Delta B = 1$ T and $T = 0.5$ K. With LiteBIRD target in mind, the material needs $B = 1.5$ T to cool from 1.8 K to 0.3 K by full demagnetization. Since such weak fields can be produced using permanent magnets, application implementations can be designed without technological complexity and heavy components.

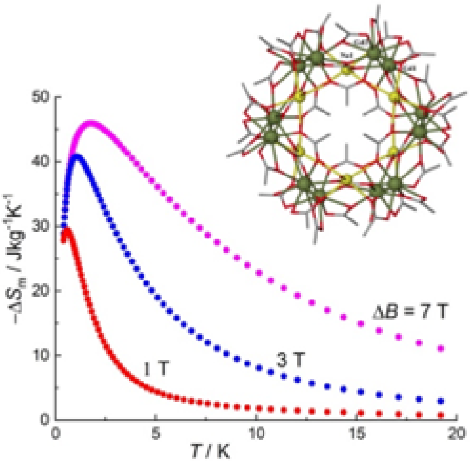

Figure 1: Molecular structure and magnetic entropy change

Acknowledgements: This work was supported by The Leverhulme Trust (RPG- 2021-176), MICINN (PID2021-124734OB-C21), HFRI (project no. 400). D.G. acknowledges financial support from the Gobierno de Aragón through a doctoral fellowship.

[1] W. F. Giauque and D. P. McDougall, Phys. Rev., 43 (1933) 768
[2] J. M. Duval *et al.*, J. Low Temp. Phys., 199 (2020) 730
[3] G. T. Thomais *et al.*, J. Am. Chem. Soc., 145 (2023) 7743

CONTRIBUTED TALK, MON./13:45

Synthesis, Crystal Structure, and Spin Crossover Behavior in an Iron(II) Complex Based on Tris(4,4'-bis-1,2,4-triazole) Ligand

X. Li[1] and Y. Garcia[1]

[1] *Université catholique de Louvain, Louvain-la-Neuve, Belgium*

email: `Xiaochun.li@uclouvain.be`

Some transition metal complexes, particularly those of the first transition series with configurations $3d^4$ to $3d^7$, can undergo spin conversion when induced by an external stimulus such as light, temperature, pressure, electric field, or guest molecules, which is called spin crossover (SCO) complexes [1, 2]. SCO compounds have been studied extensively over the last few decades for potential applications in high-density information storage devices, quantum computers and spintronics [3].

In this work, a new three-dimensional iron(II) complex based on tris(4,4'-bis-1,2,4-triazole), hereafter abbreviated as btr, has been synthesized with the formula $[\mathrm{Fe(btr)_3}](\mathrm{anion})_2$. Single-crystal X-ray diffraction showed that the complex crystallized in the $R3$ space group and the structure is three-dimensional. Two crystallographically independent iron sites were revealed, denoted as Fe1 and Fe2, respectively. The magnetic properties were studied using SQUID (Superconducting Quantum Interference Device). This compound exhibits SCO behaviour. The low-spin to high-spin transition occurs in two steps with a ca. 67 K plateau, each involving around 50% of the Fe^{2+} ions. The low-temperature step is abrupt and undergoes a thermal hysteresis with a width of 12 K from 116 K to 128 K. The high-temperature step, centred on $T_2 = 187$ K without thermal hysteresis. Fig. 1 shows Temperature dependence of $\chi_M T$ for $[\mathrm{Fe(btr)_3}](\mathrm{anion})_2$. Differential scanning calorimetry (DSC) measurements have confirmed the occurrence of the two-step spin transition. In addition, ^{57}Fe Mössbauer spectra were obtained at different temperatures, which allows us to follow the temperature dependence of the HS and LS molar fractions in an accurate way.

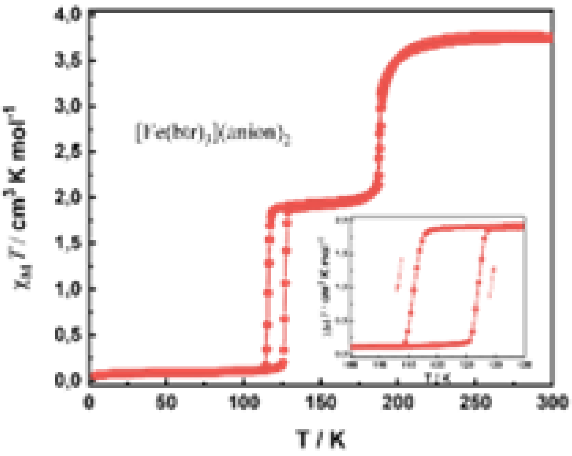

Figure 1: Temperature dependence of $\chi_M T$ for $[\mathrm{Fe(btr)_3}](\mathrm{anion})_2$.

[1] R. Hogue *et al.*, Chem. Soc. Rev., 47 (2018) 7303
[2] P. Gütlich *et al.*, Beilstein J. Org. Chem., 9 (2013) 342
[3] Y. Garcia *et al.*, Inorg. Chem., 38 (1999) 4663

CONTRIBUTED TALK, MON./14:00

A spin 1/2 Quasi-Two-Dimensional antiferromagnet $Cu(en)(H_2O)_2SO_4$ encapsulated into mesoporous silica SBA-15

P. Danylchenko[1], R. Tarasenko[1], E. Čižmár[1], V. Tkáč[1], V. Zeleňák[2], A. Orendáčová[1], and M. Orendáč[1]

[1] *Institute of Physics, Faculty of Science, P.J. Šafárik University in Košice, Park Angelinum 9, 041 54 Košice, Slovakia*
[2] *Institute of Chemistry, Faculty of Science, P.J. Šafárik University in Košice, Moyzesova 11, 041 54 Košice, Slovak Republic*

email: `petro.danylchenko@student.upjs.sk`

Despite of vast research on Cu^{+2} molecular magnets their size effect is relatively less concerned. For this reason, the main goal of this work is to successfully constrain $Cu(en)(H_2O)_2SO_4$ complex into the 6 nm pores of mesoporous silica SBA-15 with hexagonal pore arrangement to obtain new stable hybrid material. We conducted synthesis with the times 90 minutes, 24 hours, 72 hours and 14 day of the silica being left in saturated solution of $Cu(en)(H_2O)_2SO_4$. For example, the hybrid sample with time synthesis 24 hours was denoted as $Cu(en)(H_2O)_2SO_4$ @SBA15(24h).

The output of the energy dispersive X-ray analysis on a scanning electron microscope showed that for all four hybrid materials $Cu(en)(H_2O)_2SO_4$ @SBA15 the complex was evenly distributed inside the SBA-15 and during the synthesis from the nitrogen adsorption isotherms measurement were found out that the pore filling rate present up to 60 % of the total volume with the time synthesis more than 24 hours. The study of thermal analysis exhibit that water is released from the crystal structure at temperatures above 100°C and at a temperature above 200°C, ethylenediamine is exempted from the structure. It is important to note that the same result of thermal analysis was observed on the bulk $Cu(en)(H_2O)_2SO_4$ complex itself, which proving it successful impregnation into the pores SBA-15 without changing any chemical bounding between atoms in complex.

The magnetic properties were carried out by electron paramagnetic resonance (EPR) and susceptibility measurements on hybrid sample $Cu(en)(H_2O)_2SO_4$ @SBA15(72h) with further comparision with the bulk $Cu(en)(H_2O)_2SO_4$ complex [1]. At EPR spectra of the hybrid sample appears new peaks compared to the bulk $Cu(en)(H_2O)_2SO_4$, which could be originated from the distortion of the crystallofraphic structure and development of the hyperfine interaction of Cu(II) nuclei. The EPR spectras was analyzed with all mentioned above points above within Easyspin software package. The best agreement with the experimental data measured at a temperature of 2.1 K was obtained for the fit with parameters $g_z = 2.34$, $g_y = 2.10$, $g_x = 2.02$, $A_x = 121$ MHz, $A_z = 325$ MHz, $A_y = 90$ MHz and $\Delta B = 7.1$ mT. For the hybrid sample the calculated value of f-factor (g_z/A_z ratio) is 216 cm, which is reasonable near to 250 cm for tetrahedral complexes. Temperature dependence of magnetic susceptibility in ZFC and FC regimes for $Cu(en)(H_2O)_2SO_4$ complex encapsulated in SBA-15 shows paramagnetic behavior without any sign of phase transition to magnetically ordered state in contrast to the bulk $Cu(en)(H_2O)_2SO_4$ complex, where the phase transition has been evidently get sight of at $T_N = 0.91$ K [1].

Acknowledgements: This work was supported by the Slovak Research and Development Agency Project number APVV-18-0197 and VEGA Grant No. 1/0132/22 of the Scientific Grant Agency of the Ministry of Education, Science, Research and Sport of the Slovak Republic.

[1] M. Kajňaková *et al.*, Physical Review B, 71 (2005) 014435

Contributed talk, Mon./14:15

Influence of the electrodeposition parameters on the properties of FeCoNiCu nanowires

A. Nykiel[1,2], A. Walcarius[2], and M. Kąc[1]

[1]Institute of Nuclear Physic, Polish Academy of Science, Cracow, Poland
[2]Laboratory of Physical Chemistry and Microbiology for the Materials and the Environment (LCPME), Lorraine University, CNRS, Nancy, France

email: `anna.nykiel@ifj.edu.pl`

Among many potential applications of magnetic nanowires, their use in information technology is becoming more and more promising [1]. Such nanowires, due to a strong effective magnetic anisotropy and easy-to-modify morphology and distribution, can be used as magnetic data storage devices. Nanowires with their ability to smoothly propagate the domain wall at very high speed can be considered as domain wall guide for 3D magnetic recording media technology [2].

In this study, alloyed FeCoNiCu nanowires with a diameter of 50 nm and length of 6 μm were electrodeposited into polycarbonate membranes at various cathodic potentials at two different pH values (3.0 and 3.7). Nanowires were prepared using the template-assisted electrodeposition process performed in the potentiostatic mode. Morphology and elemental composition were examined using a scanning electron microscope (SEM) equipped with an energy dispersive spectrometer (EDS). The structural and magnetic properties of nanowires were investigated based on X-ray diffraction (XRD) and superconducting quantum interference device (SQUID) measurements.

A more cathodic potential resulted in a higher current and an obvious shortening of the time needed to fill the membranes. The current values recorded for different pH were shown to be about 60% higher for lower pH. As predicted, more cathodic applied potentials resulted in an increase in Ni concentration with a simultaneous decrease in Fe, Co and Cu contents. However, the content of Fe, Co and Ni, due to a small difference in pH values, did not change significantly for various pH at the appropriate voltages. Similarly, pH did not impact the crystalline structure of nanowires, while clear structural modifications were observed at applied potentials. The analysis allowed us to identify diffraction lines that correspond to the fcc FeCoNi phase. Magnetic anisotropy with the easy axis along nanowires was observed for all nanowires, regardless of their composition. Moreover, the coercivity (H_c) and squareness (M_R/M_s) varied with the chemical composition of nanowires with a tendency to increase with increasing cathodic potential. The highest value of the $H_c = 490$ Oe measured out of the membrane plane was observed at cathodic potentials of -1.4 V for both pH values, while the highest $M_R/M_s \cong 80\%$ was achieved at the most negative potential. The changes in the magnetic properties with the pH value were also noticed. Both the coercivity and squareness were larger for the nanowires deposited at higher pH except for the nanowires prepared at the lowest potential, for which both parameters were greater at pH $= 3.0$.

The studies have shown the difference in the magnetic properties of nanowires prepared at various potentials, which make them good candidates for 3D magnetic recording media technology.

Acknowledgements: This research was supported by a French Government Scholarship. A. Nykiel acknowledges financial support provided by the Polish National Agency for Academic Exchange NAWA under the Programme STER – Internationalisation of doctoral schools, Project no. PPI/STE/2020/1/00020.

[1] J. A. Moreno *et al.*, IEEE Trans. Magn., 57 (2021) 1A
[2] E. C. Burks *et al.*, Nano Lett., 21 (2021) 716

Contributed talk, Mon./14:30

Plasma irradiation: a promising technique for modifying magnetic properties in molecular magnets

D. Czernia[1] and P. Konieczny[1]

[1]*Institute of Nuclear Physics PAN, Cracow, Poland*

email: `dominik.czernia@ifj.edu.pl`

Molecular magnets are a class of metal-organic materials exhibiting unique physical properties sensitive to external stimuli such as temperature, pressure, light, or the presence of guest molecules. Although not in molecular systems yet, it was shown that the plasma treatment can also be used as a stimulus to control the desired parameters of magnetic materials.

Here, we report results obtained for the three-dimensional molecular Nb^{IV}-Mn^{II} ferrimagnet ($\mathbf{NbMn_2}$) subjected to plasma irradiation under various conditions. The long-range ordered state can be observed below $T_C = 47.5$ K, and antiferromagnetic interaction between two magnetic ions was confirmed by the saturation magnetization of 9 Bohr magnetrons per $\mathbf{NbMn_2}$ formula unit, which corresponds to two spins $S = 1/2$ and one $S = 5/2$.

The $\mathbf{NbMn_2}$ samples were ground down and scattered on the adhesive tape to ensure a large surface-to-volume ratio of exposed crystallites. Then, the samples were irradiated with plasma made of air, nitrogen, oxygen, and argon with different power and treatment time. After the irradiation, all samples were protected from air and vacuum by an additional layer of adhesive tape put at the top of the samples.

The magnetic properties after plasma treatment show a clear appearance of the second magnetic phase with T_C around 70 K (Fig. 1) for at least medium power and 10 minutes irradiation time, indicating the threshold effects. The influence of heat and ultraviolet light generated during plasma was ruled out with additional measurements. The powder X-ray diffraction measurements show the same diffraction patterns with the shift of diffraction peaks (Fig. 2) for irradiated samples towards higher angles, indicating the decrease of crystal lattice parameters due to the evaporation of the water of crystallization. It is in line with the increase of T_C, suggesting the enhancement of exchange couplings.

We show that although plasma irradiation is not a common approach to modify physical properties in molecular magnets, it indeed offers a promising way of obtaining new magnetic phases.

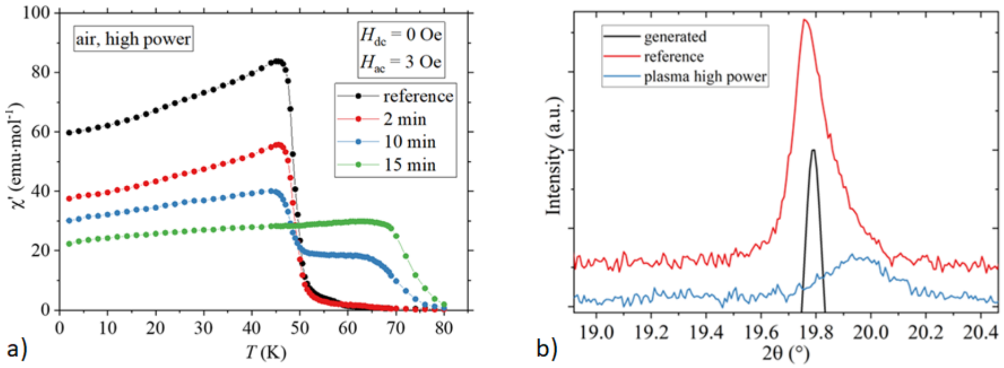

Figure 1: a) The real part of the AC magnetic susceptibility of $\mathbf{NbMn_2}$ measured for samples irradiated for 10 minutes with high-power air, nitrogen, oxygen, and argon plasma. b) One of the powder diffraction peaks of $\mathbf{NbMn_2}$ obtained from the structure file (black), the sample before (red), and after 10 minutes high-power air plasma treatment (blue).

Acknowledgements: This work was supported by the Polish Minister of Education and Science (grant No.: DI2017 006047).

Contributed talk, Mon./14:45

Experimental study of low-temperature magnetic properties of Dy-doped phosphate glass

P. Baloh[1], V. Tkáč[1], R. Tarasenko[1], E. Čižmár[1], M. Orendáč[1], A. Orendáčová[1], J. Holubová[2], E. Černošková[3], Z. Černošek[2], and A. Feher[1]

[1]*Institute of Physics, Faculty of Science, P. J. Šafárik University in Košice, Park Angelinum 9, 041 54 Košice, Slovakia*
[2]*Department of General and Inorganic Chemistry, Faculty of Chemical Technology, University of Pardubice, Studentská 573, 532 10 Pardubice, Czech Republic*
[3]*Joint Laboratory of Solid State Chemistry, Faculty of Chemical Technology, University of Pardubice, Studentská 84, 532 10 Pardubice, Czech Republic*

email: `pavlo.baloh@student.upjs.sk`

The low-temperature magnetic properties of rare-earth ion doped materials are mainly focused on the periodic and symmetrical crystal structures. In such cases, the surroundings of the ion are defined, and the crystal-electric field (CEF) is uniform. Our study is focused on the amorphous phosphate glass doped with a Dy^{3+} ion which is conformed into a random network consisting of chains of PO_4 tetrahedra of various lengths to generate different CEF sets with a random distribution of energy levels.

The $Dy(PO_3)_3$ was measured by a set of experimental techniques, including specific heat, DC susceptibility, and magnetization. Specific heat was measured in the temperature range of 0.4 – 300 K, and magnetic fields up to 9 T. The low-temperature specific heat of disordered materials is known to reveal a broad maximum, commonly accepted as Boson peak (BP). However, the lowest temperatures of magnetic samples are dominated by the Schottky anomaly, which overlaps the BP. Therefore, the specific heat of equivalent non-magnetic glass $Y(PO_3)_3$ was also measured at the same temperature range, revealing the BP at 12 K.

The magnetic susceptibility was measured from 1.8 K up to room temperature. An effective moment of 10.65 μ_B was estimated, close to the theoretical prediction for the free Dy^{3+} ion. Magnetization curves were measured in magnetic fields up to 5 T with temperatures ranging from 2 to 50 K.

X-band electron-paramagnetic resonance was measured from 0 to 1 T and temperatures from 2 to 40 K, revealing an additional absorption maximum at 100 mT. The maximum has the largest intensity at the same temperatures as the BP position in specific heat, implying a possible correlation.

Acknowledgements: This work was supported by the Slovak Research and Development Agency Project [grant numbers APVV-18-0197, APVV-SK-BY-RD-19-0008, and APVV-20-0324] and Scientific Grant Agency of the Ministry of Education, Science, Research and Sport of the Slovak Republic and the Slovak Academy of Sciences project VEGA 1/0132/22.

SESSION III: COMPUTATIONAL PHYSICS

16:00	**Iuliia Voroshylova** (Portugal) Computational study of the influence of temperature on $EMImBF_4$ – graphene interface: explanation in the framework of bilayer model	p. 23
16:15	**Surajit Basak** (Poland) A first principle study of the materials hosting chiral phonons	p. 24
16:30	**Jacek Gatlik** (Poland) Thermal Effects on the Dynamic of Kink in Heterogeneous Energy Landscapes	p. 25

CONTRIBUTED TALK, MON./15:45

Computational study of the influence of temperature on $EMImBF_4$-raphene interface: explanation in the framework of bilayer model

I. V. Voroshylova[1], H. Ers[2], P. Pikma[2], and V. B. Ivaništšev[2,3]

[1]*LAQV/REQUIMTE, Department of Chemistry and Biochemistry, Faculty of Sciences, University of Porto, Porto, Portugal*
[2]*Institute of Chemistry, University of Tartu, Tartu, Estonia*
[3]*Department of Chemistry, Center for High Entropy Alloy Catalysis, University of Copenhagen (UCPH), Copenhagen, Denmark*

email: `voroshylova.iuliia@fc.up.pt`

Ionic liquids (ILs) are electrolytes composed solely of ions. They possess exceptional physicochemical properties, such as high electrochemical stability and low vapor pressure, which makes ILs an attractive alternative for use in fuel cells, solar panels, supercapacitors, actuators, as well as in other storage and transformation electrochemical devices [1]. Taking into account the potential application of ILs in the aforementioned devices, the interfacial properties of ILs, including electric double layer (EDL), have gained fundamental interest.

Due to the ionic nature of ILs, their EDL differs from the one formed in aqueous and organic electrolytes. EDL in ILs is characterized by layered structure and an overscreening, i.e., the electrode charge is overcompensated by the electrolyte contact layer. Despite numerous theoretical [2], experimental [3] and computational [4] studies, multiple open questions about ILs interfacial properties remain. One of them - the dependence of differential capacitance on the temperature [5] – is addressed in this study.

In a series of molecular dynamics simulations and density functional theory calculations on the example of 1-ethyl-3-methylimidazolium tetrafluoroborate ($EMImBF_4$) and graphene electrode, we show how the capacitance and structure depends on the applied potential and temperature. We analyze the obtained data in terms of our newly developed bilayer model. We introduce a novel phenomenon of EDL in ILs, the ionic saturation. In our simulations, we show an overscreening phenomenon, monolayer formation, and temperature-induced smearing of the interfacial structure. With a bilayer model we relate the characteristic features of capacitance–potential dependence to the changes in interfacial structure. These insights are of fundamental and practical importance for the application in electrochemical devices.

Acknowledgements: This work was supported by FCT/MCTES through the Portuguese national funds, project UIDP/50006/2020 (LAQV/REQUIMTE). The financial support from the Estonian Research Council (grant PSG249) and from the EU through the European Regional Development Fund under project TK141 (2014-2020.4.01.15-0011) is also acknowledged.

[1] D. D. Patel and J.-M. Lee, Chem. Rec., 12 (2012) 329
[2] Z. A. H. Goodwin and A. A. Kornyshev, Electrochem. Commun., 82 (2017) 129
[3] I. V. Voroshylova *et al.*, Electrochim. Acta, 379 (2021) 138148
[4] L. Siinor *et al.*, J. Electrochem. Soc., 157 (2010) F83
[5] F. Silva *et al.*, J. Electroanal. Chem., 622 (2008) 153

CONTRIBUTED TALK, MON./16:15

A first principle study of the materials hosting chiral phonons

S. Basak[1], P. Piekarz[1], and A. Ptok[1]

[1]*Institute of Nuclear Physics, Polish Academy of Sciences, W. E. Radzikowskiego 152, PL-31-342,Krakow,Poland*

email: `surajit.basak@ifj.edu.pl`

Geometry of the compounds often allow the atoms to circulate around their equilibrium position in a circular or an elliptical trajectory. The phonons emerging from these kind of vibrations inherit the properties of its parent system and have a non zero value of Pseudo Angular Momentum (PAM) associated with them. We study the presence of chiral phonons in a system with orthorhombic symmetry (YalSi) [1], and also in systems with cubic Laves phases with chemical symbol $\mathrm{ABi_2}$($\mathrm{A} = \mathrm{K}$, Rb, Cs). However, due to the presence of inversion symmetry, the total angular momentum is zero in all the mentioned system. We then artificially break the inversion symmetry by doping and propose a couple of new systems with a non zero value of total Pseudo Angular Momentum [2]. We study the dynamical stability of the final systems $\mathrm{KRbBi_4}$, $\mathrm{RbCsBi_4}$ and show that there are no negative frequency modes in the phonon dispersion relation of any of those compounds, which indicates that they can be prepared in laboratory. A finite value of PAM indicates that we may expect a angular momentum current arising from the phonons which allows these materials to be used as platforms for studying phonon Hall effect.

[1] S. Basak and A. Ptok, Crystals 12 (2022) 436
[2] S. Basak *et al.*, arXiv:2208.14041 (2022)

Contributed talk, Mon./16:30

Thermal Effects on the Dynamic of Kink in Heterogeneous Energy Landscapes

J. Gatlik[1] and T. Dobrowolski[2]

[1] *Doctoral School, Pedagogical University of Krakow, Kraków, Poland*
[2] *Pedagogical University of Krakow, Kraków, Poland*

email: `jacek.gatlik@doktorant.up.krakow.pl`

The research focuses on the impact of thermal noise on kink motion through the curved region of the long Josephson junction. We considered the kink motion in the modified sine-Gordon model with the position dependent dispersive term

$$\partial_t^2\phi + \alpha\partial_t\phi - \partial_x(\mathcal{F}(x)\partial_x\phi) + \sin\phi = -\Gamma \tag{1}$$

where the function $\mathcal{F}(x)$ contains information about the curvature of the junction. In the equation α represents the dissipation in the system caused by quasiparticle current and Γ represents the bias current. The physical motivation for the description of curvature effects in the framework of this model has been detailed in the article [1]. Based on perturbation theory applied to the sine-Gordon equation with the perturbations from bias current (which describes the effects of non-zero temperature of the system), damping and the curved structure, a model for the kink velocity was derived. This approach, uses a method not previously applied to the sine-Gordon model, based on the projection of kink energy onto the dynamical equation of motion and was presented in detail in the article [1]. The probability distribution of the kink velocity was found on the base of the derived Fokker-Planck equation. The analytical results were compared with the simulations based on the full field model. Due to potential applications in normal and high-temperature superconductors, the comparison was made from zero to $T = 50$ K, $T = 20$ K, and $T = 5$ K [2].

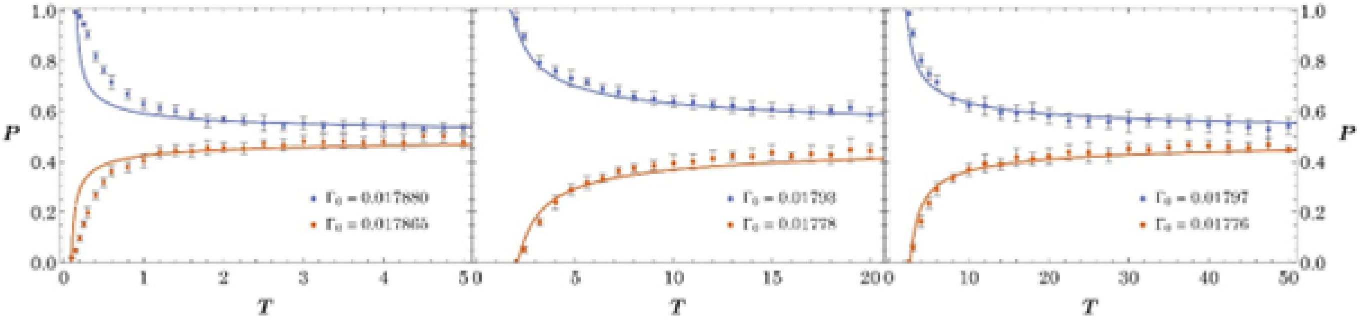

Figure 1: The probability of transition of the fluxon obtained from the field model compared in the various interval of T with the analytical formula. The blue line and points correspond to the bias current exceeding its threshold value, and the red to the bias current below its threshold value.

The agreement of the proposed model with the results from the full field model solutions is very good in the temperature range from 1 K to 50 K. For temperatures below 1 K a relativistic effect on the width of the kink was included in the analysis, but despite this, in the temperature range from 0 K to 1 K the model shows only partial agreement. The most likely reason for the discrepancy of the presented model with the results of the full model for temperatures below 1 K is the presence of resonance windows, which were detected in the studied system.

The Josephson junctions have found a wide variety of science and technical applications. Fundamental for the preparation of junctions with specific properties are the descriptions of the soliton dynamics inside the junction. The results of the research could be the basis for future development of devices based on the Josephson junction and creation of electronics based on quantum effects occurring in the junction.

[1] J. Gatlik, T. Dobrowolski, Physica D: Nonlinear Phenomena 428 (2021) 133061
[2] J. Gatlik, T. Dobrowolski, Physica D: Nonlinear Phenomena 445 (2023) 133649

SESSION IV: MULTIFUNCTIONAL MATERIALS

10:30	**Luming Zhang** (Japan) Thermal Conductivity Measurement System for Wide-Temperature Range for Single Crystals of Molecular Compounds	p. 27
10:45	**Qingping Wang** (xxxx) Pyroelectric materials for thermal sensing and harvesting	p. 28
11:00	**Sara El Houbbadi** (Poland) Experimental and Theoretical XAFS studies of the atomic structure of Copper functionalized SBA-15 mesoporous matrix	p. 29
11:15	**Veronika Mukharovska** (Ukraine) Optical properties of opal-based photonic crystal films and heterostructures	p. 30
11:30	**Mateusz Gala** (Poland) Evolution of the Verwey transition in magnetite observed through electronic transport studies under uniaxial stress	p. 31
11:45	**Bahjou Yousra** (Morocco) A new environmentally safe hybrid material aimed at removing heavy metals from contaminated water, magnetic studies of the iron(II) complex	p. 32
12:00	**Juliusz Chojenka** (Poland) Manipulating Electrical Properties of Nanopatterned Double-Barrier Schottky Junctions in Ti/TiO$_x$/Fe Systems	p. 33

CONTRIBUTED TALK, TUE./10:30

Thermal Conductivity Measurement System for Wide-Temperature Range for Single Crystals of Molecular Compounds

A. Luming Zhang[1], B. Tetsuya Nomoto[2], C. Satoshi Yamashita[1], D. Hiroki Akutsu[1], and E. Yasuhiro Nakazawa[1]

[1] *Osaka University, Graduate School of Science, Toyonaka, Osaka, 560-0043, Japan*
[2] *The University of Tokyo, Institute for Solid State Physics, Kashiwa, Chiba, 277-8581, Japan*

email: `zhangl20@chem.sci.osaka-u.ac.jp`

Thermal conductivity measurements in a wide temperature range are necessary for characterizing the materials with unique heat transport properties. They are also important for developing new functional materials with peculiar electronic and phonon properties. Unlike electrical conductivity measurements which only exhibit the nature of electron transport, thermal conductivity measurements can give the information of the heat transport by various degrees of freedom such as spin and phonons.

The steady-state method is usually available in low-temperature thermal conductivity measurements with high accuracy. However, it is required to use longer samples, typically more than a few millimetres in length. Also, highly sensitive resistance sensors are necessary for attaining enough resolution in a wide temperature region. We have developed a thermal conductivity measurement system based on the steady-state technique for tiny samples as small as 0.3 mm using small ruthenium oxide resistance thermometers [1]. Although this system can give high measurement accuracy in the temperature range of 0.1 K to 20 K, the sensitivity of the ruthenium thermometer decreases rapidly above 20 K, making it difficult to measure thermal conductivity at higher temperatures. In the present apparatus, we combined RuO_2 resistance thermometer and thermocouple in the regular 4-terminal detector setup. We used a 13-μm diameter type E thermocouple wire for the lead wire of the 4-wire resistance measurement of a resistance thermometer. In Fig. 1, we compared the standard deviation $\sigma_{\Delta T}$ of the temperature detection by several thermometers, calculated from the sensitivity of the thermometers and the accuracy of the meters. Thermocouples are sensitive to detect temperature differences at high temperatures, but their sensitivity is reduced at very low temperatures. By introducing automatic switching unit between thermocouple detection and ac resistance bridge around 10 K, we realized the continuous high accuracy thermal conductivity measurement from 0.1 K to 300 K in one setup [2]. Furthermore, we can measure the anisotropy by multiplexing thermometers and resistor heaters. The system is also suitable to measure under high magnetic fields and electric fields.

Using this apparatus, we succeeded to measure thermal conductivity of $(n\text{-}BuNH_3)_2CuCl_4$ which shows high thermal conductivity due to para-magnons. The dynamic fluctuations of the $n\text{-}BuNH^{3+}$ alkyl chain layers and electron correlations in $CuCl_4^{2-}$ layers are discussed. We also show thermal conductivity of organic charge transfer compounds.

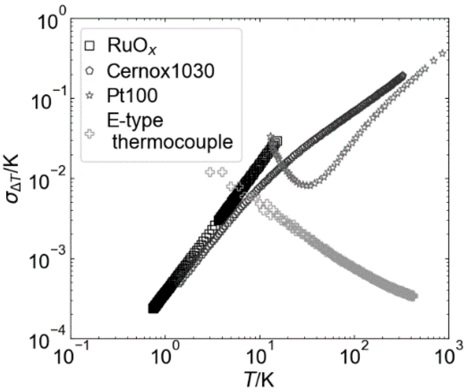

Figure 1: Temperature dependence of measurement error $\sigma_{\Delta T}$ of different types of thermometers. Lower values of $\sigma_{\Delta T}$ give better resolution.

[1] T. Nomoto *et al.*, J. Therm. Anal. Calorim., 135 (2019) 2831
[2] L. Zhang *et al.*, Low Temp. Phys.(Fiz. Nyzk. Temp.), 49 (2023) 588

Contributed talk, Tue./10:45

Pyroelectric materials for thermal sensing and harvesting

Q. Wang

email: `qw608@bath.ac.uk`

Poor heat transfer and low output energy are the main obstacles that limit the popularization and application of pyroelectric sensors and energy harvesters. To address these problems, lead magnesium niobate-lead antimony-manganese-lead zirconate titanate ($Pb[(Mn_{1/3}Nb_{2/3})_{1/2}(Mn_{1/3}Sb_{2/3})_{1/2}]_{0.04}(Zr_{95}Ti_5)_{0.96}O_3$, abbreviated as PMN-PMS-PZT) ceramics were designed and fabricated to improve the thermal conductivity of the pyroelectric material through the high thermal conductivity additive ZnO nanoparticles, and the effects of the additive on the thermal conductivity, pyroelectric coefficient, the rate of temperature change (dT/dt) and the output energy of the ceramic were investigated in detail; the effects of ZnO on the piezoelectric response and temperature change in the microzone were analyzed by PFM, along with the energy figure of merits and output energy. These results showed that the pyroelectric material with 0.3% ZnO can increase the output voltage and power up to 41.4 and 99.7%, respectively, suggesting potential prospect applications in waste heat recovery and thermal sensing, harvesting, and beyond.

Acknowledgements: Q. Wang acknowledges the National Natural Science Foundation of China (Grant No. 51902094).

Contributed talk, Tue./11:00

Experimental and Theoretical XAFS studies of the atomic structure of Copper functionalized SBA-15 mesoporous matrix

S. El Houbbadi[1,2], M. Laskowska[1], and Ł. Laskowski[1]

[1] *Institute of Nuclear Physics Polish Academy of Sciences, Krakow 31-342, Poland*
[2] *Université de Lorraine, CNRS, LCPME, Nancy F-54000, France*

email: `sara.elhoubbadi@ifj.edu.pl`

Ordered Mesoporous silica nanocomposites open up the possibility to control their physicochemical properties by introducing a wide range of functional groups inside their pores. Various approaches have been developed to functionalize these materials, which can be achieved in a few steps to ultimately reach a uniform dispersion of active anchoring units, separated by passive functionalities called spacers [1, 2]. SBA-15 with propyl phosphonic acid, which serves as anchoring units for two-valent metal ions like copper, nickel, iron, or cobalt, can be considered a potential candidate in many industrial applications. We have demonstrated previously that SBA-propyl-Cu can exhibit quite good Non-linear optical (NLO) response that can be tuned by changing the concentration of the functional unit inside the silica scaffold [3], making them intriguing materials for optoelectronic studies. X-ray absorption spectroscopy has been used to investigate the structure of incorporated copper sites inside the silica matrix.

In this work, I will present a rigorous analysis approach that adopts numerical calculations of x-ray absorption spectra of the studied system to achieve a quantitative analysis of the local structure and coordination environment information of the metallic species incorporated inside the silica. The results will be used to explain the NLO response found in the materials.

Other complementary measurements such as TEM, SEM, EDS, isothermal sorption of nitrogen, and vibrational spectroscopy, will also be presented.

Acknowledgements: Financial support for this investigation has been provided by the National Centre of Science (2020/37/B/ST8/03637, and 2021/43/D/ST8/00737).

[1] M. Laskowska *et al.*, Int. J. Mol. Sci., 21 (2020) 8137
[2] A. Fedorchuk *et al.*, Mater. Proc., 4 (2021) 66
[3] M. Laskowska *et al.*, Nanoscale, 33 (2017) 12110

Contributed talk, Tue./11:15

Optical properties of opal-based photonic crystal films and heterostructures

V. Mukharovska[1], M. Derhachov[1], and V. Moiseienko[1]

[1] *Oles Honchar Dnipro National University, Dnipro, Ukraine*

email: `mukharovska@ffeks.dnu.edu.ua`

Practical interest in fabrication and investigation of photonic crystals (PhCs) comes from their ability to control the emission and propagation of light. One of the widely used prototypes of three-dimensional PhCs is synthetic opal, that is a self-assembled periodic structure composed of monodisperse spherical silica particles (MSSPs) packed in face-centered cubic lattice. Development of heterogeneous opal-based PhC is a new step towards engineering functional devices - this approach enables multiple-frequency lasing from a single PhC chip, complex light filtering, and the realization of PhC resonator or superlattice [1].

Initially MSSPs were synthesized using the modified Stöber–Fink–Bohn (SFB) method by tetraethyl orthosilicate hydrolysis in ethanol–water solution in the presence of ammonia hydroxide. To investigate the effect of the synthesis components concentration on the diameter of MSSPs the reaction solutions were prepared with large variety of components molarity: 9–20 M of H_2O, 0.3–2 M of NH_3, 10–13 M of C_2H_5OH, and 0.14–0.32 M of $SiC_8H_{20}O_4$. Thereupon for obtaining synthetic opals, MSSPs were deposited on a glass substrate using the method of vertically moving meniscus. To make PhC band gap wider, PhC dual heterostructure were obtained by using MSSPs of another diameter (close to initial) prepared by the multistage SFB method. The second layer of opal film heterostructure was crystalized on the first one acting like a substrate using the abovementioned method.

Reflectance spectra (Fig. 1) of both single-film and double-film structures were registered by using modified spectrometer based on a double monochromator DFS-12 equipped with a photon counting system. The diameter D of MSSPs was determined from the spectral position λ_m of the reflectance maximum in the corresponding spectrum, according to the Bragg law.

The Bragg light diffraction model provides a remarkable coincidence with the obtained angular dependences of the single-film reflectance, thereby enabling us to utilize it as a tool for controling the diameter of the MSSPs. The latter can be altered significantly by adjusting the molarity of $SiC_8H_{20}O_4$, H_2O and NH_3. Moreover, the multistage SFB method can be employed to obtain a more predictable MSSPs diameter, which is crucial for fabricating dual heterostructures. Angular dependence of dual heterostructure reflectance exhibits the similar behavior as a single-film with a 'blue shift' of reflectance maximum with increasing the angle of light incidence. However, it's spectrum can be seen as a superposition of the spectra of the films composing the structure, resulting in a noticeably wider PhC band gap. One should also take note of the substantial contribution of the interface to light scattering and the attenuation of the reflected light beam. The obtained heterostructures can serve as templates for laser-active systems by infiltrating them with an appropriate substance.

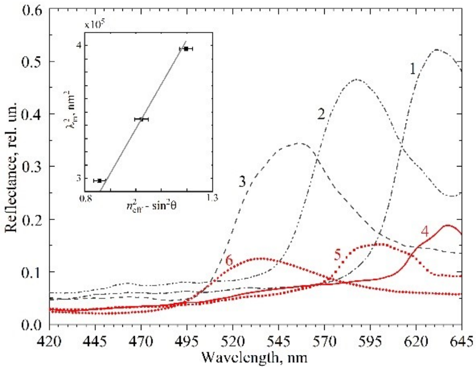

Figure 1: The single film (1-3) and heterostructure (4-6) spectra at angle $\Theta = 40°$ (1, 4), 50° (2, 5), 60° (3) and 65° (6). Inset shows linear approximation of angular dependence of the reflectance maximum position for the single film based on Bragg law.

[1] A.S. Kuchyanov *et al.*, Optoelectron. Instrum. Data Process., 52 (2016) 96

Contributed talk, Tue./11:30

Evolution of the Verwey transition in magnetite observed through electronic transport studies under uniaxial stress

M. A. Gala[1], K. Komędera[1], A. Kozłowski[1], D. Rybicki[1], and W. Tabiś[1,2]

[1] *AGH University, Faculty of Physics and Applied Computer Science, 30-059 Krakow, Poland*
[2] *Institute of Solid State Physics, TU Wien, 1040 Vienna, Austria*

email: `mgala@agh.edu.pl`

Magnetite is one of the most extensively investigated magnetic materials nowadays. Despite its simple chemical composition, it is a strongly correlated electronic system with many co-existing orderings. Magnetite is mostly known for the still not entirely understood Verwey transition (VT) occurring at $T_V \approx 123$ K. The VT is reflected in measurements of fundamental physical properties like AC susceptibility, heat capacity or electrical resistivity. It also involves change of the structure from cubic to monoclinic and conductive properties from semi-metallic to insulating. Even though much attention of the scientific community has been paid to understanding properties of magnetite for more than a century, the VT still requires a consistent theoretical and experimental description [1].

T_V can be systematically decreased by introducing oxygen non-stoichiometry or substituting the iron positions in the spinel structure with cations like Ti, Ni, or Zn [2]. Furthermore, it is also possible to manipulate the VT by applying external pressure to the material. Although, in general, hydrostatic pressure was shown to systematically decrease T_V, and cause metallization of the material at critical pressure of 8 GPa [3], the uniaxial pressure studies of the VT are still very limited [4].

I will present the electronic transport measurements performed on single crystals of stoichiometric magnetite under uniaxial pressure, which is so far the only known external stimulus capable of increasing T_V.

The resistivity was measured as the lattice was compressed along (100) direction. We studied the electrical resistivity as a function of temperature and uniaxial stress systematically increasing from 0 up to 500 MPa (see Fig. 1). The T_V was determined from marking the inflection point at the VT of the resistivity curves. This analysis indicated that the application of uniaxial pressure along (100) direction systematically increased T_V. The changes of TV turned to be a linear relation of the applied uniaxial pressure.

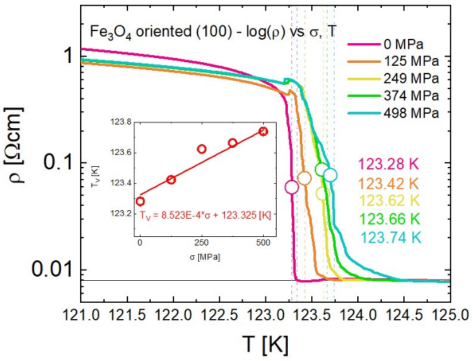

Figure 1: Temperature dependence of resistivity in the region of the Verwey transition, measured for a single crystal of magnetite for different values of uniaxial pressure. Inset: T_V as a function of uniaxial compression along (100) direction.

Acknowledgements: We acknowledge the support from the National Science Centre, Poland, grant OPUS: UMO-2021/41/B/ST3/03454, National Science Centre, Poland, grant No. 2018/30/E/ST3/00377, and the Polish National Agency for Academic Exchange under 'Polish Returns 2019' Program: PPN/PPO/2019/1/00014.

[1] E.J. Verwey *et al.*, Physica, 8 (1941) 979
[2] Z. Kąkol *et al.*, Solid State Sci., 2 (2000) 737
[3] T. Muramatsu *et al.*, J. Appl. Phys., 119 (2016) 135903
[4] Y. Nagasawa *et al.*, JPSJ, 76 (2007) 110

Contributed talk, Tue./11:45

A new environmentally safe hybrid material aimed at removing heavy metals from contaminated water, magnetic studies of the iron(II) complex

B. Yousra[1,2], R. Smaail[2], and Y. Garcia[2]

[1]*LCAE, Department of Chemistry, Faculty of Science, University Mohamed I, Oujda, Morocco*
[2]*Institute of Condensed Matter and Nanosciences, Molecular Chemistry, Materials and Catalysis (IMCN/MOST), Université Catholique de Louvain, Belgium*

email: `yousra.bahjou@uclouvain.be`

C-N junctional tetrazole and triazole motif ligands can readily form different types of coordination networks that have attracted much attention due to their variety of architectures and topologies [**?**], as well as to their broad potential applications, for example, in molecular magnetism, photoluminescence, and cancer therapeutics [2, 3]. A series of new tetrazole and C,N-triazole ligands, 2-(3-(3,5-dimethyl-1H-pyrazol-1-yl)-1H-1,2,4-triazol-1-yl)acetonitrile (**L1**) and 5-((3-(3,5-dimethyl-1H-pyrazol-1-yl)-1H-1, 2,4-triazol-1-yl)methyl)-1H-tetrazole (**L2**), were prepared and identified by different spectroscopic methods including ^{1}H-NMR, ^{13}C-NMR, FT-IR and HRMS. The reaction of **L1** and **L2** with several transition metals: Ni(II), Cu(II), Co(II), Fe(II) and Cd(II) led to the formation of coordination complexes, namely: $[\mathrm{Ni}(\mathbf{L1})_3](\mathrm{ClO}_4)_2$ (**1**), $[\mathrm{Cd}(\mathbf{L1})]\mathrm{C})_2$ (**2**), $[\mathrm{Cu}(\mathbf{L1})_2(\mathrm{NO}_3)]\mathrm{NO}_3$ (**3**), $[\mathrm{Co}(\mathbf{L1})_3](\mathrm{ClO}_4)_2$ (**4**), $[\mathrm{Fe}(\mathbf{L1})_3](\mathrm{ClO}_4)_2$ (**5**), $\mathrm{Cu}\mathbf{L2}\mathrm{Cl}_2$ (**6**) and $[\mathrm{Ni}(\mathbf{L2})_3](\mathrm{ClO}_4)_2$ (**7**). In addition, the iron(II) analogue was studied by ^{57}Fe Mössbauer spectroscopy and SQUID magnetometry [4].

The main goal was to use model complexes to realize the simultaneous synthesis of a new hybrid material based on silica **M1**, whose surface is decorated with the ligand **L2**, which was prepared and identified using standard methods of solid material characterization: FT-IR, elemental analysis, TGA, BET and SEM. The purpose of this **M1** hybrid material research is to assess its efficiency and contribution to the removal of heavy metals from aqueous and real solutions (Figure 1).

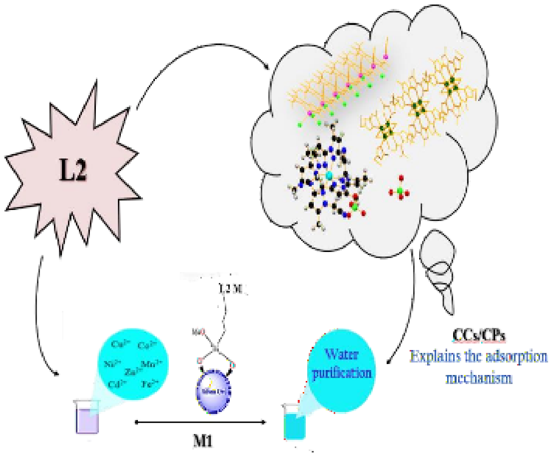

Figure 1: Illustration of main work.

[1] D.A. Safin *et al.*, CrystEngComm, 18 (2016) 7284
[2] H. Benaissa *et al.*, Cryst. Growth Des., 21 (2021) 3562
[3] M. El-Massaoudi *et al.*, J. Cleaner Prod., 284 (2021) 124757
[4] Y. Bahjou *et al.*, submitted

CONTRIBUTED TALK, TUE./12:00

Manipulating Electrical Properties of Nanopatterned Double-Barrier Schottky Junctions in Ti/TiO$_x$/Fe Systems

J. Chojenka[1], A. Zarzycki[1], M. Perzanowski[1], T.Fodor[2], K. Mróz[3], V. Takáts[2], K. Vad[2], M. Krupiński[1], and M. Marszałek[1]

[1]*Institute of Nuclear Physics Polish Academy of Sciences, Krakow, Poland*
[2]*Institute for Nuclear Research, Hungarian Academy of Sciences, Debrecen, Hungary*
[3]*Faculty of Chemistry, Jagiellonian University in Krakow, Krakow, Poland*

email: `juliusz.chojenka@ifj.edu.pl`

In this work, we focuses on investigating electrical transport and magnetoresistance phenomena in heterostructures based on transition metal oxides. Specifically, we utilized anodized porous titanium oxide, a wide bandgap semiconductor, combined with a ferromagnetic iron layer to create heterojunctions controllable by a magnetic field. The anodization method used is fully scalable, enabling cost-effective mass production of such systems and opening up new application perspectives. Our work primarily focuses on understanding the structural, electrical, and magnetic phenomena on the surfaces and interfaces of porous titanium oxide/iron heterostructures, which hold significant relevance in modern oxide semiconductor-based spintronics [1, 2].

In our findings, we observed a distinctive dual magnetoresistance behavior, which can be attributed to the distinct properties of the individual interfaces: titanium-titanium oxide and titanium oxide-iron. This magnetoresistance consists of two components, each exhibiting different temperature dependencies. The positive component arises from the paramagnetic constituents of the junctions and dominates the behavior at room temperature, while the negative component arises from iron and predominantly contributes at lower temperatures. This type of complex behavior has not been observed previously and seems to be associated with the introduction of pores to the metal-metal oxide interfaces. Furthermore, we demonstrate an enhancement in magnetoresistance as the size of the pores increases. This enhancement is linked to the larger surface area of the titanium oxide, leading to a more pronounced interface development of the iron layer.

Acknowledgements: The support from the NCN grant 2015/19/D/ST3/01843 is gratefully acknowledged. This work was also supported by the project 2019-2.1.7-ERANET-2021-00021, financed by the National Research, Development and Innovation Fund of the Ministry for Innovation and Technology, Hungary.

[1] A. Zarzycki *et al.*, Materials, 14:9 (2021) 2390
[2] J.C. Chojenka *et al.*, Materials, 16:1 (2023) 289

SESSION V: SOFT MATTER AND GLASS-FORMERS

13:30	**Marcin Piwowarczyk** (Poland) Thermochromism of mesogenic mixtures containing liquid-crystalline azo and chiral compounds	p. 35
13:45	**Aleksandra Deptuch** (Poland) Crystallization kinetics vs. fluorosubstitution of the molecular core - the study of four chiral compounds forming the smectic phases	p. 36
14:00	**Valeria Morales Alvarez** (Poland) Effect of alkyl chain length on phase transitions and ion dynamics of phosphonium ionic liquids at ambient and elevated pressure	p. 37
14:15	**Beibei Yao** (Poland) Liquid-liquid phase transition promotes the decoupling of ion diffusion from structural dynamics in aprotic ionic liquids	p. 38

CONTRIBUTED TALK, TUE./13:30

Thermochromism of mesogenic mixtures containing liquid-crystalline azo and chiral compounds

M. Piwowarczyk[1], E. Juszyńska-Gałązka[1], A. Drzewicz[1], M. Gałązka[1], and Z. Galewski[2]

[1]*Institute of Nuclear Physics, Polish Academy of Sciences, Kraków, Poland*
[2]*Faculty of Chemistry, University of Wrocław, Wrocław, Poland*

email: `marcin.piwowarczyk@ifj.edu.pl`

The possibility to modulate properties of system is the main reason why the use of liquid crystal mixtures is preferred to design materials for applications. An example of a broadly known application is thermography. It is a method of imaging surface temperature. Thermography allows the measurement of a physical object's temperature and records it in the form of coloured images. It is based on the phenomenon of the thermochromic effect - a selective reflection of specific wavelengths (as a function of temperature) when illuminated by white light [1].

A number of two-component mixtures were prepared, containing different concentrations (mole fractions) of individual compounds. The first component belongs to the mesogenic azo compounds from the homologous series of (E)-4-((4-heptyloxyphenyl)diazenyl)phenyl alkanoates (7OABOOCm, where m = 5 or 8). While the second is one of selected chiral liquid-crystalline compounds - cholesteryl pelargonate (PCh) [2] or (E)-4-((undecylphenyl)diazenyl)phenyl 2-chloropropanoate (P1) [3].

Polarized Optical Microscopy (POM) and Differential Scanning Calorimetry (DSC) methods were used to investigate phase situation dependence on mixture composition. The emphasis is on describing the thermochromic effect of mixtures with respect to pure PCh compound [4].

Acknowledgements: MP has been partly supported by the EU Project POWR.03.02.00-00-I004/16.

[1] H.F. Gleeson, *Thermography Using Liquid Crystals*, in: edited by J. Goodby *et al.*, *Handbook of Liquid Crystals Vol. 8*, Academic Press Inc., New York, 2014
[2] G.W. Gray, J. Chem. Soc., 0 (1956) 3733
[3] A. Włodarczyk *et al.*, Proceedings SPIE, 3319 (1998) 40
[4] J.L. Fergason *et al.*, Mol. Cryst., 1 (1966) 309

Contributed talk, Tue./13:45

Crystallization kinetics vs. fluorosubstitution of the molecular core – the study of four chiral compounds forming the smectic phases

A. Deptuch[1], E. Juszyńska-Gałązka[1,2], M. Jasiurkowska-Delaporte[1], A. Drzewicz[1], M. Piwowarczyk[1], M. Urbańska[3], and S. Baran[4]

[1] *Institute of Nuclear Physics Polish Academy of Sciences, Kraków, Poland*
[2] *Research Center for Thermal and Entropic Science, Graduate School of Science, Osaka University, Osaka, Japan*
[3] *Institute of Chemistry, Military University of Technology, Warsaw, Poland*
[4] *Jagiellonian University, Faculty of Physics, Astronomy and Applied Computer Science, M. Smoluchowski Institute of Physics, Kraków, Poland*

email: `aleksandra.deptuch@ifj.edu.pl`

The kinetics of melt crystallization (during/after cooling) or cold crystallization (during/after heating) is investigated for four chiral liquid crystalline compounds denoted as $5X_1X_26$ with the formula $C_3F_7CH_2OC_5H_{10}O$-Ph(X_1,X_2)-COO-Ph-Ph-C∗H(CH_3)C_6H_{13}. Ph is the phenyl ring and X_1 = H or F, X_2 = H or F indicate the fluorosubstitution of the phenyl ring at 3 and 2 position, respectively [1–4]. The main experimental methods involved in the study of glass transition and crystallization are differential scanning calorimetry (DSC) and broadband dielectric spectroscopy (BDS). Additionally, the polarizing optical microscopy (POM) and X-ray diffraction (XRD) methods are applied where necessary. The density functional theory (DFT) calculations are used to facilitate the interpretation of dielectric relaxation processes. The fluorosubstitution has a significant impact on the crystallization process, which is the fastest for 5FF6 and the slowest for 5HF6. The structure of the smectic glass is also affected by the fluorosubstitution, as 5HH6 forms the hexatic SmX_A* glass, 5HF6 and 5FF6 form the SmC_A* glass and 5FF6 forms apparently the glass of the conformationally-disordered crystal phase (CONDIS). The fragility parameter, describing the deviation of the α-relaxation process from the Arrhenius dependence on temperature, is equal to 89 for 5HH6, 105 for 5FF6 and 107 for 5HF6, while for 5FH6 the α-relaxation is not observed. 5HH6 is therefore the strongest glassformer, despite it crystallizes easier than 5HF6 with a larger fragility index.

Acknowledgements: Empyrean 2 (PANalytical) diffractometer with Cryostream 700 Plus (Oxford Cryosystems) temperature attachment were purchased thanks to European Regional Development Fund Operational Program Infrastructure and Environment (contract no. POIS.13.01.00-00-062/08). The DFT calculations were carried out thanks to the computational resources from the Academic Computer Centre Cyfronet AGH (PL-Grid Infrastructure). The research was supported in part by the Excellence Initiative - Research University Program at the Jagiellonian University in Kraków.

[1] A. Deptuch *et al.*, Phys. Chem. Chem. Phys., 23 (2021) 19795
[2] A. Deptuch *et al.*, J. Phys. Chem. B, 126 (2022) 6547
[3] A. Deptuch *et al.*, J. Mol. Liq., 368 (2022) 120612
[4] A. Deptuch *et al.*, Phase Trans., 96 (2023) 166

Contributed talk, Tue./14:00

Effect of alkyl chain length on phase transitions and ion dynamics of phosphonium ionic liquids at ambient and elevated pressure

V. Morales Alvarez[1], B. Yao[1], and Z. Wojnarowska[1]

[1] *University of Silesia in Katowice, Institute of Physics, Chorzow, Silesia, PL*

email: `v.moralesalvarez@o365.us.edu.pl`

The liquid-liquid phase transition (LLT) is the process of conversion from one liquid to another through a first-order transition. The study of liquids can be further advanced by better understanding of the LLT, since it has been proposed that some of the distinctive properties of materials such as water can be associated to the LLT [3]. In recent time, research has provided insight into the self-organization of ions in quaternary phosphonium-based ILs, it has been considered that this phenomenon is an origin of the liquid-liquid phase transition [1, 2]. As a modern example, on cooling [P666,14][BH4] was transformed from one supercooled liquid state to another one with different local structures, static dielectric permittivity, and thermodynamic properties [1]. Although non-ionic systems have exhibited LLT, such as systems of silicon, phosphorus, liquid carbon, liquid water, or triphenyl phosphite, and other mixtures [3, 4]. The LLT in [P666,14][BH4] can be classified as a genuine first-order phase transition since both supercooled liquids in this state are able to flow. It has also been demonstrated that an exchange of borohydride anion to another anion such as: [TFSI], [TCM], [SCN], or taurine, keeps both liquid phases and does not considerably affect the temperature of LLT [5]. Additionally, it was found that the LLT occurred at a similar time scale of ionic motions (from 0.3-13 ms) no matter the anion in the sample.

All these facts lead to the implication that tendency of amphiphilic phosphonium ILs to have a LLT is irrespective of the anion and more of a consequence of its ability to form local structures. Hence the importance of understanding: *What is the effect of the alkyl chain length in formation of local domains and consequently what is the effect on the LLT and LGT phase transitions within a single-component system?* To further the understanding of this phenomena we have studied the difference that arises from variations in the alkyl chain length. For this study we have chosen ILs with trihexyl-alkylphosphonium cation, [P666,n]+ ($n = 2, 6, 8, 12, 14$), combined [TFSI] anion. To verify whether the chosen systems undergo LLT, differential scanning calorimetry (DSC) at different heating and cooling rates was be employed, revealing a LLT transition only for the sample with 14-carbon alkyl chains. The effect of cation self-assembly on the ion dynamics was examined using dielectric spectroscopy at ambient and elevated pressure.

Acknowledgements: This research was funded in whole by National Science Centre, Poland [Opus 21, 2021/41/B/ST5/00840].

[1] M.A. Harris *et al.*, PNAS, 118 (2021) 11
[2] S. Sastry *et al.*, Nat. Mater., 2 (2003) 739
[3] H. Tanaka *et al.*, Phys. Rev. E, 62:5 (2000) 6968
[4] H. Tanaka *et al.*, Phys. Rev. Lett., 92 (2004) 025701
[5] Z. Wojnarowska *et al.*, Nat. Commun., 13 (2022) 1342

CONTRIBUTED TALK, TUE./14:15

Liquid-liquid phase transition promotes the decoupling of ion diffusion from structural dynamics in aprotic ionic liquids

B. Yao[1], M. Paluch[1], J. Paturej[2], S. McLaughlin[2], A. McGrogan[2], M. Swadzba-Kwasny[2], and Z. Wojnarowska[1]

[1] *Institute of Physics, Silesian Centre for Education and Interdisciplinary Research, University of Silesia in Katowice, Chorzów, Poland*
[2] *The QUILL Research Centre, School of Chemistry and Chemical Engineering, The Queen's University of Belfast, NI, UK*

email: `Beibei.yao@smcebi.edu.pl`

Ionic liquids (ILs), remarkable for their compositional versatility, reveal considerable potential as multifunctional materials in diverse fields such as energy storage, catalysis, and biotechnology. In particular, ILs have emerged as promising electrolyte candidates for lithium-ion batteries. Here, we reported three amphiphilic ILs exhibiting liquid-liquid phase transition (LLT) as the first example of conductivity independent from viscosity in neat aprotic ILs. As one of the most intriguing physical phenomena, LLT between two distinct phases of singlecomponent material enriches the physiochemical properties of the system. By performing the broadband dielectric spectroscopy (BDS) and rheological measurements on the examined ILs containing the tetra(alkyl)phosphonium cation and different anions, i.e., thiocyanate $[SCN]^-$, dicyanamide $[DCA]^-$, and tricyanomethanide $[TCM]^-$, we found that charge transport of all three ILs is viscosity-controlled at high temperatures (in liquid 1 phase); however, ion diffusion is much faster than structural dynamics in supercooled liquid 2 state. In other words, through LLT, the time scale of ion diffusion (τ_σ) and structural dynamics (τ_α) start to decouple, which is shown in Fig. 1. The decoupling phenomenon can be detected by isobaric cooling and isothermal compression. Furthermore, highpressure dielectric measurements reveal a nonmonotonic behavior of the decoupling in the case of small anions, indicating different decoupling degrees for different anion sizes. Finally, the volume fluctuation accompanying LLT has been calculated using the Clausius-Clapeyron equation. Our findings present a novel perspective on the charge transport mechanism in aprotic ILs with the LLT phenomenon, thereby offering valuable insights for developing high-quality electrolytes and innovative design strategies.

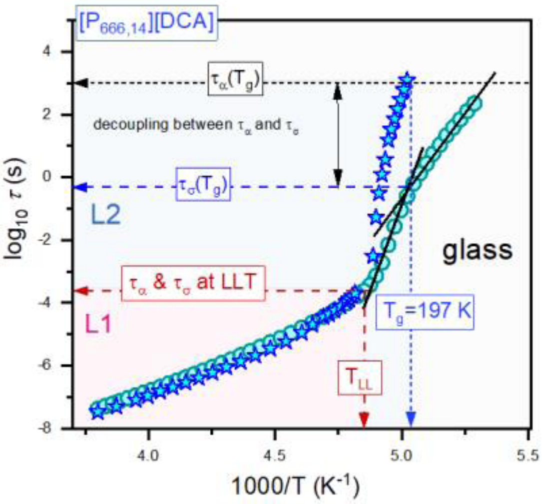

Figure 1: Direct comparison between conductivity relaxation time τ_σ (circles) obtained from BDS and structural relaxation time τ_α determined from rheology (stars) as a function of temperature for $[P_{666,14}][DCA]$.

Acknowledgements: This research was funded in whole by National Science Centre, Poland [Opus 21, 2021/41/B/ST5/00840].

SESSION VI: MULTIFERROIC

15:00	**Franco Di Rino** (France) Surface tension assisted polar phases in one-dimensional ferroelectrics	p. 40
15:15	**Anna Szeremeta** (Poland) The electrical properties of bismuth manganite -– lead titanate – epoxy composite	p. 41
15:30	**Tina Tasheva** (Bulgaria) Structural characterization and magnetic properties of glass-ceramics with high iron oxide concentration	p. 42
15:45	**Leo Boron** (France) Topological polar phases in ferroelectric nanowires	p. 43

CONTRIBUTED TALK, TUE./15:00

Surface tension assisted polar phases in one-dimensional ferroelectrics

F. Di Rino[1,2], L. Boron[1], S. Kondovych[3], M. Pavlenko[1], and Y. Tikhonov[1]

[1]*Laboratoire de Physique de la Matière Condensée, Université de Picardie, 80080 Amiens, France*
[2]*Instituto de Física Rosario, CONICET-Universidad Nacional de Rosario, Rosario 2000, Argentina*
[3]*Institute for Theoretical Solid State Physics, IFW Dresden, 01069 Dresden, Germany*

email: `dirino@ifir-conicet.gov.ar`

Ferroelectric materials possess unique dielectric, ferroelastic, and piezoelectric properties, bringing about novel functionalities at the nanoscale. Recent advances in the study of nanosized ferroelectric systems have unveiled new topological excitations, challenging our notion of the uniformity of the polar ground state. However, there is still a significant effort underway to comprehensively understand the polar structures in ferroelectrics.

Thermodynamic properties of uniform polarization states in one-dimensional nanostructures have been extensively investigated [1, 2]. At the same time, recent studies have demonstrated the emergence of unconventional topological states such as vortex and helix states [3, 4] in ferroelectric 1-D systems. However, there is still a lack of understanding regarding the underlying causes of their occurrence.

In this study, we examined $PbTiO_3$ nanowires of different sizes, chosen as a representative ferroelectric material, using the atomistic second-principles approach combined with the Ginzburg- Landau-Devonshire (GLD) model and the phase-field method. Our investigations utilizing the core-shell model in free-standing configurations revealed a strong size effect on the resulting polar texture. This dependency can be attributed to the influence of surface tension, which not only manifests laterally through Laplace pressure but also longitudinally.

To gain a deeper understanding, we adapted the GLD functional by incorporating the surface energy term. By employing both simulation techniques in line with analytical calculations, we constructed a radius-temperature phase diagram, which demonstrated a good agreement of methods. We identified two polar phases: the vortex phase, characterized by swirling polarization around the nanowire's caxis, and the uniform c-phase. At low temperatures, the predominant polar state in small particles was observed to be the vortex phase, transitioning to the uniform c-phase beyond a critical size.

The demonstrated tunability of properties makes one-dimensional ferroelectrics applicable for the realization of advanced ferroelectric-based device components, such as multilevel logic units [5, 6] or neuromorphic computing circuits [7]. In particular, the targeted design of nanowires with account of surface tension allows to achieve desirable range of functionalities already at the production stage and ensure the further efficient implementation into nanoelectronic devices.

Acknowledgements: We thank our colleagues and co-authors, Marcelo Sepliarsky, Anais Sene, Anna Razumnaya, and Igor Lukyanchuk who also participated in the presented calculations. The work was supported by H2020-MSCA programs, ITN-MANIC, RISE-MELON and CONICET (No. PUE-IFIR 2017-2022 N0076).

[1] W. Ma *et al.*, Appl. Phys. A, 96 (2009) 915
[2] J. Wang *et al.*, Phys. Rev. B, 91 (2015) 125432
[3] I.I. Naumov *et al.*, Nature, 432 (2004) 737
[4] M. Pavlenko *et al.*, Crystals, 12 (2022) 453
[5] L. Baundry *et al.*, Sci. Rep., 7 (2017) 42196
[6] A. Razumnaya *et al.*, Neuromorph. Comput. Eng., 3 (2023) 024003
[7] S. Oh *et al.*, APL Mater., 7 (2019) 091109

Contributed talk, Tue./15:15

The electrical properties of bismuth manganite – lead titanate – epoxy composite

A. Z. Szeremeta[1], A. Nowok[4], M. Zubko[2,3], S. Pawlus[1], I. Gruszka[1], J. Koperski[1], and A. Molak[1]

[1] *August Chełkowski Institute of Physics, University of Silesia in Katowice, ul. 75 Pułku Piechoty 1, 41-500 Chorzów, Poland*
[2] *Institute of Materials Engineering, University of Silesia in Katowice, ul. 75 Pułku Piechoty 1, 41-500 Chorzów, Poland*
[3] *Department of Physics, Faculty of Science, University of Hradec Králové, Hradec Králové, Czech Republic*
[4] *Department of Experimental Physics, Wrocław University of Science and Technology, Wybrzeże Wyspiańskiego 27, 50-370, Wrocław, Poland*

email: `anna.szeremeta@us.edu.pl`

Composite is defined as two- or multi-component material, the building blocks of which are mixed together [1]. Compared to ceramics, composites are characterized by higher electric strength and easier processing at low temperatures [2]. Hence, they help produce batteries, sensors, and electronic devices.

In our studies, we showed the electrical features of a new sintered 0.88 BM–0.12 PT ceramics and its organic-inorganic composite by using several interdisciplinary methods: X-ray diffraction, scanning electron microscopy, and broadband dielectric spectroscopy over a wide temperature and pressure ranges. We focus on dielectric losses – an essential parameter for materials applicable in the electronics sector. In this respect, we present two paths possibilities of decrease its: application of hydrostatic pressure and preparing the composite from ceramics powder and organic matrix. We showed the high sensitivity of the studied ceramics in terms of its electrical properties to pressure changes, which making this material attractive for application in micro-electromechanical sensors. Furthermore, we found that surprisingly the changes caused by embedding the inorganic material in the organic matrix and applying high hydrostatic pressure on the ceramics are similar. Hence, we show the utility of high-pressure dielectric studies of bulk inorganics to foresee their behavior in composite materials. Finally, we showed that the introduction of structural disorder in the inorganic material increases its electrical order. The interfacial stresses in the composite are proved not to destroy the electrical ordering in the crystal lattice.

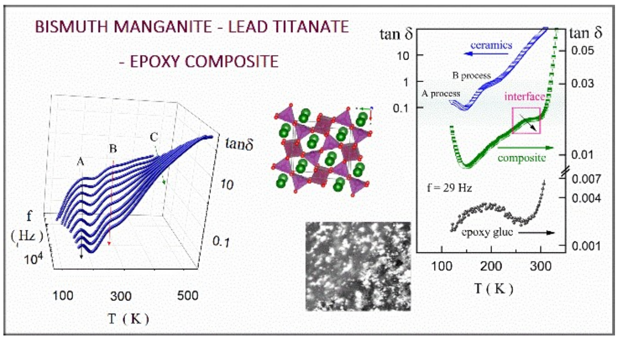

[1] R.M. Jones, Mechanics of Composite Materials, 2nd ed., Taylor & Francis: Blacksburg, Virginia, 1984
[2] A. Soulintzis *et al.*, J. Polym. Sci. Part B Polym. Phys., 47 (2009) 445

Contributed talk, Tue./15:30

Structural characterization and magnetic properties of glass-ceramics with high iron oxide concentration

T. Tasheva[1], R. Harizanova[1], I. Mihailova[1], Z. Cherkezova-Zheleva[2], D. Paneva[2], M. Georgieva[3], D. Tzankov[3], G. Avdeev[4], and C. Rüssel[5]

[1] *University of Chemical Technology and Metallurgy, Sofia, Bulgaria*
[2] *Institute of Catalysis, Bulgarian Academy of Sciences, Sofia, Bulgaria*
[3] *University of Sofia, Faculty of Physics, Sofia, Bulgaria*
[4] *Institute of Physical Chemistry "Rostislaw Kaischew", Bulgarian Academy of Sciences, Sofia, Bulgaria*
[5] *Otto Schott Institute of Materials Research, University of Jena, Jena, Germany*

email: `tina.tasheva@uctm.edu`

Magnetic glass-ceramic materials containing iron oxides attract the attention of the scientific community due to various possible applications such as magnetic storage devices, biodetection, contrast agents, magnetic hyperthermia, etc.

The glass-ceramics in the system Na_2O-CaO-SiO_2-Fe_2O_3, containing 20, 25 and 30 mol% Fe_2O_3, have been investigated. These materials are synthesized by applying a traditional melt-quenching technique in air ambient. The high iron oxide concentrations stimulate the spontaneous crystallization of the melt while pouring and quenching them. Thus, the main goal of the performed investigation is to establish the relation among the chemical and phase composition, microstructure, redox-ratio and magnetic properties of the obtained glass-ceramics.

In all samples the crystallization of magnetite (Fe_3O_4) and hematite (α-Fe_2O_3) is detected by X-ray diffraction, XRD analysis while in the sample with 25 mol% Fe_2O_3 an additional phase occurs whose structure corresponds to ε-Fe_2O_3. The volume fraction of the precipitated crystalline phase varies from 2 to 17 wt% and increases with increasing Fe_2O_3 concentration. The investigation of the microstructure of the glass-ceramics by Scanning Electron Microscopy, SEM reveals that the typical morphology of the occurring crystals corresponds to needles aggregates and dendrites with varying sizes. The information on the chemical compositions of the crystalline phases supplied by energy dispersive X-ray spectroscopy, EDS confirms that these are iron oxide containing ones.

The data from Mössbauer spectroscopy renders information on the coordination and oxidation state of Fe ions in the glass and in the occuring crystalline phases and confirms the findings of the XRD and EDS about the phase composition. Furthermore, it reveals the distribution of the Fe ions at the various crystallographic positions in the respective crystalline phases, i.e., magnetite, hematite and ε-Fe_2O_3. The Mössbauer spectra deconvolution suggests both octahedral and tetrahedral coordinations for the Fe^{3+} ions while Fe^{2+} is present in octahedral coordination in the amoprhous phase. The estimated ratio Fe^{3+}_{tetra} / Fe^{3+}_{octa} changes from approximately 3 to about 8 with increasing iron oxide concentration from 20 to 30 mol% and consequently, with increasing Fe-oxide concentration, ferric ions prefer to occupy tetrahedral positions.

Magnetic measurements at room temperature confirm the ferromagnetic nature with well defined hysteresis curves of the glass-ceramics containing 25 and 30 mol% Fe_2O_3.

Acknowledgements: This work is financially supported by contract KP-06-N48/4 with the Bulgarian National Science Fund.

Contributed talk, Tue./15:45

Topological polar phases in ferroelectric nanowires

L. Boron[1], M. Pavlenko[1], Yu. Tikhonov[1], and F. Di Rino[1,2]

[1] *Laboratoire de Physique de la Matière Condensée, Université de Picardie, 80080 Amiens, France*
[2] *Instituto de Fisica Rosario, CONICET-Universidad Nacional de Rosario, Rosario 2000, Argentina*

email: `leo.boron@u-picardie.fr`

Ferroelectric materials manifest unique dielectric, ferroelastic, and piezoelectric properties. In the past decade, some new topological states have been discovered in nanoscale ferroelectrics, turning the prevailing view that the polar ground state in these materials is uniform. However, the systematic understanding of the topological polar structures in ferroelectrics is still on track.

In two-dimensional and quasi-two-dimensional ferroelectric thin films and superlattices there is a variety of topological excitations such as soft domains [1], vortices [2], skyrmions [3], and merons [4] that are now understood reasonably well. Compared with these systems, quasi-one-dimensional ferroelectric nanowires are investigated to a much lesser extent and restricted mostly to general issues of the thermodynamic properties of the uniform polarization states [5–8]. Altghough the possibility of the emergence of unconventional topological vortex states in elongated nanorods was realized already in the early work on nanoscale ferroelectrics [9], only a few studies considered these states systematically [10–12]. In particular, the important practical aspects of operations with the different topological states remain underexplored.

Here we develop a general approach for describing ferroelectrics based on the Ginzburg-Landau-Devonshire model, combined with the phase field method to carry out the numerical calculations. $PbTiO_3$ loaded nanowires were studied, as an exemplary ferroelectric material, and a variety of the topological polarization states were revealed. This allows the construction of the strain–temperature phase diagram. Three polar phases were discovered: the vortex state (v phase) with polarization swirling around the nanowire c axis; the helical state (h phase), with the polarization screwing along the c axis; and the uniform polarization state extending along the c axis (c phase). We provide an overview of the unique physical properties of these states that are suitable for applications. In particular, the h phase hosts the spontaneously broken polarization chirality, easily tunable by the applied strain and temperature. This property of tunable chirality is of prime importance for optoelectronics and quantum communication technologies and does not have natural analogs. Additionally, the switching between different states can be implemented for a multilevel logic element in non von-Neumann computing circuits.

Acknowledgements: We thank our colleagues and co-authors, Svitlana Kondovych, Anais Sene, Anna Razumnaya, Marcelo Sepliarsky and Igor Lukyanchuk who also participated in the presented calculations. The work was supported by H2020-MSCA programs, ITN-MANIC and RISE-MELON.

[1] V.A.) Stephanovich *et al.*, Phys. Rev. Lett., 94 (2005) 047601
[2] A. Yadav *et al.*, Nature, 530 (2016) 198
[3] S. Das *et al.*, Nature, 568 (2019) 368
[4] Y. Wang *et al.*, Nat. Mater., 19 (2020) 881
[5] A.N. Morozovska *et al.*, Phys. Rev. B, 73 (2006) 214106
[6] A.N. Morozovska *et al.*, Phys. Rev. B, 76 (2007) 014102
[7] W. Ma *et al.*, Appl. Phys. A, 96 (2009) 915
[8] J. Wang *et al.*, Phys. Rev. B, 91 (2015) 125432
[9] I.I. Naumov *et al.*, Nature, 432 (2004) 737
[10] L. Lahoche *et al.*, Integr. Ferroelectr., 99 (2008) 60
[11] Z. Liu *et al.*, Phys. Rev. Appl., 8 (2017) 034014
[12] A.N. Morozovska *et al.*, Phys. Rev. B, No. (year) page

SESSION VII: SPECTROSCOPIC AND DIFFRACTION METHODS

09:00	**Rikumaru Saito** (Japan) ^{13}C NMR study on π-d interaction system, λ-$(BEST)_2$FeCl$_4$	p. 45
09:15	**N. S. Dhami** (Croatia) High-Pressure studies on non-centrosymmetric EuTGe$_3$ (T= Co, Rh and Ir) Materials	p. 46
09:30	**Oleksandr Tomchuk** (Poland) Neutron scattering study of LC ordering in cylindrical mesopores	p. 47
09:45	**Tsunehisa Kihara** (Japan) Low Temperature Crystal Structure of $\beta" - (BEDT - TTF)_2Hg(SCN)_2Cl$	p. 48
10:00	**Aleksandr Bamburov** (Portugal) Intolerance of Ruddlesden-Popper $La_2NiO_{4\pm\delta}$ structure to A-site cation deficiency	p. 49
10:15	**Andrius Pakalniškis** (Lithuania) Temperature Induced Magnetic and Crystal Structure Transition in Novel Sc doped Lutetium ferrite	p. 50
10:30	**Kinga Łucak** (Poland) The supramolecular structures in propanol and its halogen derivatives	p. 51

Contributed talk, Wed./9:00

^{13}C NMR study on π-d interaction system, λ-(BEST)$_2$FeCl$_4$

R. Saito[1], Y. Iida[1], T. Kobayashi[2], H. Taniguchi[2], S. Fukuoka[1], N. Matsunaga[1], and A. Kawamoto[1]

[1] *Hokkaido University, Sapporo, Japan*
[2] *Saitama University, Saitama, Japan*

email: `maruriku0702@eis.hokudai.ac.jp`

λ type salts are quasi-two-dimensional organic conductors, in which donor and anion layers are alternately stacked. Introducing Fe ions with S=5/2 into the anion layer causes π-d interactions between the π electrons in the donor layers and the localized 3d spins, and the interaction generates characteristic physical properties. λ-(BETS)$_2$FeCl$_4$, where BETS is bis(ethylenedithio)tetraselenafulvalene, is one of the molecular π-d systems. The compound undergoes an antiferromagnetic (AF) transition with a magnetic anisotropy [1]. Specific heat measurements reveled that the π electrons are ordered antiferromagnetically and 3d spins are passive under the exchange fields through the π-d interaction [2]. The π-d interaction plays an important role in the emergence of the magnetic anisotropy. In studying the role of the π-d interaction in Fe salts, comparison between Fe and Ga salts is informative, and λ type salts with the same ground state are desired. However, λ-(BETS)$_2$GaCl$_4$ exhibits a superconducting transition and cannot be a reference for λ-(BETS)$_2$FeCl$_4$ citeSaito-3.

Also, the estimation of $J_{\pi d}$ is important for understanding the π-d interaction. There are some NMR approaches to estimate $J_{\pi d}$. In the approaches, the correction by the demagnetization factor from the crystal outline is required. In the previous studies of λ-FeCl$_4$, the factor was calculated using the ellipsoid approximation on a thin rectangle outline with fixed dimensions because it is difficult to evaluate the factor experimentally [4, 5]. Hence, there is ambiguity in the estimation of $J_{\pi d}$.

We have focused on BEST salts, where BEST is bis(ethylenediseleno)tetrathiafulvalene, in order to resolve the two problems described above. ^{13}C NMR measurements on λ-(BETS)$_2$GaCl$_4$ showed that the AF transition occurred at 22 K.[6] Mössbauer measurements on λ-(BETS)$_2$FeCl$_4$ showed a development of the internal field on Fe sites below 26 K, and we concluded that the AF transition in donor layers occurred even in λ-(BETS)$_2$FeCl$_4$.[7] However, Mössbauer measurements focus on the Fe sites and are not suitable for investigating the magnetism on the π electron systems.

In this study, we performed ^{13}C NMR measurements on λ-(BETS)$_2$FeCl$_4$. The measurements can provide selectively information on the π electron systems. Figure 1 shows temperature dependence of nuclear spin-lattice relaxation rate $1/T_1$. $1/T_1$ shows a sharp peak at 25 K, indicating that λ-(BETS)$_2$FeCl$_4$ undergoes the AF transition in donor layers. We confirmed that BEST salts have the same ground state of the π electron systems. In addition, we evaluated $J_{\pi d}$ with the estimation of the demagnetization factor experimentally. In this conference, we will explain the results of ^{13}C NMR measurements in detail and discuss the estimation of $J_{\pi d}$.

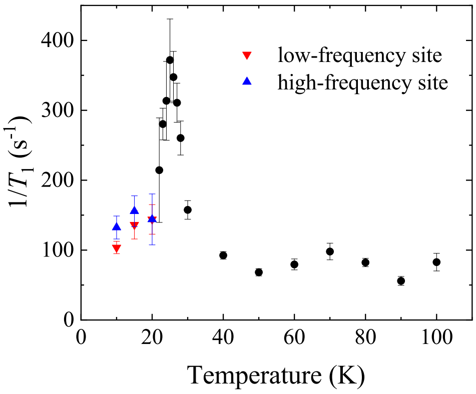

Figure 1: Temperature dependence of $1/T_1$.

Acknowledgements: This work was supported by JST SPRING, Grant Number JPMJSP2119.

[1] M. Tokumoto *et al.*, Synth. Met., 86 (1997) 2161.
[2] H. Akiba *et al.*, J. Phys. Soc. Jpn., 78 (2009) 033601
[3] A. Kobayashi *et al.*, Chem. Lett., 22 (1993) 2179
[4] K. Hiraki *et al.*, J. Phys. Soc. Jpn., 76 (2007) 124708
[5] S. Fukuoka *et al.*, Phys. Rev. B, 105 (2022) 124427
[6] A. Ito *et al.*, Phys. Rev. B, 106 (2022) 045114
[7] R. Saito *et al.*, Phys. Rev. B, 105 (2022) 165115

CONTRIBUTED TALK, WED./9:15

High-Pressure studies on non-centrosymmetric EuTGe$_3$ (T= Co, Rh and Ir) Materials

N. S. Dhami[1], V. Balédent[2], O. Bednarchuk[3], D. Kaczorowski[3], S. R. Shieh[4], J. M. Ablett[5], J.-P. Rueff[5,6], J. P. Itié[5], C. M. N. Kumar[1], P. Popčević[1], and Y. Utsumi[1]

[1] *Institute of Physics, Zagreb, Croatia*
[2] *Université Paris-Saclay, CNRS, Laboratoire de Physique des Solides, Orsay, France*
[3] *Institute of Low Temperature and Structure Research, Polish Academy of Sciences, Poland*
[4] *Department of Earth Sciences, Department of Physics and Astronomy, University of Western Ontario, Canada*
[5] *Synchrotron SOLEIL, Saint-Aubin, France*
[6] *Laboratoire de Chimie Physique-Matière et Rayonnement, Sorbonne Université, CNRS, Paris, France*

email: `nsdhami@ifs.hr`

Intermetallic EuTX_3 (T: transition metal, X= Si/Ge) forms a non-centrosymmetric BaNiSn$_3$-type structure (space group I4mm). It has been attracting considerable attention due to complex magnetic structures and unique pressure phase diagram that potentially accommodates superconductivity under pressure [1]. At ambient pressure, all EuTGe$_3$ series host divalent Eu ions ($4f^7$, J=7/2) and exhibit antiferromagnetic ordering at low temperatures ($<$ 15 K). In order to study the T-dependent pressure behavior of the electronic and crystal structures of EuTGe$_3$ (T= Co, Rh, Ir), we performed high energy resolution fluorescence detected x-ray absorption spectroscopy (XAS) and powder x-ray diffraction (XRD) as a function of pressure at the GALAXIES and PSICHE beamlines of SOLEIL Synchrotron. In all compounds, a prominent Eu^{2+} peak was observed in the Eu L_3 XAS spectra at ambient pressure. With increasing pressure, these spectra revealed a continuous change towards an intermediate Eu valence state. The mean Eu valence reached ~2.4 near 40 GPa in EuRhGe$_3$ [2], and ~2.5 and ~2.3 near 50 GPa in EuIrGe$_3$ and EuCoGe$_3$ [3], respectively. In the latter compound, the Ge K and Co K edge XAS spectra showed no remarkable changes against pressure [3]. The results of high-pressure powder XRD exhibited a smooth contraction of the lattice volume without any symmetry changes in EuRhGe$_3$ and $EuCoGe_3$. While the result of EuIrGe$_3$ indicated a pressure-induced structural transition around 34 GPa. Our study revealed the pressure evolution of Eu valence and crystal structure of EuTGe$_3$. In the talk, pressure responses of Eu valence and crystal structure in EuTGe$_3$ arising from different nature among 3d, 4d, and 5d transition metal ions will be discussed, and our recent progress in electrical resistivity measurement under pressure will be presented as well.

Acknowledgements: The work is supported by the Croatian Science Foundation project numbers UIP-2019-04-2154 and IP-2020-02-9666 and by project from the Cryogenic Centre at the Institute of Physics—KaCIF (Grant No. KK.01.1.1.02.0012), co-financed by the Croatian Government and the European Union through the European Regional Development Fund— Competitiveness and Cohesion Operational Programme.

[1] M. Nakashima *et al.*, J. Phys. Soc. Jpn., 86 (2017) 034708
[2] Y. Utsumi *et al.*, Electron. Struct., 3 (2021) 034002
[3] N. S. Dhami *et al.*, Phys. Rev. B., 107 (2023) 155119

Contributed talk, Wed./9:30

Neutron scattering study of LC ordering in cylindrical mesopores

O. Tomchuk[1,2], A. Drzewicz[1], W. Zając[1], E. Juszyńska-Gałązka[1,3], A. Len[4,5], and V. Ryukhtin[6]

[1] *Henryk Niewodniczański Institute of Nuclear Physics, PAS, Kraków, Poland*
[2] *Taras Shevchenko National University of Kyiv, Kyiv, Ukraine*
[3] *Osaka University, Osaka, Japan*
[4] *Centre for Energy Research, Budapest, Hungary*
[5] *University of Pécs, Pécs, Hungary*
[6] *Nuclear Physics Institute, ASCR, v.v.i., Řež, Czechia*

email: `oleksandr.tomchuk@ifj.edu.pl`

In recent years, there has been growing research interest in studying the behavior of liquid crystals when confined in porous materials, such as porous glasses, porous silica, or Anodic Aluminium Oxide (AAO). This confinement, ranging from micro pores to mesopores (2-50nm), offers unique sample environment conditions not available in bulk specimens. By using mesoporous matrices, researchers can explore the boundary layer of the sample, which exhibits both homogeneous intermolecular interactions within the sample and heterogeneous sample-container interactions.[1] This spatial confinement also allows for control over the volume available to the liquid crystal molecules resulting in extended free intermolecular volume due to steric hindrance.

In this study, we have applied small-angle neutron scattering (SANS) to analyze the ordering in cylindrical pores in an AAO matrix over a wide range of sizes for some partially fluorinated liquid crystals. Additionally, ultra-SANS (USANS) was used to cover the submicron size scale. The results testify in favor of the paranematic ordering of liquid crystal molecules at the periphery of mesosized pores, while no effect is observed for 200 nm pores.

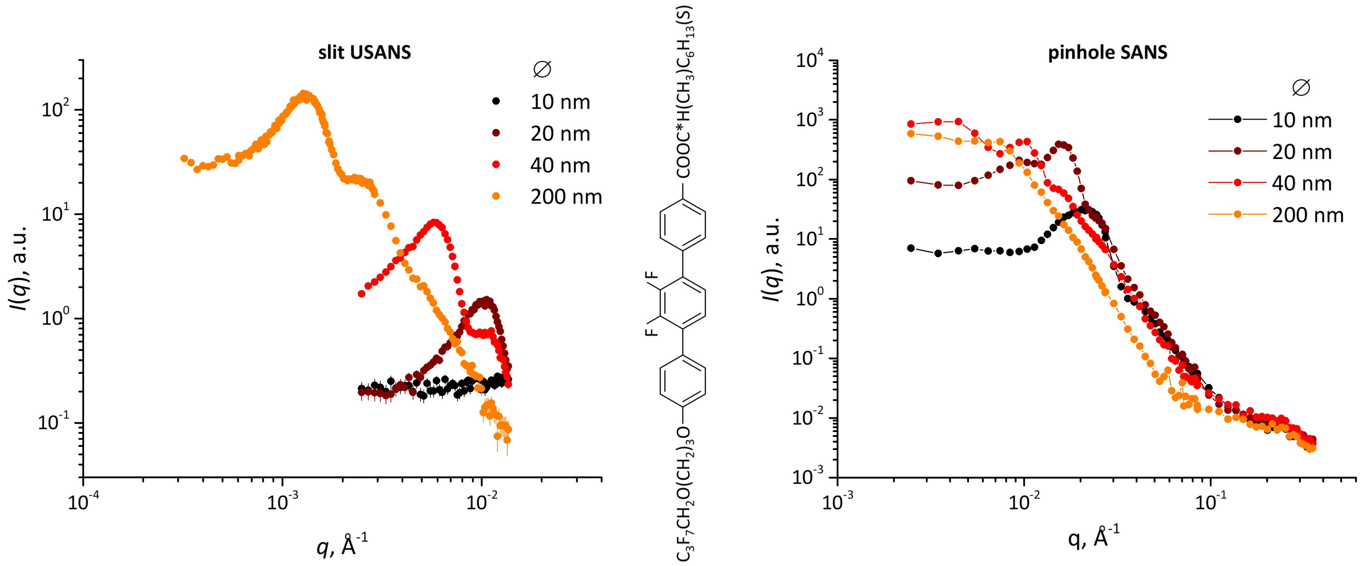

Figure 1: USANS (left) and SANS (right) from LC (middle panel) in nanopores depending on pore mean diameter.

Acknowledgements: The USANS measurements at the NPI ASCR were performed using the CANAM infrastructure (MAUD ultra-small-angle diffractometer). The SANS experiments carried-out at the Yellow Submarine instrument (Budapest Neutron Centre) are also gratefully acknowledged. O.T. acknowledges financial support from the National Science Centre of Poland (grant no. 2022/06/X/ST3/01208).

[1] E. Juszyńska-Gałązka *et al.*, Phase Transit., 96 (2023) 89

CONTRIBUTED TALK, WED./9:45

Low Temperature Crystal Structure of β"-(BEDT-TTF)$_2$Hg(SCN)$_2$Cl

T. Kihara[1], R. Saito[1], T. Kobayashi[2], H. Taniguchi[2], S. Fukuoka[1], and A. Kawamoto[1]

[1]*Hokkaido University, Sapporo, Japan*
[2]*Saitama University, Saitama, Japan*

email: `ekurea8721@eis.hokudai.ac.jp`

β"-(BEDT-TTF)$_2$Hg(SCN)$_2$Cl is a quasi-two-dimensional organic conductor. BEDT-TTF molecules form conducting layers and anion components of (Hg(SCN)$_2$ Cl$^-$) form insulating layers, and they stacked alternately. β”-type salts have been intensively studied from the viewpoint of the superconducting mechanism caused by charge fluctuations.

At ambient pressure, the electrical resistivity of β"-(BEDT-TTF)$_2$Hg(SCN)$_2$Cl shows metallic behavior down to 150 K. The electrical resistivity became minimum at T_m=150 K. With further decreasing temperatures, semiconducting behavior was observed from 150 to 72 K. Below 72 K, the resistivity showed a steep increase, suggesting that the metal-insulator transition occurred.[1] The optical conductivity spectra by infrared spectroscopy revealed that a broad peak was observed at room temperature. Upon cooling, it split into double peaks around 100 K. Below 72 K, the double peaks split into four well-distinct peaks. It can be inferred that a doubling of the lattice or a disappearance of inversion symmetry from P-1 to P1 at T_{CO}=72 K. This study aims to get the information of structural charge at Tm and T_{CO} and reveal the crystal structure below T_{CO} of β"-(BEDT-TTF)$_2$Hg(SCN)$_2$Cl by x-ray structural analysis.

In this study, we performed X-ray structural analysis on a single crystal of β"-(BEDT-TTF)$_2$Hg(SCN)$_2$Cl from room-temperature to 25 K using HyPix-AFC in Institute for Molecular Science and in Research Institute for Electronic Science Hokkaido University. The crystal structure was solved by CryAlis(Pro) and Olex2. Figure 1 shows the temperature dependence of the lattice parameters in the temperature range 287 K to 15 K. At around T_{CO}=72 K, no significant change in the lattice constant can be observed, and superlattice reflections due to the lattice doubling have not been observed, suggesting that below the T_{CO} temperature, the inversion symmetry is broken with the space group change from P-1 to P1. Furthermore, we solved the crystal structure at 30K with P1 symmetry, and estimated the charges on the molecules from the interatomic distances.[2]

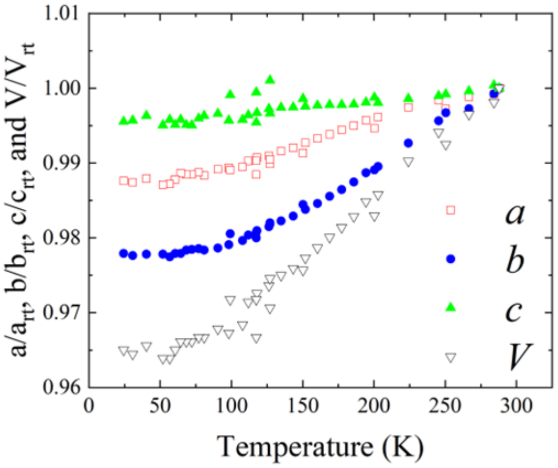

Figure 1: The temperature dependence of the lattice parameters

[1] W. Li *et al.*, J. Chem. Phys., 147 (2017) 064503
[2] P. Guionneau *et al.*, Synthetic Metals, 86 (1997) 1973

Contributed talk, Wed./10:00

Intolerance of Ruddlesden-Popper $La_2NiO_{4\pm\delta}$ structure to A-site cation deficiency

A. D. Bamburov[1], E. N. Naumovich[2,3], D. D. Khalyavin[4], and A. A. Yaremchenko[1]

[1] *CICECO – Aveiro Institute of Materials, Department of Materials and Ceramic Engineering, University of Aveiro, Aveiro, Portugal*
[2] *Institute of Power Engineering, Department of High Temperature Electrochemical Processes, Warsaw, Poland*
[3] *CTH2 - Center for Hydrogen Technologies, Institute of Power Engineering, Augustowka 36, Warsaw, Poland*
[4] *ISIS Facility, Rutherford Appleton Laboratory, Harwell Oxford, Didcot, UK*

email: `aleksandr.bamburov@ua.pt`

Mixed ionic-electronic conductors derived from Ruddlesden-Popper $Ln_2NiO_{4+\delta}$ ($Ln =$ La, Pr, Nd) attract significant attention as oxygen electrode materials for solid oxide fuel and electrolysis cells. However, literature data on the impact of A-site deficiency on the phase relationships and functional properties of $Ln_2NiO_{4+\delta}$-based phases are contradictory. While some works report an accommodation of A-site vacancies up to x = 0.15 in $La_{2-x}NiO_{4\pm\delta}$, others indicate difficulties in the synthesis of single-phase $La_{2-x}NiO_{4+\delta}$ even for low x values. The present work explores the impact of the nominal A-site deficiency on the phase composition and electrical transport properties of $La_{2-x}NiO_{4\pm\delta}$ ceramics.

Ceramics with the nominal composition $La_{2-x}NiO_{4\pm\delta}$ (x = 0, 0.02, 0.05, 0.10) were synthesized by the glycine-nitrate technique and sintered at 1350-1450°C. While XRD analysis suggested the formation of single-phase materials with orthorhombic K_2NiF_4-type structure, the lattice parameters remained independent of composition within the experimental uncertainty. Neutron diffraction studies of x = 0 and 0.05 samples revealed that the lattice parameters, La:Ni atomic ratio (2:1) and oxygen sites occupancy remain identical for both samples, while the presence of impurity NiO phase (0.4 wt.%) was detected for $La_{1.95}NiO_{4\pm\delta}$. SEM/EDS inspection of ceramic samples confirmed the presence of nickel-rich inclusions for $x \geq 0.02$, which could not be eliminated by increasing the temperature and time of sintering. The volume fraction of inclusions increased with x. The experimental observations are supported by the atomistic simulations showing that the coexistence of cation-stoichiometric $La_2NiO_{4+\delta}$ with nickel-rich $La_4Ni_3O_{10}$ or NiO is more favorable compared to cation-deficient $La_{1.95}NiO_{4\pm\delta}$. Molecular dynamics simulations of $La_{1.95}NiO_{4\pm\delta}$ lattice demonstrated that the introduction of La vacancies leads formation of instability zone in the rock-salt-type layer and destabilization of the crystal lattice. The intolerance of $La_2NiO_{4+\delta}$ lattice to A-site vacancies and coexistence of $La_2NiO_{4+\delta}$ with traces of Ni-rich secondary phase in the samples with the nominal composition $La_{2-x}NiO_{4\pm\delta}$ results in an insignificant variation of electrical transport properties with x.

Acknowledgements: This work was developed within the scope of the project CARBOSTEAM (POCI-01-0145-FEDER-032295) funded by FEDER through COMPETE2020 - Programa Operacional Competitividade e Internacionalizacao (POCI) and by national funds through FCT/MCTES, and the project CICECO-Aveiro Institute of Materials (UIDB/50011/2020, UIDP/50011/2020 & LA/P/0006/2020) financed by national funds through the FCT/MCTES (PIDDAC). A.B. acknowledges the PhD scholarship by the FCT (grant SFRH/BD/150704/2020).

CONTRIBUTED TALK, WED./10:15

Temperature Induced Magnetic and Crystal Structure Transition in Novel Sc doped Lutetium ferrite

A. Pakalniškis[1], G. Niaura[2], D. Karpinsky[3], G. Rogez[4], P. Rabu[4], S. Chen[5,6], T. C. Yang[5,6], R. Skaudžius[1], and A. Kareiva[1]

[1] *Institute of Chemistry, Vilnius University, Vilnius, Lithuania*
[2] *Department of Organic Chemistry, Center for Physical Sciences and Technology (FTMC), Vilnius, Lithuania*
[3] *Namangan Engineering-Construction Institute Namangan, Uzbekistan*
[4] *IPCMS, Strasbourg, France*
[5] *Precision Analysis and Materials Research Center, National Taipei University of Technology, Taipei, Taiwan*
[6] *Department of Chemical Engineering and Biotechnology, National Taipei University of Technology, Taipei Taiwan*

email: `andrius.pakalniskis@chgf.vu.lt`

Complex oxides are a group of materials that based on their crystal structure, elemental composition, and preparation method can obtain a wide variety of different properties. However, nowadays the requirements for practical applications of such compounds are more demanding than ever before. One such area of development involves combining sever different properties in one material. The most famous class of such materials is referred to as multiferroic. For a compound to be multiferroic it has to possess at least two of the primary ferroic orders. While the application of multiferroic compounds would be quite vast, there are still severe problems that they are currently facing. Firstly, the electrical and magnetic orders arise from opposing electronic structures. Since magnetic properties usually require the 3d layer to be partially filled by electrons, electrical properties arise from empty 3d orbital hybridization. While this is still an issue, currently there are several ferroelectricity mechanisms known that do not help bypass this problem. Such as lone pair and spin-driven mechanisms, that do not require empty electron shells.[1] The second issue is that in most cases these orderings only coexist at temperatures drastically below room temperature, thus hindering the applicability. Lastly, even if the desired magnetic and electric properties are maintained at room temperature the so-called multiferroic coupling is often too weak for application purposes. While most research has focused on a model-type multiferroic $BiFeO_3$, a new promising hexagonal variant of $LuFeO_3$ has recently attracted a lot of attention in this field. It should be noted, that the preparation of hexagonal compounds is quite difficult and the crystal structure can be modified either using the chemical substitution or via preparing the compounds in the form of thin films as the crystal lattice is unstable and tends to form an orthorhombic structure.[2, 3]

As such we provide insights into stabilizing the hexagonal structure in doped $LuFeO_3$ prepared using aqueous sol-gel synthesis procedure. While also providing further clarification on the concentration ranges of the different structural phases present in the system and analyzed using SEM, room temperature X-ray diffraction techniques, and Raman spectroscopy. We also investigate temperature driven polar to nonpolar transitions through temperature-dependent X-ray diffraction. Lastly, we provide additional insight into the magnetic structure and its changes at low and room temperatures.

Acknowledgements: This project has received funding from the European Union's Horizon 2020 research and innovation programme under the Marie Skłodowska-Curie grant agreement No 778070 – TransFerr – H2020-MSCA-RISE-2017.

[1] M. Kumar *et al.*, Mater. Lett., 277 (2020) 128369
[2] J. Luxová *et al.*, J. Therm. Anal. Calorim., 138 (2019) 4303
[3] L. Zhang *et al.*, Solid State Commun., 149 (2009) 1317

Contributed talk, Wed./10:30

The supramolecular structures in propanol and its halogen derivatives

K. Łucak[1], A. Z. Szeremeta[1], and S. Pawlus[1]

[1]*Institute of Physics, Faculty of Science and Technology, University of Silesia in Katowice, 75 Pułku Piechoty 1, 41-500 Chorzów, Poland*

email: `kinga.lucak@us.edu.pl`

Monohydroxy alcohols (MAs) uniquely form various supramolecular clusters through hydrogen bonds (HBs). This phenomenon is commonly observed in dielectric measurements as an exponential response function - called Debye (D) relaxation. MAs are also distinguished by faster α – relaxation. [1] Chemical modifications of MAs lead to different patterns of association. Depending on the terminal or non-terminal position of the OH group attached to the alkyl chain, these structures can be chain-like or ring-like. The attached functional group, e.g., a phenyl group (devoid of the dipole moment), behaves as a steric hindrance preventing the formation of effective HBs. It inhibits the self-association phenomenon and unifies the time scales of the α and D processes. [2]

Surprisingly, much less is done on the systems where an additional dipole moment comparable to the one generated by the hydroxyl moiety is introduced to the structure. As shown in Fig. 1, adding Cl, Br, and I atoms into the molecule structure of propanol influences the intensity of both relaxations. Introducing an atom of high electronegativity to the molecule causes additional dipole-dipole halogen-halogen interactions as well as halogen-based HBs that may compete with the “classical” HBs. The question arises as to how much adding these large atoms affect the sizes and architectures of supramolecular structures and their local molecular order? We will try to answer these questions based on our recent studies of propanol and its halogen derivatives.

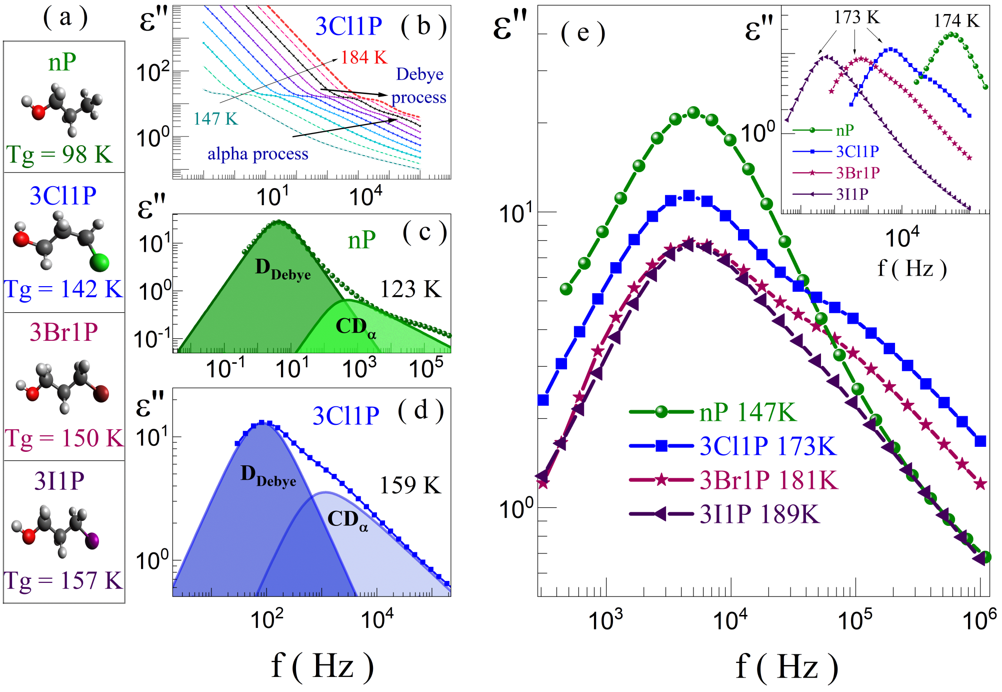

Figure 1: Molecular structure models and glass transition temperatures of the studied alcohols: nP, 3Cl1P, 3Br1P, and 3I1P (a). Dielectric loss spectra for 3Cl1P (b). Dielectric loss spectrum for: nP at 123 K (c) and 3Cl1P (d) at 159 K obtained after subtraction of dc-conductivity. The respective solid lines are the results of fitting with the use of the Debye and Cole-Davidson functions. Comparison of the D process characterized by the same relaxation times for all studied alcohols (e). The inset shows the dielectric loss spectra after subtraction of conductivity.

[1] R. Böhmer *et al.*, Phys. Rep., 545 (2014) 125
[2] A. Nowak *et al.*, J. Phys. Chem. Lett., 12 (2021) 2142

SESSION VIII: MISCELLANY

11:15	**Mohammad Sadegh Shakeri** (Poland) Synthesis of $CuFe_2O_4$-Cu_2O composite using pulsed laser irradiation of cupric-magnetite-ethanol suspension for photocatalysis application, experimental and DFT calculation approaches	p. 53
11:30	**Samuel Diaz Escribano** (Israel) Semiconductor-Superconductor-Ferromagnetic Heterostructure as a Platform for Topological Superconductivity	p. 54
11:45	**Dimitrios Tzitzilis** (Greece) Wenzel-to-Cassie transition on lubricant-impregnated surfaces	p. 55
12:00	**Yousra El Fannassi** (France) Microencapsulation of a water-soluble ruthenium (II) complex derived from limonene as an effective tool against pathogenic bacterial biofilms	p. 56
12:15	**Rui Pinto** (Portugal) Characterization and Performance Evaluation of $PrVO_y$-$CaVO_y$ Oxides for Solid Oxide Fuel Cells	p. 57
12:30	**Michał Adamek** (Poland) Synthesis and structural characterization of spherical silica nanoparticles with different diameters	p. 58

Contributed talk, Wed./11:15

Synthesis of $CuFe_2O_4$-Cu_2O composite using pulsed laser irradiation of cupric-magnetite-ethanol suspension for photocatalysis application, experimental and DFT calculation approaches

M. S. Shakeri[1] and Z. Swiatkowska-Warkocka[1]

[1] *Institute of Nuclear Physics Polish Academy of Sciences, PL-31342 Krakow, Poland*

email: `ms.shakeri@ifj.edu.pl`

In the last decade, low-energy nano-pulse lasers have been used to fabricate heterostructures by irradiating suspended nanoparticles. The final composition of the irradiated particles depends on several factors, mainly controlled by the laser and suspension parameters. [1] The mechanism of phase formation in pulsed laser irradiation of suspensions (PLIS) consists of a physical phase transition of the particles enabled by the absorption of laser energy and the chemical interaction at the interface between the heated sphere and the dissociated solvent (Figure 1). Here, we irradiated CuO and Fe_3O_4 nanoparticles suspended in ethanol with nanosecond pulses of a Nd:YAG laser with different fluences. The energy of the laser is sufficient to physically convert CuO into Cu_2O, while the released oxygen participates in the oxidation of ethanol. [2] On the other hand, some of the Fe atoms are replaced by Cu, resulting in copper ferrite as the second dominant phase in the structure. The final composition is $CuFe_2O_4$-Cu_2O, with both components known for their fabulous catalytic properties. We analyzed the oxidation states of the samples irradiated with different laser power using X-ray photoelectron spectroscopy (XPS) and X-ray absorption spectroscopy (XAS) methods to see how the laser energy affects the phase formation during PLIS. The structure of the resulting powders was examined using high resolution transmission electron microscopy (HRTEM) images to see the progress of phase formation. The absorption and fluorescence characteristics of the resulting powders were discussed in detail to describe the electronic structure of photocatalysis of drug degradation. In characterizing and analyzing the formation mechanism of PLIS, density functional theory (DFT) calculations were used as tools to support our experimental observations. We believe that our results are not only able to present a high-tech powder for photocatalyst applications, but also could be used by other scientists in this field to control the PLIS process for their desired heterostructure.

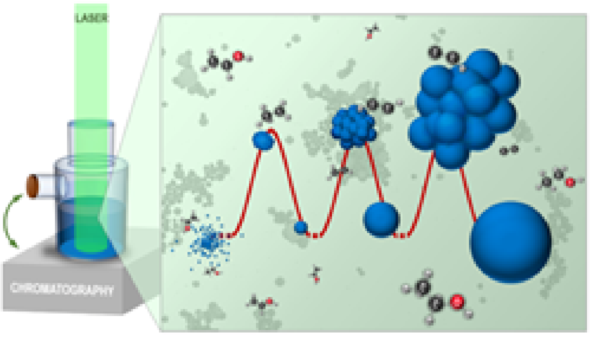

Figure 1: Schematic illustration of the mechanism of particle formation during pulsed laser irradiation of suspended nano-particles

Acknowledgements: This work is supported by the Polish National Science Center under Program No. 2022/06/X/ST3/01743. The calculations were performed in the Prometheus Cluster, Cyfronet, under grant number PLG/2022/015573. The XAS measurements were performed at the ELETRRA synchrotron center in Trieste, Italy, under application number 20232086. We thank the Polish National Synchrotron Center (SOLARIS) for providing the jfeff license to calculate the XAS spectra. We also thank Dr. Giuliana Aquilanti for her efforts in the XAS measurements.

[1] M. S. Shakeri *et al.*, Sci. Rep., 12 (2022) 11950
[2] M. S. Shakeri *et al.*, Submitted in: Adv. Mater., Under Review

Contributed talk, Wed./11:30

Semiconductor-Superconductor-Ferromagnetic Heterostructure as a Platform for Topological Superconductivity

S. D. Escribano[1], A. Maiani[2], M. Leijnse[3], K. Flensberg[2], Y. Oreg[1], A. L. Yeyati[4], E. Prada[5], and R. S. Souto[3]

[1] *Weizmann Institute of Science, Rehovot, Israel*
[2] *University of Copenhagen, Copenhagen, Denmark*
[3] *Lund University, Lund, Sweden*
[4] *Universidad Autónoma de Madrid, Madrid, Spain*
[5] *Instituto de Ciencia de los Materials (ICMM-CSIC), Madrid, Spain*

email: `samuel.diazes@gmail.com`

Hybrid structures [see Fig. 1(a)] comprising semiconducting (SM) nanowires, epitaxially grown superconductors (SC), and ferromagnetic-insulator (FI) layers have been experimentally and theoretically explored as alternative platforms for achieving topological superconductivity at zero magnetic field [1]. In this work [2], we analyze a tripartite SM/FI/SC heterostructure realized in a planar stacking geometry, where the thin FI layer acts as a spinpolarized barrier between the SM and the SC [see Fig. 1(b)]. We optimize the system's geometrical parameters using microscopic simulations to find the range of FI thicknesses for which the hybrid system can be tuned into a quasi-one-dimensional topological regime. Within this range, and due to the vertical confinement provided by the stacking geometry, trivial and topological phases alternate regularly as the external gate is varied, displaying a hard topological gap that can reach half of the SC gap. This represents a significant improvement compared to setups using hexagonal nanowires. Additionally, we propose a specific x-y pattern for the SC that would enable the development of a quasi-two-dimensional topological superconducting phase on this platform. Our results offer new possibilities for designing topological superconducting devices without the need for a magnetic field.

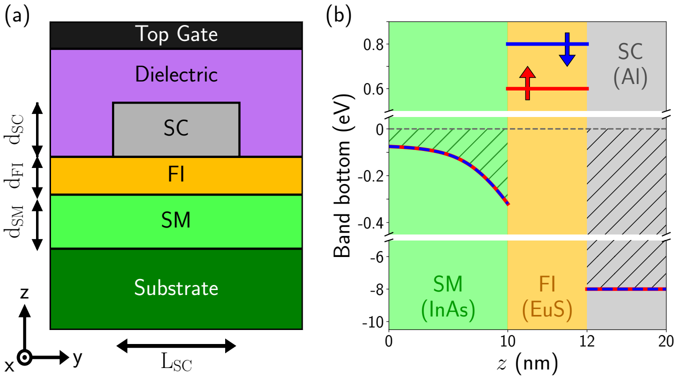

Figure 1: (a) Sketch of the device: 2D semiconductor (SM)/ferromagnetic insulator (FI)/superconductor (SC) heterostructure stacked in the z-direction. The top gate can be used to confine the wavefunction below the grounded SC. (b) Schematics of the conduction-band bottom along the heterostructure stacking direction for a specific choice of materials (InAs/EuS/Al). Red and blue colors represent different spin directions.

Acknowledgements: this work was supported by the Spanish Ministry of Economy and Competitiveness through Grant No. PCI2018-093026.

[1] S. Vaitiekėnas *et al.*, Nat. Phys., 17 (2022) 43
[2] S. D. Escribano *et al.*, npj Quantum Mater., 7 (2022) 81

Contributed talk, Wed./11:45

Wenzel-to-Cassie transition on lubricant-impregnated surfaces

D. Tzitzilis[1], I. Ntakoumis[1], C. Tsekeridis[1], and P. Papadopoulos[1]

[1] *University of Ioannina, Ioannina. Greece*

email: `phyuoi7698tzitzilis@gmail.com`

Lubricant impregnated surfaces (LIS) are microstructured surfaces impregnated with a low surface tension lubricant. They have shown great promise in various applications that require non-wettable superhydrophobic surfaces. These surfaces belong to the class of liquid-repellent and non-adhesive surfaces.

The present work aims to investigate the possibility of switching between Wenzel and Cassie states, through the injection of lubricant into microstructured hygrophobic surfaces. The "key" to the transition from Wenzel to Cassie is the change of the microscopic contact angle of the drops, which is due to the change in the environment of the drop, from air to another liquid which acts as a "lubricant". In addition, the role of the morphology of microstructured surfaces, the roughness and the surface tension of the lubricant-drop liquids in the realization or not of the aforementioned transition was studied.

To observe the Wenzel-Cassie transition of droplets on the microstructred we used a homemade laser scanning confocal microscopy (LSCM) in reflection interference mode. To calculate the interfacial surface tensions, we used an optical tensiometer. In this work we make numerical calculations of the shape of the droplet surface to study the geometrical limits within which the Wenzel-Cassie transition occurs. We minimize the Gibbs energy of the drop using the Steepest Descent algorithm and determine the deepest point more accurately than empirical relations.

The results of our measurements and calculations show that the transition of droplets from the Wenzel state to the Cassie state by lubricant injection is feasible and is favored on surfaces with large heights and short interpillar distances.

Contributed talk, Wed./12:00

Microencapsulation of a water-soluble ruthenium (II) complex derived from limonene as an effective tool against pathogenic bacterial biofilms

Y. El Fannassi[1,2], S. Khelissa[1], M. Amin El Amrani[2], A. Gharsallaoui[3], and N. Chihib[1]

[1] *Univ Lille, CNRS, INRAE, Centrale Lille, UMR 8207 - UMET - Unité Matériaux et Transformations, F-59000 Lille, France*
[2] *Laboratoire de Chimie Organique Appliquée, Université Abdelmalek Essaadi, Faculté des Sciences, BP 2121-93002, Tetouan, Morocco*
[3] *Univ Lyon, Université Claude Bernard Lyon 1, CNRS, LAGEPP UMR 5007, 43 bd 11 Novembre 1918, 69622 Villeurbanne, France*

email: `Elfannassi.youssra@gmail.com`

In the present work bioactive aminooxime ligands based on optically pure (R)-Limonene have been synthesized. Their Ruthenium (II) cationic water-soluble [1] complex was prepared by a reaction between dichloro (para-cymene) Ruthenium (II) dimers and aminooxime ligands in a 1:2 molar ratio. Antibacterial and antibiofilm activities of the synthetized complex were assessed against *Staphylococcus aureus* , *Escherichia coli*, *Listeria monocytogenes* and *Enterococcus faecalis.*

The results revealed that the Ruthenium (II) complex has higher antibacterial and antibiofilm activities in comparison to free ligands or the enantiopure (R)-Limonene. Moreover, microencapsulation of this complex reduced its cytotoxicity and improved their minimum inhibitory concentration and antibiofilm activity towards the considered bacteria.

The Ruthenium (II) complex targets the bacterial cell membrane which leads to rapid leakage of intracellular potassium and proteins. Our study suggests that the developed Ruthenium (II) complexes could be useful as an alternative to conventional disinfectants [2].

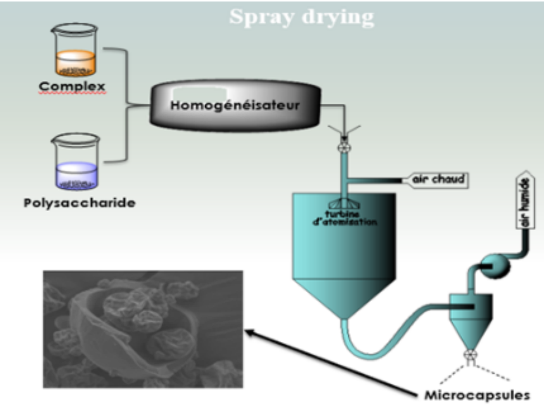

[1] M. S. Ibn El Alami *et al.*, Chirality, 24 (2012) 675-682
[2] S. Khelissa *et al.*, Front. Microbiol. Sec. Food Microbiology, 12 (2021)

Contributed talk, Wed./12:15

Characterization and Performance Evaluation of $PrVO_y$-$CaVO_y$ Oxides for Solid Oxide Fuel Cells

R. Pinto[1], B. Arias-Serrano[1,2], and A. Yaremchenko[1]

[1] *CICECO – Aveiro Institute of Materials, University of Aveiro, Aveiro, Portugal*
[2] *The Iberian Energy Storage Research Center (CIIAE), Polígono 13, Parcela 31, "El Cuartillo", 10004 Cáceres, Spain*

email: `ruigpinto@ua.pt`

Rare-earth and alkaline-earth vanadates have garnered significant attention as promising materials for electrochemical applications, especially as redox-reversible components for fuel electrodes in solid oxide fuel cells (SOFC) [1, 2] An indispensable advantage of (Ln,A)VO_y derived components (A - alkaline-earth metal cation) in SOFC anodes is their expected resistance to carbon deposition and sulfur-containing impurities, making them crucial for the efficient operation of hydrocarbon- and biogas-fueled solid oxide fuel cells (SOFCs). The current study primarily investigated the oxides within the $PrVO_4$-$Ca_2V_2O_7$ system as precursors for fuel electrodes, with a specific emphasis on phase formation, redox and thermomechanical behaviour, as well as electrical properties. $PrVO_4$, $Ca_2V_2O_7$, and ceramics with the nominal composition $Pr_{1-x}Ca_xVO_{4-\delta}$ (x = 0.02-0.20) were synthesized using the conventional solid-state route. Ceramics samples were sintered at 1000°C for $Ca_2V_2O_7$ and 1300°C for other materials. XRD demonstrated the formation of phase-pure $Pr_{1-x}Ca_xVO_{4-\delta}$ solid solutions with the tetragonal zircon-type structure for up to 5 at.% of calcium in the Pr sublattice. At the same time, SEM/EDS suggest a lower solubility indicated by the presence of Ca-V-O phase impurities. The introduction of calcium through doping enhances the ionic-electronic conductivity of Pr(Ca)VO_4 ceramics, particularly under oxidizing conditions.

The electronic contribution is p-type and decreases with reducing p(O_2. The reduction of $Pr_{1-x}Ca_xVO_{4-\delta}$ ceramics in a 10% H_2-N_2 atmosphere at 800°C induces phase separation, forming perovskite-like $PrVO_3$ and $CaVO_3$ phases. The redox behaviour of $PrVO_4$-$Ca_2V_2O_7$ ceramics was investigated through isothermal cycling between air and 10% H_2-N_2, employing techniques such as impedance spectroscopy, thermogravimetry, dilatometry, and post-mortem XRD analysis.

Acknowledgements: This work was supported by the FCT/MCTES/FEDER (projects CARBOSTEAM (POCI-01-0145-FEDER-032295) and CICECO-Aveiro Institute of Materials (UIDB/50011/2020, UIDP/ 50011/2020 & LA/P/ 0006/2020), and PhD grant 2020.04654.BD).

[1] L. Adijanto *et al.*, J. Mater. Chem., 22 (2012) 11396
[2] E.V. Tsipis *et al.*, J. Mater. Chem., 12 (2002) 3738

Contributed talk, Wed./12:30

Synthesis and structural characterization of spherical silica nanoparticles with different diameters

M. Adamek[1], M. Laskowska[1], A. Karczmarska[1], O. Kowalska[2], A. Maximenko[3], and Ł. Laskowski[1]

[1]*Intitute of Nuclear Physics Polish Academy of Sciences, Cracow, Poland*
[2]*Institute of Catalysis and Surface Chemistry Polish Academy of Sciences, Cracow, Poland*
[3]*SOLARIS National Synchrotron Radiation Centre, Jagiellonian University, Cracow, Poland*

email: `michal.adamek@ifj.edu.pl`

In today's physics, chemistry, material engineering, and nanotechnology, much of the collective scientific effort is dedicated to designing, synthesizing, and developing novel, multifunctional composite nanomaterials for future use in fields such as i.e., spintronics, quantum computing, and nanoelectronics. Given the need for certain functional molecules or units to be placed on the right kind of platform in order to operate efficiently, nanoparticles are often the most reasonable choice for that purpose. This is the case in our team, where we use spherical silica nanoparticles to functionalize them with magnetic molecules Mn_{12}, thereby producing composite nanomaterial with extraordinary magnetic properties at the nanoscale. We find SiO_2 nanospheres especially useful because of their chemical inertness and stability, biocompatibility, homogeneity, large specific surface area, and ease of functionalization.

By applying the Stöber method [1] and adjusting the reaction conditions such, as concentration of reagents and reaction temperature, we are able to obtain monodisperse, uniform SiO_2 spherical nanoparticles with desired diameter, typically between 50 and 500 nm, in a highly reproducible manner.

In our recent work, we performed a series of synthesis procedures on this nanomaterial and established the influence of reaction temperature and reagent concentrations on the diameter of the obtained nanospheres. By analyzing microphotographs taken using SEM microscopy, we determined the diameters of nanospheres in each produced sample. For every sample, we prepared a histogram presenting the size distribution of the spheres (see Fig. 1). Basing on the diameters, we selected five representative samples (50, 100, 200, 300, and 400 nm) and subjected them to a series of further structural studies using various experimental techniques, in order to comprehensively characterize the nanomaterial. These techniques included BET nitrogen physisorption analysis, DLS analysis, FT-IR spectroscopy, XRD diffractometry, and XANES absorption spectroscopy. This work will present the results of the experiments conducted.

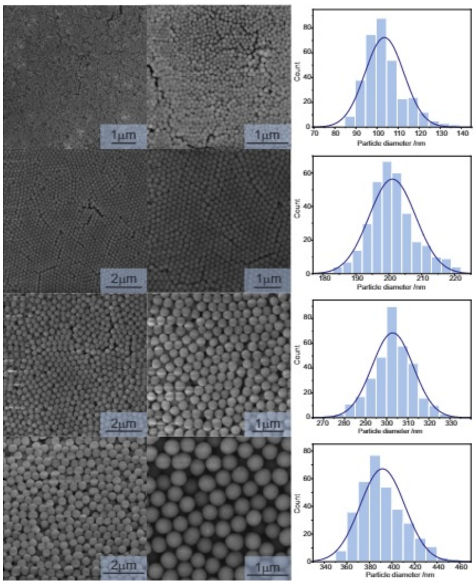

Figure 1: SEM microphotographs of samples with diameters of 100, 200, 300, and 400 nm, respectively.

Acknowledgements: Financial support for this investigation has been provided by the National Centre of Science (2020/37/B/ST8/03637, and 2021/43/D/ST8/00737)

[1] W. Stöber *et al.*, J. Colloid Interface Sci., 26 (1968) 62-69

POSTERS SESSION

1.	**Tanya Malakova** (Bulgaria) Characterization of LSCO and LCCO perovskite oxides as candidates for the development of bifunctional catalysts in zinc-air batteries	p. 61
2.	**Karolina Kosińska** (Poland) Synthesis of titanium oxide nanoparticles and studies of their effect on healthy human cells	p. 62
3.	**Ha Nguyen** (Poland) Ab-initio study of electronic structure and optical properties of Ba_2MnWO_6	p. 63
4.	**Patricia Osorio Ferreira** (Brazil) The influence of water in the crystallization of valsartan and naringenin coamorphous	p. 64
5.	**Tomoko Kubota** (Japan) Development a Synthesis Method for Metal-Substituted Tetratitanium Heptoxide	p. 65
6.	**Volodymyr Sagan** (Ukraine) Heat transfer in dod phases of cyclic hydrocarbons	p. 66
7.	**Izumi Akihiro** (Japan) Schiff base liquid crystal compounds exhibiting HexB phase, 2MBAC and 4MBAC	p. 67
8.	**Diana Vantyukh** (Ukraine) The Use of natural clinoptilolite as addition to building materials	p. 68
9.	**Maksym Barabashko** (Ukraine) Features in the Heat capacity and Thermal expansion of 1D atomic Xe chains	p. 69
10.	**Yulija Horbatenko** (Ukaraine) Thermal Conductivity Analysis for Complex Crystals formed via Superlattice Structure	p. 70
11.	**Martin Pernikov** (Bulgaria) Synthesis, physico-chemical and structural investigation of glasses from the system $Na_2O/BaO/ZrO_2/TiO_2/SiO_2/B_2O_3/Al_2O_3$ as potential material for the preparation of ferroelectric glass-ceramics	p. 71
12.	**Anna Karachevtseva** (Ukraine) Phase diagrams of cyclic hydrocarbons with heteroatom as an illustration of the state of matter	p. 72
13.	**Diana Hurova** (Ukraine) Temperature behavior of the thermal factor of scattering in the ordered phase of solid Nitrogene-15	p. 73
14.	**Greta Inkrataitė** (Lithuania) A study on Endogenous Dynamic Nuclear Polarization (DNP) is being carried out using Garnet Structure samples synthesized through Sol-Gel methods	p. 74
15.	**Tomasz Tarnawski** (Poland) LC-TEM observations of growth and dissolution of CeO_2 NPs and their decoration by Au NPs	p. 75
16.	**Shintaro Akagi** (Japan) Spin-Flop Transition in a One-Dimensional Nickel-Octacyanidotungstate Magnet	p. 76
17.	**Shuntaro Nagashima** (Japan) Direct observation of surface magnetization on magnetic thin films of ternary-metal-hexacyanide molecule-based magnet using magnetic force microscopy	p. 77
18.	**Riku Seiki** (Japan) Synthesis of λ-Ti_3O_5 using Titanium Chloride as starting material	p. 78
19.	**Veronika Mukharovska** (Ukraine) Interpretation of photoluminescence spectrum of $Eu(CH_3COO)_3 \cdot H_2O$ salt and its dependance over excitation radiation intensity	p. 79
20.	**Dimitrios Tzitzilis** (Greece) Wenzel-to-Cassie transition on lubricant-impregnated surfaces	p. 80
21.	**Dominik Czernia** (Poland) Plasma irradiation: a promising technique for modifying magnetic properties in molecular magnets	p. 81

Poster No. 1

Characterization of LSCO and LCCO perovskite oxides as candidates for the development of bifunctional catalysts in zinc-air batteries

T. Malakova[1], E. Mihaylova-Dimitrova[2], V. Terziev[2], G. Raikova[2], and K. Krezhov[1,3]

[1] *Institute of Electronics, Bulgarian Academy of Sciences, 1784 Sofia, Bulgaria*
[2] *Institute of Electrochemistry and Energy Systems, Bulgarian Academy of Sciences, 1113 Sofia, Bulgaria*
[3] *Institute for Nuclear research and Nuclear Energy, Bulgarian Academy of Sciences, 1784 Sofia, Bulgaria*

email: `tanya_malakova@abv.bg`

Bifunctional catalysts for the oxidation/reduction process in the metal-air battery are an important group of materials that determine its reversibility, i.e. the ability to recharge the battery. Rechargeability can be improved by developing new bifunctional oxygen electrocatalysts which facilitate both the oxygen reduction reaction (ORR) and the oxygen evolution reaction (OER) [1].

Materials based on Lanthanum cobaltite ($LaCoO_3$) and its doped derivatives $La_{1-x}(Ca,Sr)_xCoO_3$ are often used as bifunctional catalysts in metal-air batteries. Substitution of La^{3+} with Ca^{2+} increases the concentration of oxygen-free lattice sites and the occurrence of vacancies accordingly supports the transport of oxygen ions. Since the Ca^{2+} cation size is smaller than La^{3+}, the substitution can also cause a lowering of the crystal symmetry. An important merit of the Ca-substituted derivatives is that they are stable with respect to thermal expansion, and of the Sr-substituted ones that they have metallic conductivity for $x > 0.3$. However, Ca-substituted compositions show instability in long-term tests in alkaline electrolytes. This problem and the prohibitive cost and scarcity of noble metal catalysts required to catalyze the ORR in fuel cells and metal-air batteries have severely affected the commercialization scope of these clean energy technologies.

In this report, we describe results related to the development of carbon-free gas-diffusion electrodes in zinc-air rechargeable batteries. The performance of test electrodes prepared by a specific innovative procedure using catalytic materials of both commercially available and nanostructured powders of $La_{0.6}Sr_{0.4}CoO_3$, (LSCO) and $La_{0.6}Ca_{0.4}CoO_3$ (LCCO) was investigated. Doping with calcium or strontium affects the local structure of the system, which in addition depends on the temperature treatment. The temperature-induced changes in the perovskite-like crystal structure can be caused by different effects: 1) formation of oxide compounds based on cobalt and dopant, 2) distortion of the perovskite structure and 3) partial replacement of La^{3+} by Ca^{2+} or Sr^{3+} ions. The details of structural changes were investigated by X-ray and neutron diffraction and scanning electron microscopy in an attempt to deepen the understanding of the properties relevant to the particular case. Electrochemical tests performed on both types of oxide-based electrodes show greater stability of that produced with $La_{0.6}Sr_{0.4}CoO_3$.

Acknowledgements: The author E. Mihaylova -Dimitrova kindly acknowledged for financial support to “National Program "YOUNG SCIENTISTS AND POST-DOCTORAL STUDENTS-2", financed by the Ministry of Education and Science – 2022”.

[1] J. Suntivich *et al.*, Nat. Chem., 3 (2011) 546-550

Poster No. 2

Synthesis of titanium oxide nanoparticles and studies of their effect on healthy human cells

K. Kosińska[1], B. Klębowski[2], and M. Parlińska-Wojtan[2]

[1]*Ignacy Łukasiewicz Rzeszow University of Technology, Rzeszow, Poland*
[2]*Institute of Nuclear Physics Polish Academy of Sciences, Kraków, Poland*

email: `k.kosinska99@gmail.com`

Nanotechnology is a dynamically developing branch of science due to the unique properties of nanomaterials and nanoparticles (NPs). The present study is focused on the synthesis and evaluation of the biological activity of titanium oxide NPs (TiO_2 NPs).

Until recently, TiO_2 was widely used as a food additive (E171). Currently, TiO_2 can only be used as an ingredient in cosmetics, medicines, paints or plastics. TiO_2 NPs can induce different biological effects depending on their crystalline form, size and shape [1], as they can lead to disruption of homeostasis, inflammation and apoptosis of cells in the large intestine and spleen [2, 3]. TiO_2 is especially dangerous when inhaled, as it causes inflammation in the lungs and increases the risk of lung cancer [4].

In this study, different ratios of oleylamine and oleic acid in reaction with titanium tetrafluoride (precursor) were used in order to obtain of TiO_2 NPs with different morphologies (spherical and rod-like NPs – Figure 1a and 1b). The obtained and purified TiO_2 NPs were characterized by scanning transmission electron microscopy (STEM), selected area electron diffraction (SAED), UV-Vis spectroscopy and measurements of their zeta potential. Then, MTS viability test will be carried out, to evaluate the cytotoxicity of the synthesized TiO_2 NPs on normal colon epithelium cells (CRL-1790). Contact of TiO_2 NPs with the intestine may cause disturbances in the functioning of intestinal microvilli, reducing the absorption of other nutrients, such as zinc, iron or fatty acid [5]. The CRL-1790 cells were cultured with the addition of spherical and rod-like TiO_2 NPs in the concentration range from 5 to 150 μg/ml.

The preliminary results of our research showed that both types of TiO_2 NPs, obtained by the same synthesis method and having a similar values of zeta potentials, at concentrations up to 50 μg/ml do not cause a significant decrease in cell survival. For higher concentrations, the mortality is already statistically significant (Figure 1c). However, there were no significant differences in the cytotoxicity of spherical and rod-like TiO_2 NPs. The obtained information on the cytotoxicity of the synthesized TiO_2 NPs may enable further research on the use of these NPs in biomedicine in the future, e.g. as drug delivery systems (DDS).

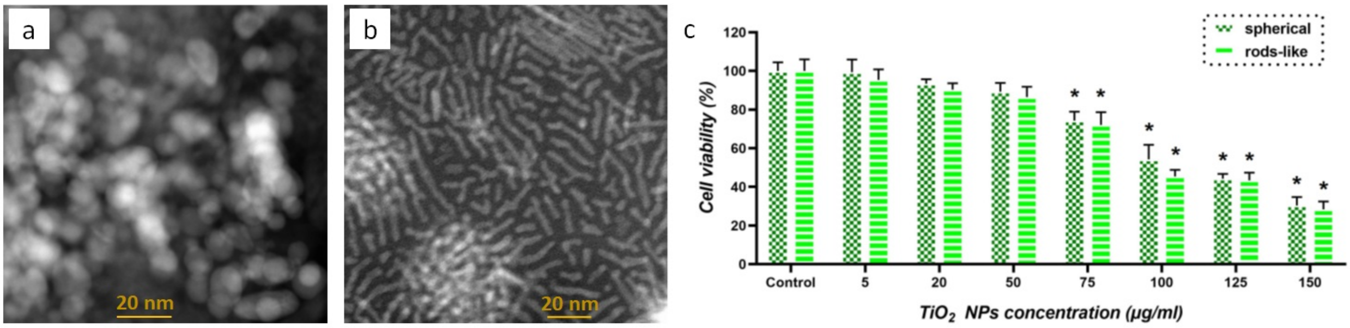

Figure 1: STEM images of (a) spherical and (b) rod-like TiO_2 NPs, as well as (c) cytotoxicity of TiO_2 NPs against CRL-1790 cells after 24 h of incubation. Differences were considered significant when *p-value $<$0.05 vs control.

[1] S. Jarmakiewicz-Czaja *et al.*, Gastroenterology Rev., 16 (2021) 106
[2] S. Tada-Oikawa *et al.*, Int. J. Mol. Sci., 17 (2016) 576
[3] S. Yang *et al.*, J. Nanosci. Nanotechnol., 18 (2018) 2387
[4] K. E. Driscoll *et al.*, Front. Public Health, 10 (2022) 907318
[5] Z. Guo *et al.*, NanoImpact, 5 (2017) 70

Poster No. 3

Ab-initio study of electronic structure and optical properties of Ba_2MnWO_6

T. T. H. Nguyen[1], M. Sahakyan[2], and V. H. Tran[2]

[1] *Pedagogical University of Cracow, Cracow, Poland*
[2] *Institute of Low Temperature and Structure Research, Polish Academy of Sciences, Wrocław, Poland*

email: `ha.nguyen@doktorant.up.krakow.pl`

Double perovskites with the chemical formula $A_2MM'O_6$ ($A=$ alkali, alkaline earth or rare earth ions, M and M' = metal ions) have gained attention in recent years due to their prospective applications as magnetocaloric and optoelectronic materials. One of the magnetically ordered double perovskites with semiconducting characteristics is Ba_2MnWO_6. Based on neutron diffraction measurements, Mutch et al. found that the compound undergoes a long-range antiferromagnetic ordering at 8 K [1]. The magnetic structure characterizes with a propagation vector k = (1/2, 1/2, 1/2), with the Mn moment of 4.5 μB/Mn lying in the (111) plane.

In this report, we used the generalized gradient approximation (GGA) and on-site Coulomb interaction of localized 3d electron (Hubbard U parameter) to examine the magnetic and electronic properties of this compound. We studied several magnetic configurations, including both nonmagnetic and antiferromagnetic. In the ordered state, we assume the Mn^{2+} moments arranged in the (001) or (111) planes. Furthermore, our results show that Ba_2MnWO_6 is an indirect band gap semiconductor with a gap energy of 0.36 eV and a band gap up to 1.76 eV when $U_{\text{eff}} = 3$ eV ($U = 4$ eV, $J = 1$ eV) [2]. We discovered that Mn-3d orbitals have the greatest influence on the valence band maximum (VBM), whereas W-5d orbitals have a large impact on the conduction band minimum (CBM). Notably, our findings indicate that the Ba_2MnWO_6 absorbs ultraviolet light very well, making it a viable material for optical applications such as solar cells.

[1] H. Mutch *et al.*, Phys. Rev. Mater., 4 (2020) 014408
[2] T. T. Nguyen *et al.*, Low Temp. Phys., 49 (2023) 247

Poster No. 4

The influence of water in the crystallization of valsartan and naringenin coamorphous

P. O. Ferreira[1,3], A. C. Almeida[1], L. T. Ferreira[2], M. E. S. Eusébio[3], R. A. E. Castro[3,4], and F. J. Caires[1,2]

[1] *School of Sciences, São Paulo State University, Bauru, Brazil*
[2] *Institute of Chemistry, São Paulo State University, Araraquara, Brazil*
[3] *CQC/IMS, Chemistry Department, University of Coimbra, Coimbra, Portugal*
[4] *Faculty of Pharmacy, University of Coimbra, Coimbra, Portugal*

email: `patricia.osorio@unesp.br`

Coamorphous phases are homogeneous multicomponent amorphous systems that exhibit kinetic stability due to intermolecular interactions between the components or to mixing effects. They have been highlighted as a strategy to stabilize amorphous phases that also have the possibility of improving physicochemical properties of drugs [1]. The APIs (active pharmaceutical ingredients) chosen for this work are valsartan (VAL), an antihypertensive drug, that has low aqueous solubility, been classified by the Biopharmaceutical Classification System (BCS) as a class II drug (low solubility – high permeability) [2], and naringenin (NAR) a flavonoid characterized as functional food ingredient, that has several biopharmaceutical properties, such as cardiovascular protection [3]. The plasticizing effect of water in amorphous systems has been reported, but for coamorphous phases there are not many reports [4]. In this work, we investigate the effect of moisture on the crystallization of an equimolar valsartan+naringenin coamorphous system (1:1-VAL+NAR).

The samples were prepared through mechanochemical synthesis and then characterized by differential scanning calorimetry (DSC), infrared spectroscopy (FTIR), and powder X-ray diffraction (PXRD). For physical stability studies, the samples were incubated in climatic chambers for 8 weeks at different temperature and relative humidity (RH) (25 °C / RH 60%; 30 °C/ RH 65%; 40 °C/ RH 70%), and for about 24 weeks under dry conditions in a desiccator.

The equimolar VAL-NAR mixture is an amorphous system as confirmed by PXRD, with a single glass transition (T_g) event, as expected for a coamorphous phase, at 58 °C. The experimental T_g temperatures of other VAL-NAR molar ratio mixtures have a negative deviation from those predicted by the Gordon-Taylor equation [5]. Investigation of the physical stability of the 1:1 VAL+NAR coamorphous sample shows that increasing relative humidity induces crystallization of naringenin, as shown in Figure 1. The sample kept under dry conditions, at room temperature, for about 6 months remained highly amorphous, which shows the role of relative humidity in the crystallization of the 1:1-VAL-NAR coamorphous system.

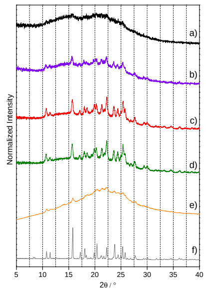

Figure 1: PXRD of 1:1-VAL-NAR system under different environmental conditions: a) freshly prepared; b) 8 weeks 25 °C / RH 60%; c) 2 weeks 30°C / RH 65%; d) 1 week 40 °C / RH 70%; e) 6 months under dry conditions (desiccator); and f) pure NAR.

Acknowledgements: This work was financed in part by the Brazilian Federal Agency for Support and Evaluation of Graduate Education (CAPES), in the scope of the Program CAPES-PrInt, Mobility number 88887.571008/2020-00. CQC/IMS is supported by Portugal national funds through FCT – Fundação para a Ciência e a Tecnologia, I.P., under the project UIDB/00313/2020.

[1] A. Shayanfar *et al.*, J. Mol. Liq., 187 (2013) 171
[2] R. Hamed *et al.*, AAPS PharmSciTech, 19 (2013) 2213
[3] D. K. Jha *et al.*, Int. J. Pharm., 583 (2020) 119363
[4] J. Liu *et al.*, Int. J. Pharm., 605 (2021) 120802
[5] M. Gordon *et al.*, J. Appl. Chem., 2 (1952) 493

Poster No. 5

Development a Synthesis Method for Metal-Substituted Tetratitanium Heptoxide

T. Kubota[1], R. Seiki[1], A. Fujisawa[1], A. F. Fadilla[1], S. Ohkoshi[2], and H. Tokoro[1]

[1]*Department of Material Science, Faculty of Pure and Applied Sciences, University of Tsukuba, 1-1-1 Tenno-dai, Tsukuba, Ibaraki 305-8577, Japan*
[2]*Department of Chemistry, School of science, University of Tokyo, 7-3-1 Hongo, Bunkyo-ku, Tokyo 113-8654, Japan*

email: `s2320340@u.tsukuba.ac.jp`

[Introduction] Titanium oxides containing Ti^{3+} have various polymorph, i.e., dititanium trioxide (Ti_2O_3), tritanium pentoxide (Ti_3O_5), tetratitanium heptoxide (Ti_4O_7), and so on. Among titanium oxides materials, Ti_4O_7 has the highest electrical conductivity and moreover exhibits a two-step phase transition from metal to semiconductor (150 K) and semiconductor to semiconductor (140-130 K) phases which is interesting field of study. In this study, we have tried to develop a synthesis method for single-phase tetratitanium heptoxide. Furthermore, by this synthesis method, we try to obtain metal-substituted tetratitanium heptoxide.

[Method] Sample **1**; a microemulsion of H_2O, $TiCl_4$, and NH_3 was prepared in a flask and stirred in an oil bath at 50 °C for 20h to form $Ti(OH)_4$ precipitate. The precipitate was gained by centrifugation, washed with ethanol, and heated at 60 °C for 24h on a hot plate. The obtained precipitate which was then called by precursor calcinated under hydrogen flow 0.5 $dm^3 min^{-1}$ at 1,000 °C for 5h, which produced black powder sample. Sample **2**; as a metal-substituted sample, we prepared the microemulsion of H_2O, $TiCl_4$, $GaCl_3$ and NH_3, adding $GaCl_3$ of 5% of the titanium molar ratio in the flask. Then, the precursor was synthesized, and it was sintered under hydrogen flow 1.0 $dm^3 min^{-1}$ at 900 °C for 5h, which produced black powder sample.

[Result] X-ray diffraction (XRD) pattern and Rietveld analysis at room temperature of the sample **1** were shown in Figure 1. The sample **1** is a single-phase of Ti_4O_7 with triclinic crystal structure (space group P1) of the lattice constants of $a = 5.5972$ Å, $b = 7.1208$ Å, $c = 12.4586$ Å, $\alpha = 95.051°$, $\beta = 95.172°$, $\gamma = 108.753°$. The crystallite size estimated by Rietveld analysis is 32.1 ± 0.4 nm. As for sample 2, the results of XRD pattern and Rietveld analysis will be presented at the poster session.

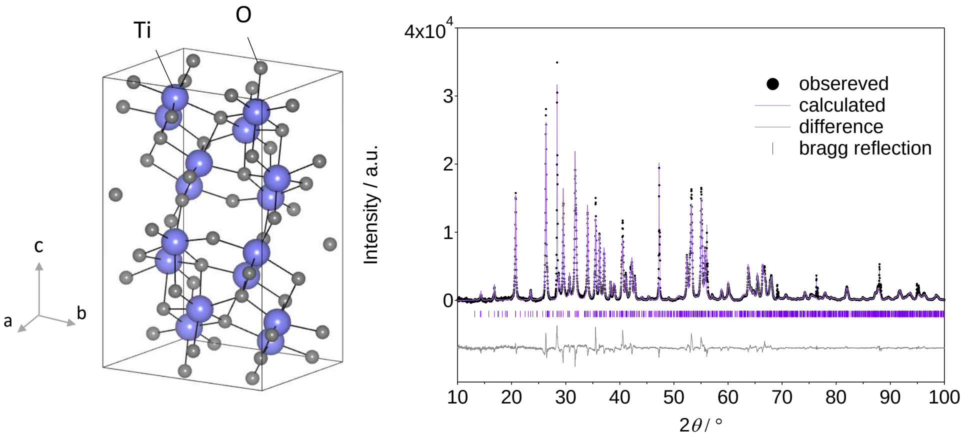

Figure 1: Crystal Structure of Ti_4O_7 (left) and XRD pattern and Rietveld analysis (right).

Poster No. 6

Heat transfer in dod phases of cyclic hydrocarbons

V. V. Sagan[1], V. A. Konstantinov[1], A. I. Krivchikov[1], and A. V. Karachevtseva[1]

[1]*B.Verkin Institute for Low Temperature Physics and Engineering of the National Academy of Sciences of Ukraine, 47 Nauky Ave., Kharkiv 61103, Ukraine*

email: `sagan@ilt.kharkov.ua`

Experimental results of the dependence of isochoric thermal conductivity for the densest samples of cyclic compounds – benzene (C_6H_6), cyclohexane (C_6H_{10}), cyclohexene (C_6H_{12}), furan (C_4H_4O), thiophene (C_4H_4S), and cyclopentane (C_5H_{10}) showed that in all dynamically orientationally disordered phases of cyclic hydrocarbons the thermal conductivity increases with increasing temperature. Earlier, the increase in isochoric thermal conductivity with growing temperature in the DOD phases of molecular crystals was qualitatively explained by a decrease in the probability of scattering of acoustic phonons on collective rotational excitations due to weakening of interaction between translational and orientational subsystems. [1]

Recently, it has been suggested that such behavior may be related alternatively to the thermal activation contribution to the thermal conductivity, which can be described by the Arrhenius expression. In this case, thermal conductivity can be described as $\kappa(T) = A/T + B + \kappa_{TA}(T)$, where $\kappa_{TA}(T){=}\kappa_0 \exp(-E/kT), \kappa_0$ is the pre-exponential factor, E is the activation energy. [2–6]

In present work, for the first time, we analyzed our experimental data on the isochoric thermal conductivity in the dynamically orientationally disordered phases of cyclic hydrocarbons in order to determine how satisfactorily they can be described by the thermal activation mechanism of heat transfer and Arrhenius dependence.

It is shown that the increase in thermal conductivity with growing temperature in the number of cyclic hydrocarbons can be described by the hopping thermal activation mechanism, with constant activation energy and a pre-exponential factor depending on the density. Activation energies and pre-exponential factors are determined. The dependence of the pre-exponential factor on the activation energy was analyzed. It was found out that for cyclic compounds discussed κ_0 does not depend on E for low activation energies ($E < 200$ K).

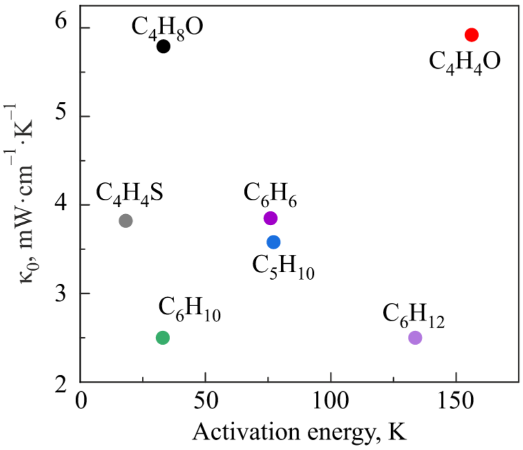

Figure 1: The dependence of the pre-exponential factor κ_0 on the acti-vation energy E for a number of cyclic compounds in DOD phases.

Acknowledgements: This work was supported by the National Research Foundation of Ukraine (Grant № 2020.02/0094).

[1] V. A. Konstantinov *et al.*, InTech Open Access Publisher (2011) 157
[2] M. T. Agne *et al.*, Energy Environ. Sci., 11 (2018) 609
[3] M. Simoncelli *et al.*, Nat. Phys., 15 (2019) 809
[4] A. Jezowski *et al.*, AIP Adv., 9 (2019) 015121
[5] Y. V. Horbatenko *et al.*, J. Phys.Chem. Solid., 127 (2019) 151
[6] V. A. Konstantinov *et al.*, Solid State Commun., 329 (2021) 114241

Poster No. 7

Schiff base liquid crystal compounds exhibiting HexB phase, 2MBAC and 4MBAC

I. Akihiro[1], Y. Yamamura[2], and K. Saito[2]

[1] *Degree Programs in Pure and Applied Sciences Graduate School of Science and Technology, University of Tsukuba, Tsukuba, Ibaraki, Japan*
[2] *Department of Chemistry, Faculty of Pure and Applied Sciences, University of Tsukuba, Tsukuba, Ibarak, Japan*

email: `s2220191@s.tsukuba.ac.jp`

We have investigated the molecular packing structure of the orthogonal smectic liquid crystal phases (SmA, CrB, SmE) based on the alkyl-chain length dependence of layer spacing.[1–3] However, the molecular packing structure of the HexB phase, which is one of the SmB phases, has not been studied because mesogens exhibiting the HexB phase are rare.

Two Schiff base compounds, ethyl-4-[(4-methoxybenzylidene)amino]cinnamate (2MBAC) and butyl-4-[(4-methoxybenzylidene)amino]cinnamate (4MBAC), have been reported to exhibit three liquid crystal phases (N, SmA, SmB), and crystal polymorphs during the cooling process.[4–7] However, the type of SmB phase has not been specified. Therefore, we reexamined the phase behavior of 2MBAC and 4MBAC as candidates for the mesogen exhibiting the HexB phase and investigated their phase transitions between liquid crystal phases in this study.

DSC measurements of the two compounds revealed that they exhibit N, SmA, and SmB phases and an unknown smectic one. To identify the SmB phase, we performed wide-angle X-ray diffraction measurements. The observed diffraction patterns show that a broad reflection around $2\vartheta \approx 20^\circ$ for the SmA phase becomes sharp without significant growth in the interlayer order for the SmB phase with decreasing temperature. This change results from the enhanced ordering in the intralayer molecular arrangement. Thus, we concluded that the SmB phase is the HexB phase.

The molecular packing structure and phase transition of the smectic phases of 2MBAC and 4MBAC will be discussed.

[1] Y. Yamamura *et al.*, Phys. Chem. Chem. Phys., 19 (2017) 25518
[2] Y. Yamamura *et al.*, J. Phys. Chem. B, 121 (2017) 1438
[3] Y. Yamamura *et al.*, Phys. Chem. Chem. Phys., 19 (2017) 19434
[4] I. G. Chistyakov *et al.*, Mol. Cryst. Liq. Cryst., 7 (1969) 279
[5] J. Nakauchi *et al.*, Bull. Chem. Soc. Jpn., 46 (1973) 3321
[6] C. E. Tarr *et al.*, Mol. Cryst. Liq. Cryst., 22 (1973) 123
[7] M. Harada *et al.*, J. Phys. Soc. Jpn., 54 (1985) 998

Poster No. 8

The Use of natural clinoptilolite as addition to building materials

D. E. Vantyukh[1]

[1] Uzhhorod National University, Uzhhorod, Ukraine

email: `vantiukh.diana@uzhnu.edu.ua`

Zeolites is a mineral group as a result of variation of volcanic ashes in the aquatic environment millions of years ago consisting of alkaline and soil alkaline's hydrated natural silicates. [1] More than 40 minerals belonged to the group of Natural zeolites. The most important and widespread of them is clinoptilolite. One of the most famous deposits of natural clinoptilolite in Europe is located in the village Sokyrnytsia, Transcarpathian region, Ukraine. Sokyrnytsia' zeolites have wide range usage areas such as agriculture, water and gas storage, fisheries, radioactive cleaning, solar energy.[1] But the most famous is building industry.[2]

The most frequent and beneficial uses of natural clinoptilolite addition in civil engineering is the use of it in concrete. Concrete is a nanostructured, multi-phase, composite material that ages over time. It is composed of an amorphous phase, nanometer to micrometer size crystals, and bound water.[3] It is used in almost all construction, from roads, to bridges, to buildings. Concrete can be modified in numerous ways; one of which is to add clinoptilolite in it. Our results of Sokyrnytsia' zeolite containing cement testing have shown that the addition of dry and particularly burned zeolite in 15% quantity into cement composition improves its physical-mechanical properties. Terms of hardening consists from 2.30 to 4 hour-second, limit strength on compression – $300 kg/cm^2$ 28 days, the water/cement ratio 30.0. In addition, composite cement is characterized by spreading 117 mm cone. But compressive strength after 28 days of hardening is 42.2 MPa, which less than nearly 10% corresponds to the 400 brand cement.

Our study showed that addition of clinoptilolite in 15% quantity improved the durability properties of concrete, but decreased strength and setting time as well as workability of cementitious composites which demands further researches.

[1] O. Bilgin, Int. J. Eng. Res., 3 (2014) 741-744
[2] T. Markiv *et al.*, Archiv. Civ. Mech. Eng. 16 (2016) 554-562
[3] K. Hossain *et al.*, Eur. J. Sustain. Dev. Res. 4 (2015) 161-166

POSTER NO. 9

Features in the Heat capacity and Thermal expansion of 1D atomic Xe chains

M. Barabashko[1], M. Bagatskii[1], A. Dolbin[1], and V. Sumarokov[1]

[1]*B.Verkin Institute for Low Temperature Physics and Engineering of NAS of Ukraine,47 Nauky Ave.,*
Kharkiv, 61103, Ukraine

email: `msbarabashko@gmail.com`

The formation of quasi-1D and -2D physically adsorbed atomic and molecular structures is possible due to a unique structure of bundles of single-walled carbon nanotubes (c-SWCNTs): the length of nanotubes is several orders of magnitude larger than their diameter. The study of the low-temperature heat capacity of carbon nanomaterials with physically adsorbed gases is useful for obtaining knowledge about the dynamics of low-dimensional adsorbate structures and thermal effects in nanomaterials.

Recently, heat capacities of $C_P(T)$ at constant pressure for one-dimensional chains of Xe, N_2, and CH_4 adsorbed in grooves on the outer surfaces of bundles of single-walled carbon nanotubes (c-SWCNTs) have been experimentally investigated.[1–3] The temperature dependence of the coefficient of radial thermal expansion $\alpha r(T)$ for bundles of c-SWNTs with Xe atoms adsorbed on the outer surface of the bundles was also studied.[4]

In this work, we analyze and compare the temperature dependence of the heat capacity $C_P(T)$ of one-dimensional chains of xenon atoms in the grooves on the outer surface of bundles of single-walled carbon nanotubes with closed-caps (c-SWCNTs) and the contribution $\alpha(T)$ of adsorbed Xe atoms to the radial thermal expansion of the system c -SWCNTs-Xe to identify common features on the $C_P(T)$ and $\alpha(T)$ curves, which may be caused by the effects of spatial redistribution of xenon atoms.

In the temperature range of 2–75 K, the analysis and comparison were performed for: (i) experimental $C_P(T)$ and theoretical $C_V(T)$ heat capacity of 1D chains of xenon atoms adsorbed in grooves on the outer surface of bundles of single-walled carbon nanotubes with closed ends (c-SWNTs); (ii) the experimental $C_P(T)$ and the experimental contribution to the radial thermal expansion $\alpha(T)$ of Xe that adsorbed to the grooves of c-SWCNTs. There is an anomaly near 60 K on the $C_P(T)$ and $\alpha(T)$ curves due to the contribution of the spatial redistribution of Xe atoms between the chains and the outer surface of c-SWCNTs. It was found that the dependencies of $C_P(T)$ and $\alpha(T)$ are qualitatively similar below 60 K. The anomaly near 60 K in the $C_P(T)$ curve indicates the complete of fragmentation of 1D Xe atomic chains. The obtained result is important for understanding the kinetics of gas impurity sorption/desorption processes in c-SWCNTs.

Acknowledgements: The work was supported by the National Research Foundation of Ukraine (NRFU project No 2020.02/0094).

[1] M. Barabashko *et al.*, Netsu Sokutei, 48 (2021) 164-170
[2] M. I. Bagatskii *et al.*, J. Low Temp. Phys., 187 (2017) 113-123
[3] M. I. Bagatskii *et al.*, Low Temp. Phys., 39 (2013) 441-445
[4] A.V. Dolbin *et al.*, Low Temp. Phys., 35 (2009) 484-490

Poster No. 10

Thermal Conductivity Analysis for Complex Crystals formed via Superlattice Structure

Yu. V. Horbatenko[1], A. I. Krivchikov[1], O. O. Romantsova[1], and O. A. Koroluyk[1]

[1] *B. Verkin Institute for Low Temperature Physics and Engineering, Kharkiv, Ukraine*

email: `horbatenko@ilt.kharkov.ua`

The analysis of thermal conductivity κ for different complex crystals, which are built by superlattice structure, or so called ‘superlattices’ were made. In particular, we analyzed temperature dependences of thermal conductivity for thin films of LMO$_n$/SMO$_n$ [1], AlN–GaN [2, 3], $(\mathrm{AlN})_{4nm}$–$(\mathrm{GaN})_y$ [4] with different thicknesses of GaN-layer and etc. It was shown that all temperature dependences of κ exhibit their exponentional growth while temperature increase similar to expression $\kappa_C = \kappa_0 \exp(-E/T)$, where κ_0 and E are parameters characterize excitations responsible for heat transfer processes. Also it was found that values of energy E differs slightly (±10 K) for crystals Si/SiGe with superlattice structure and Si/SiGe-nanowires, but κ_0 differs in two times [5]. It was shown that such representation of $\kappa(T)$ can be used for description of “coherent” contribution of thermal conductivity, or wave-like mechanism of heat transfer according to unified theory of thermal transport that declares - $\kappa(T)$ consists of the sum of two contributions - particle-like propagation and wave-like tunneling of excitations in crystals [6].

Acknowledgements: This work has received funding from the National Research Foundation of Ukraine (NRFU project No. 2020.02/0094).

[1] D. Meyer *et al.*, arXiv preprint, arXiv:2108 (2021) 05860
[2] J. Alvarez-Quintana *et al.*, Appl. Phys. Lett., 93 (2008) 013112
[3] Y. K. Koh *et al.*, Adv. Funct. Mater., 19 (2009) 610
[4] D. Li *et al.*, Appl. Phys.Lett., 83 (2003) 3186
[5] C. Chiritescu *et al.*, Science, 315 (2007) 351
[6] M. Simoncelli *et al.*, Nature Physics, 15 (2019) 809

POSTER NO. 11

Synthesis, physico-chemical and structural investigation of glasses from the system $Na_2O/BaO/ZrO_2/TiO_2/SiO_2/B_2O_3/Al_2O_3$ as potential material for the preparation of ferroelectric glass-ceramics

M. Pernikov[1], R. Harizanova[1], T. Tasheva[1], V. Lilova[1], S. Nedev[1], M. Nedkova[1], and C. Rüssel[2]

[1]*University of Chemical Technology and Metallurgy, Sofia, Bulgaria*
[2]*Otto Schott Institute of Materials Research, Jena, Germany*

email: `martin.pernikov@gmail.com`

Sodium-aluminoborosilicate glasses with high concentrations of alkaline and alkaline-earth metal oxides show tendency for phase separation and after appropriate choice of the composition glass-ceramics containing dielectric phases such as $BaTiO_3$ and/or $BaZr_xTi_{1-x}O_3$ could be prepared. The obtained materials may find applications in electronics and medicine as parts of different sensors and electronic as well as opto-electronic devices and for energy storage.

This work reports on oxide glasses in the compositional series $20.1Na_2O/(23.1\text{-}y)BaO/yZrO_2/23TiO_2/21SiO_2/9.8B_2O_3/3Al_2O_3$ by applying a traditional melt-quenching technique. Glasses were obtained for $y = 0.5$, 1, 2, 3 and 6 mol% ZrO_2. The densities were measured by using a helium pycnometer and served to determine physico-chemical characteristics of the prepared glasses such as molar volume, oxygen packing density and refractive index. The obtained results reveal that the values of all estimated physico-chemical characteristics increase with increasing ZrO_2 concentration. Furthermore, the characteristic temperatures, i.e., glass transition and crystallization peak maximum temperature were determined by using differential scanning calorimetry. The obtained values reveal that both the glass transition and crystallization peak maximum temperatures increase with increasing zirconium oxide concentration. The structure of the glasses was investigated by Infrared Spectroscopy on powdered samples and the existence of Si-O-Si/O-B-O bending, Si-O-Si rocking, B-O-B bending and B-O-B/B-O-Si stretching vibrations was observed in the spectra. The presence of BO_3, BO_4 and SiO_4 interconnected as well as isolated structural units was suggested. At approximately 570-580 cm^{-1}, a peak typical for the compound $BaTiO_3$ was also registered for all samples.

Acknowledgements: This study is funded by the European Union-Next Generation EU, through the National Recovery and Resilience Plan of the Republic of Bulgaria, project No. BG-RRP-2.004-0002, "BiOrgaMCT".

Poster No. 12

Phase diagrams of cyclic hydrocarbons with heteroatom as an illustration of the state of matter

A. Karachevtseva[1], V. Konstantinov[1], and V. Sagan[1]

[1] *B. Verkin ILTPE of NASU, Kharkiv, Ukraine*

email: `zvonaryova@ilt.kharko.ua`

This thesis devoted graphical representation of the equilibrium states of a substance as a function of temperature, pressure and volume. Directly to phase diagrams. Each substance has a number of phase states. For example, stable phases can exist for an unlimited time. Metastable phases have the lifetime of which is limited.

At normal atmospheric pressure, the transitions between solid-solid, solid-liquid and gas-liquid phases can be considered as points on the temperature scale, characteristic for each substance. If the pressure varies, it leads to changes of the phase transition temperature. The "triple point" is the point at which the liquid, solid, and vapor phases can exist together. $V - T$ diagrams allow you to visually observe the position of phase boundaries in isochoric studies of thermal properties, such as thermal conductivity, heat capacity, dielectric properties, etc.

The substances which considered here, quite often form a metastable phase. We analyzed the experimental data for such heterocyclic hydrocarbons like furan (C_4H_4O) [1], thiophene (C_4H_4S) [2] and tetrahydrofuran (C_4H_8O) [3].

All studies of thermal conductivity were carried out on the setup, using the method of stationary heat flow in a cell of coaxial geometry. The setup, samples growing procedure and experimentation is described in detail in [4].

The changes in molar volume during melting and the boundaries of the existence of high temperature phases have been determined. The magnitudes of thermal pressure of cyclic hydrocarbons studied were obtained. Experimental values of dP_m/dT on melting line were compared with those calculated by the Clapeyron-Clausius formula.

Acknowledgements: This work was supported by the National Research Foundation of Ukraine (Grant No.197/02.2020).

[1] V. A. Konstantinov *et al.*, Low Temp. Phys., 39 (2013) 473
[2] V. A. Konstantinov *et al.*, Low Temp. Phys., 41 (2015) 213
[3] V. A. Konstantinov *et al.*, Low Temp. Phys., 40 (2014) 1008
[4] V. A. Konstantinov *et al.*, Instr. Eksp. Tech., 42 (1999) 133

POSTER NO. 13

Temperature behavior of the thermal factor of scattering in the ordered phase of solid Nitrogene-15

D. E. Hurova[1], A. I. Erenburg[2], N. A. Aksenova[3], L. A. Alekseeva[1], and N. N. Galtsov[1]

[1]*B. Verkin Institute for Low Temperature Physics and Engineering of NAS of Ukraine, Kharkiv, Ukraine*
[2]*Ben-Gurion University of Negev, P.O.B 653, 84105 Beer-Sheva, Israel*
[3]*Ukrainian State University of Railway Transport, Kharkiv, Ukraine*

email: `hurova@ilt.kharkov.ua`

In solid Nitrogen-15, as well as in solid Nitrogen-14, an order-disorder phase transition is observed, which is accompanied by a change in the symmetry of the crystal lattice $Pa3 - P6_3/mmc$. In the ordered phase $^{15}N_2$ molecules are oriented along the $< 111 >$ direction of the cubic lattice. In the disordered phase, $^{15}N_2$ molecules rotate quasi freely forming a hexagonal lattice.

We have carried out structural studies, the purpose of which was to determine the value of mean square displacements (MSD) of molecules from the lattice site and the orientational order parameter (OOP) using structural data for the low-temperature phase of Nitrogen-15.

Structural researches were carried out on a DRON-2 x-ray powder diffractometer in Kα radiation from a copper anode. The measurements were taken in the temperature range of existence of the Nitrogen-15 solid phase.

Using the approach proposed in [1, 2] for analyzing the intensity of diffraction peaks, the temperature dependences of the behavior of the orientational order parameter and mean square displacements from the lattice site were plotted. Also, the OOP and MSD values obtained for Nitrogen-15 were compared with the values for Nitrogen-14 [1].

[1] N. N. Galtsov *et al.*, Low Temp. Phys., 38 (2012) 221
[2] L. A. Alekseeva *et al.*, Low Temp. Phys., 48 (2022) 113

POSTER NO. 14

A study on Endogenous Dynamic Nuclear Polarization (DNP) is being carried out using Garnet Structure samples synthesized through Sol-Gel methods

G. Inkrataitė[1], V. Klimavičius[2], D. Vištorskaja[1], A. Kareiva[1], and R. Skaudžius[1]

[1]*Institute of Chemistry, Faculty of Chemistry and Geosciences, Vilnius University, Vilnius, Lithuania*
[2]*Faculty of Physics, Vilnius University, Vilnius, Lithuania*

email: `greta.inkrataite@chgf.vu.lt`

Nuclear magnetic resonance spectroscopy (NMR) is a universal method in materials science, suitable for studying ceramics, nano-materials, catalysts and perovskites. Its disadvantage is low sensitivity due to the small energy difference between the energy levels of nuclear spins. Dynamic nuclear polarization (DNP), a hyperpolarization technique that increases the filling difference in energy levels, solves this problem. DNP-based electron spin polarization transfers from stable radicals or paramagnetic centers to the studied nuclei. In the last years, it has become possible to perform the DNP experiment in high magnetic fields. This results in higher resolution and higher signal-to-noise ratio. For DNP studies, the test system must have paramagnetic centers. Therefore, a new DNP signal enhancement strategy can be immediately used to obtain good results using paramagnetic centers that are naturally present in the sample. Samples with a garnet structure also have such paramagnetic centers [1, 2]. Garnet structure samples are very little studied in this application. For this reason, the main goal is to synthesize using Sol-Gel method and verify the applicability of these samples using the DNP technique.

This thesis will discuss the aqueous Sol-Gel synthesis and properties of yttrium aluminum garnets ($Y_3Al_5O_{12}$) doped with vanadium (V^{3+}), sodium (Na^+), potassium (K^+). The structural properties of garnets were studied by X-ray diffraction analysis (XRD), scanning electron microscope (SEM) and energy-dispersive X-ray spectroscopy (EDS). The doping distribution and levels were tested EPR spectroscopy at X- and Q- bands. Further analysis was performed using ^{27}Al MAS solid state NMR spectroscopy and spin-lattice T_1 relaxation analysis.

Acknowledgements: Funding by Vilnius University Science Promotion Foundation (MSF-JM-5/2022).

[1] T. Wolf *et al.*, J. Am. Chem. Soc., 141(1) (2019) 451
[2] J. Leggett *et al.*, Phys. Chem. Chem. Phys., 12 (2010) 5883

POSTER NO. 15

LC-TEM observations of growth and dissolution of CeO_2 NPs and their decoration by Au NPs

T. Tarnawski[1], J. Depciuch[1], A. Maximenko[2], Miroslawa Pawlyta[3], and M. Parlińska[1]

[1]*Institute of Nuclear Physics Polish Academy of Sciences, PL-31-342 Krakow, Poland*
[2]*SOLARIS National Synchrotron Radiation Centre, Czerwone Maki 98, 30-392 Kraków, Poland*
[3]*Materials Research Laboratory, Faculty of Mechanical Engineering, Silesian University of Technology, Konarskiego 18A, 44-100 Gliwice, Poland*

email: `tomasz.tarnawski@ifj.edu.pl`

Liquid cell TEM (LC-TEM)is a highly advanced method, which allows to observe in situ reactions inside the TEM. With this method, investigation of the growth dynamics is possible. It allows to verify what factors affect the nucleation and aggregation during synthesis.

In the presented research, the growth and dissolution of CeO_2 NPs, as well as their decoration by gold nanoparticles (CeO_2@Au NPs) were investigated using LC-TEM. The synthesized nanosystems were used in ethanol oxidation reaction (EOR), to investigate their catalytic activity. Furthermore, they were compared with pure Au nanocatalyst. Cyclic voltammetry was used for electrochemical measurements and in-situ FTIR was used to verify what are the products of the EOR and to establish the stability of the CeO_2@Au catalyst. X-ray absorption near edge structure (XANES) was used to determine the oxidation state of CeO_2 before and after ethanol oxidation reaction.

The LC-TEM analysis showed that depending on the electron beam energy, the CeO_2 NPs were synthesized or dissolved. The electrochemical results showed, that CeO_2 enhance the EOR. The XANES measurement revealed, that the ceria NPs were actually a mixture of two phases: CeO_2 and Ce_2O_3. However, it has been observed, that after the EOR, the amount of Ce^{3+} decreased in favor of Ce^{4+}.

Acknowledgements: This research was founded by the grant from the National Science Foundation 2019/35/B/ST5/04140.

Poster No. 16

Spin-Flop Transition in a One-Dimensional Nickel-Octacyanidotungstate Magnet

S. Akagi[1], J. Wang[1], K. Imoto[2], S. Ohkoshi[2], and H. Tokoro[1]

[1]*Department of Materials Science, Faculty of Pure and Applied Science, University of Tsukuba, Ibaraki, Japan*
[2]*Department of Chemistry, School of Science, The University of Tokyo, Tokyo, Japan*

email: `s2330077@u.tsukuba.ac.jp(S.Akagi),tokoro@ims.tsukuba.ac.jp(H.Tokoro)`

Introduction: Cyano-bridged bimetal assemblies are molecule-based magnets that can exhibit various magnetic functionalities such as photomagnetism, magnetization-induced second harmonic generation phenomena, gas-sensitive magnetic properties and so on [1]. In this work, we synthesized cyano-bridged Ni-W bimetal assemblies, $[\mathrm{Ni}^{II}(\mathrm{imidazole})_6][\mathrm{Ni}^{II}(\mathrm{imidazole})_4][\mathrm{W^V(CN)_8}]_2\cdot 4\mathrm{H_2O}$ (**NiW**), where Ni and W were selected as the magnetic centers. We present a detailed synthesis, single-crystal structure determination, and complete magnetic characterization of both polycrystalline and single-crystal samples of **NiW** [2].

Experiment: Single crystals of **NiW** were prepared by the slow diffusion of an aqueous solution of $\mathrm{NiCl_2\cdot 6H_2O}$ and imidazole into a $\mathrm{Cs_3[W(CN)_8]\cdot 2H_2O}$ aqueous solution at room temperature for two weeks. Valence states were evaluated using an IR spectrometer (JASCO FT/IR - 4700). The crystal structures were determined by Single-crystal X-ray structural analysis (Rigaku R-axis rapid). Magnetic properties were measured by SQUID magnetometer (Quantum Design MPMS).

Result: The chemical composition of **NiW**, $[\mathrm{Ni}^{II}(\mathrm{imidazole})_6][\mathrm{Ni}^{II}(\mathrm{imidazole})_4]$ $[\mathrm{W^V(CN)_8}]_2\cdot 4\mathrm{H_2O}$, was determined using elemental analysis, IR spectroscopy and single-crystal X-ray structural analysis. Single-crystal X-ray structural analysis indicated that **NiW** had a monoclinic structure ($C2/m$). **NiW** consists of one-dimensional (1D) anionic $[\mathrm{Ni}^{II}(\mathrm{imidazole})_4][\mathrm{W^V(CN)_8}]_n^{n-}$ chains, isolated counter cations $[\mathrm{Ni}^{II}(\mathrm{imidazole})_6]^{2+}$, and crystallization water as shown in Fig. 1a. Magnetic studies on $[\mathrm{Ni}^{II}(\mathrm{imidazole})_4][\mathrm{W^V(CN)_8}]_n^{n-}$ chains showed that Ni^{II} ($S = 1$) and $\mathrm{W^V}$ ($S = 1/2$) are ferromagnetically coupled within the chain via cyanido bridges. However, owing to the markedly short W–W intermetallic distance between the chains perpendicular to the *ab* plane, the magnetization was cancelled out by the antiferromagnetic interchain interaction below a Néel temperature of 8.5 K. Such interchain interactions can be overcome by an externally applied magnetic field of over 1 T at 2 K; thus, a field-induced spin-flop transition is observed in the **NiW** chain magnet (Fig. 1b). Notably, the isolated cationic $[\mathrm{Ni}^{II}(\mathrm{imidazole})_6]^{2+}$ complex plays a pivotal role in attracting the $[\mathrm{Ni}^{II}(\mathrm{imidazole})_4][\mathrm{W^V(CN)_8}]_n^{n-}$ chains close to each other ensuring the metamagnetism of **NiW**.

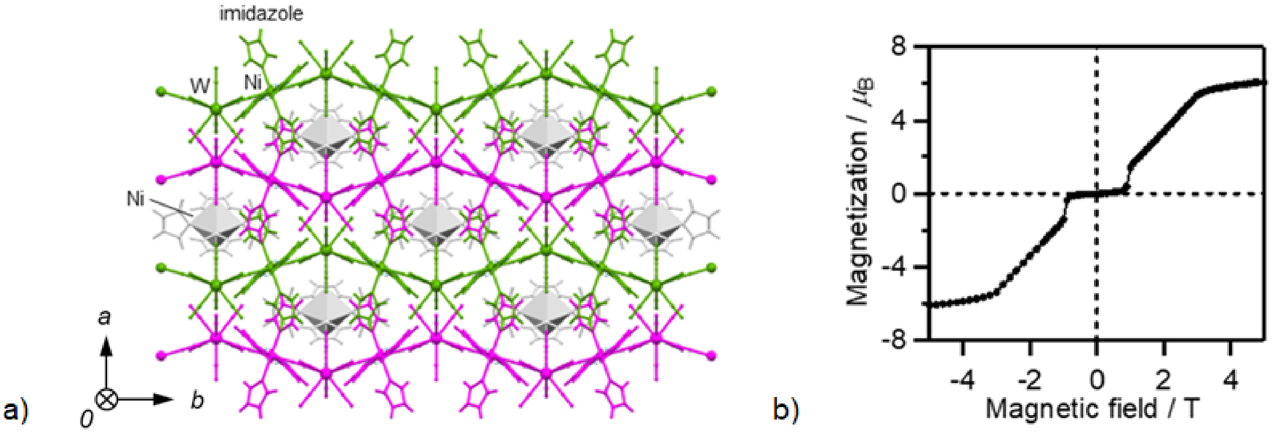

Figure 1: a) Crystal packing view along the *c* axis, neighboring chains are colored alternatively in green and purple, and the isolated $[\mathrm{Ni}^{II}(\mathrm{imidazole})_6]^{2+}$ complex is presented in gray polyhedron style for clarity. b) $M - H$ curve of single crystal of **NiW** after removing the contribution from $[\mathrm{Ni}^{II}(\mathrm{imidazole})_6]^{2+}$ under an applied field perpendicular to the *ab* plane.

[1] S. Ohkoshi *et al.*, Nat. Chem., 12 (2020) 338
[2] S. Akagi *et al.*, Cryst. Growth Des., 23 (2023) 1972

Poster No. 17

Direct observation of surface magnetization on magnetic thin films of ternary-metal-hexacyanide molecule-based magnet using magnetic force microscopy

S. Nagashima[1], Y. Yahagi[1], S. Ohkoshi[2], and H. Tokoro[1]

[1] *Department of Materials Science, Faculty of Pure and Applied Sciences, University of Tsukuba, Ibaraki 305-8573, Japan*
[2] *Department of Chemistry, School of Science, The University of Tokyo, 7-3-1 Hongo, Bunkyo-ku, Tokyo 113-0033, Japan*

email: `s2330082@u.tsukuba.ac.jp`

Introduction: Magnetic domains are important properties related to the recording magnetic media, and much research has been done so far. On the other hand, molecule-based magnets have interesting characteristic to design magnetic functionality [1]. In this study, we investigated the surface magnetization state of a ternary-metallic iron chromate hexacyanochromate [2] that exhibits temperature-induced magnetization reversal.

Experiment: The target sample of $(\mathrm{Fe}^{II}_{0.20}\mathrm{Cr}^{II}_{0.80})[\mathrm{Cr}^{III}(\mathrm{CN})_6]_{2/3}\cdot 5.3\mathrm{H_2O}$ (**1**) were prepared by reducing aqueous solutions containing $\mathrm{FeCl_3\cdot 6H_2O}$, $\mathrm{CrCl_3\cdot 6H_2O}$, and $\mathrm{K_3[Cr(CN)_6]}$. Characterization was performed using UV-vis spectrum, IR spectrum, SEM, and AFM. Magnetic properties were measured by a SQUID magnetometer and surface magnetization was observed using a magnetic force microscopy (MFM).

Result: **1** was obtained as a purple thin film on $\mathrm{SnO_2}$-coated glass. In UV-vis spectrum, a broad absorption band originating from intervalence transfer between Fe^{II} and Cr^{III} was observed around 450 nm. In the IR spectrum, the CN stretching mode of mixed Fe^{II}-NC-Cr^{III} and Cr^{II}-NC-Cr^{III} was observed at 2181 cm^{-1}. From SEM images, a thickness of this film was 1.76 ± 0.05 μm. AFM images revealed a smooth surface with a roughness of 0.45 ± 0.14 μm. The magnetization vs temperature curve showed a spontaneous magnetization below Curie temperature (T_C) of 222 K. Further cooling reversed the magnetization from positive to negative at the compensation temperature (T_{comp}) of 134 K (Fig. 1 (a)). This temperature-induced magnetization reversal originates from mixed ferro-ferrimagnetism, which involves two types of exchange couplings: a ferromagnetic interaction between Fe^{II} ($S = 2$) and Cr^{III} ($S = 3/2$) and an antiferromagnetic interaction between Cr^{II} ($S = 2$) and Cr^{III} [?]. From MFM images, no magnetic signal was detected at room temperature (Fig. 1 (b)). After cooling below T_C, magnetic domains were observed as clear contrast (Fig. 1 (c)). The size of the magnetic domains was one-to-several μm, which is larger than the roughness of the sample surface (ca. 0.45 μm).

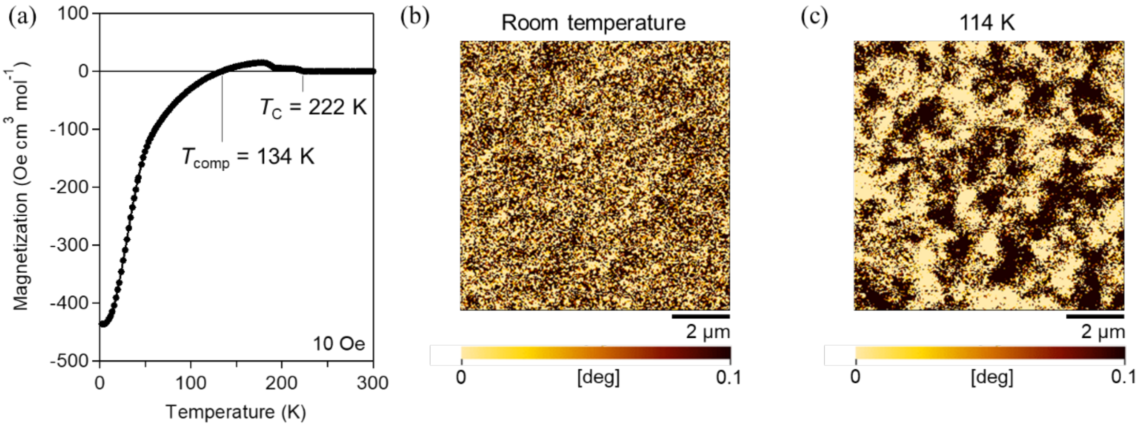

Figure 1: (a) Magnetization vs temperature curve of **1**, MFM images of **1** at (b) Room temperature and (c) 114 K.

[1] S. Ohkoshi *et al.*, Nature Chem., 12 (2020) 338
[2] S. Ohkoshi *et al.*, J. Am. Chem. Soc., 120 (1998) 5349

POSTER NO. 18

Synthesis of λ-Ti_3O_5 using Titanium Chloride as starting material

R. Seiki[1], A. Fujisawa[1], A.F. Fadilla[1], F. Jia[2], S. Ohkoshi[2], and H. Tokoro[1]

[1] *Department of Material Science, Faculty of Pure and Applied Sciences, University of Tsukuba, 1-1-1 Tenno-dai, Tsukuba, Ibaraki 305-8577, Japan*
[2] *Department of Chemistry, School of Science, University of Tokyo, 7-3-1 Hongo, Bunkyo-ku, Tokyo 113-8654, Japan*

email: `s2220343@u.tsukuba.ac.jp`

[Introduction] Titanium oxides that have a composition of Ti_nO_{2n-1} (n = 3-9) are called the Magneli phase, and exhibit metal-semiconductor phase transition by changing temperature. In particular, the lambda-type trititanium-pentoxide (λ-Ti_3O_5) (Fig. 1a) nanoparticles are reported to show a reversible phase transition to the beta-type trititanium-pentoxide (β-Ti_3O_5) by various external stimuli: light, heat, pressure, and electric current [1, 2]. This material is expected to be applied as a heat storage material because of its properties [2]. In this study, we developed a synthesis method for λ-Ti_3O_5 nanoparticles by preparing a precursor using titanium chloride ($TiCl_4$) liquid as the starting material.

[Experiment] We synthesized λ-Ti_3O_5 nanoparticles by the following process. First, a mixed solution of H_2O, $TiCl_4$, and NH_3 was prepared in a round bottom flask, and stirred in an oil bath at 50°C for 20 hours to form $Ti(OH)_4$ precipitation. Then the precipitation was extracted from the solution by centrifugation with ethanol, and we obtained a precursor by heating at 60°C for 24 hours on a hot plate. The precursor was sintered under a hydrogen flow of 0.5 dm^3min^{-1} at 1100°C for 5 hours.

[Result] The powder X-ray diffraction (PXRD) pattern of the obtained sample with Rietveld analysis indicated that the obtained sample is a single phase of λ-Ti_3O_5 (monoclinic, C2/m; a = 9.8332 $\AA$, b = 3.7857 $\AA$, c = 9.9690 $\AA$, β = 91.2567°) (Fig. 1b). Scanning electron microscopy (SEM) image showed that the particles size is 303 ± 56 nm. A pressure-induced phase transition was confirmed with the pressure threshold (ca. 300 MPa), and pressure-produced β-Ti_3O_5 returned to λ-Ti_3O_5 by heating above 490 K. Hence, the obtained λ-Ti_3O_5 exhibited a reversible phase transition on account of pressure and heat.

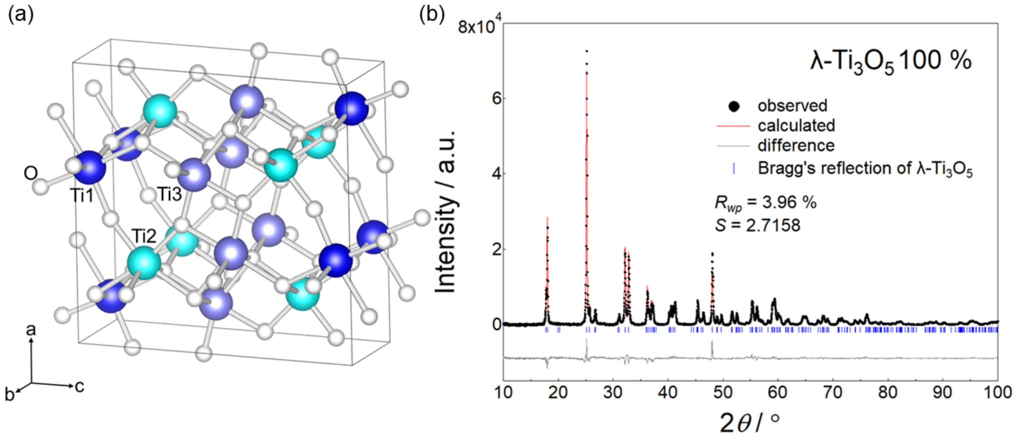

Figure 1: (a) Crystal structure of λ-Ti_3O_5. (b) PDXL pattern of the obtained sample with Rietveld analysis. Black dots, red lines, and gray lines show the observed plots, calculated pattern, and their difference, respectively. Blue bars show the calculated Bragg's reflection of λ-Ti_3O_5.

[1] S. Ohkoshi *et al.*, Nature Chem., 2 (2010) 539
[2] H. Tokoro *et al.*, Nature Commun., 6 (2015) 7037

Poster No. 19

Interpretation of photoluminescence spectrum of $Eu(CH_3COO)_3{\cdot}H_2O$ salt and its dependance over excitation radiation intensity

V. Mukharovska[1], M. Derhachov[1], and V. Moiseienko[1]

[1] *Oles Honchar Dnipro National University, Dnipro, Ukraine*

email: `mukharovska@ffeks.dnu.edu.ua`

Europium ions have gained significant attention as spectroscopic probes due to their unique optical properties, including sharp emission lines and long luminescence lifetimes. These characteristics make europium ions valuable for a wide range of applications such as sensing, imaging, and biological assays.

In this work the photoluminescence (PL) spectra of the $Eu(CH_3COO)_3{\cdot}H_2O$ salt were measured under different excitation intensities. The excitation of the salt was carried out in forward scattering geometry under 410 nm semiconductor laser continuous radiation.

Measured spectra consist of the three emission bands (Fig. 1) with the barycenter of 17250 cm^{-1}, 16900 cm^{-1}, and 16200 cm^{-1}, which correspond to the $^5D_0 \rightarrow {}^7F_0$, $^5D_0 \rightarrow {}^7F_1$ and $^5D_0 \rightarrow {}^7F_2$ transitions in the Eu spectrum, respectively. The maximum number of Stark components for $^5D_0 \rightarrow {}^7F_2$ transition, defined by Stark splitting pattern, is five. However, this result does not match the obtained spectrum. To explain this discrepancy, we assume that the Eu ions occupy two non-equivalent sites: (I) and (II) within the host complex. By employing spectral decomposition technique, the analysis was carried out using the minimum number of Gaussian line profiles. This approach considered the equidistant arrangement of Stark splitting components for every transition, along with the limitations imposed by the possible point symmetry groups of the Eu site(1). Based on the obtained spectral agreement, it is proposed that site (I) possesses C_1 symmetry, while site (II) has either C_3 or C_{3v} point group symmetry. This conclusion is derived from considering the assumed sets of components, which provided the closest match to the observed spectrum.

Furthermore, it is essential to emphasize the robust correlation between the measured spectra and the intensity of the excitation radiation (Fig. 1). The augmentation of excitation intensity gives rise to a marked broadening of spectral lines, thereby instigating the devastating destruction of the spectrum. Additionally, it is worth noting that variations in the excitation intensity provoke discernible changes in the relative intensities of distinct PL components. The observed changes are assumed to find their origin in the influence of local heating. Notably the thermal quenching of PL, augmentation of energy transfer amid the Eu ions and the host lattice, migration of Eu ions to sites with different coordination environment, and consequential structural modifications within the host complex. Furthermore, one can posit that the structural changes induced by local heating are irreversible, as the original spectrum (dashed curve in Fig. 1) becomes non-reproducible beyond a certain excitation intensity.

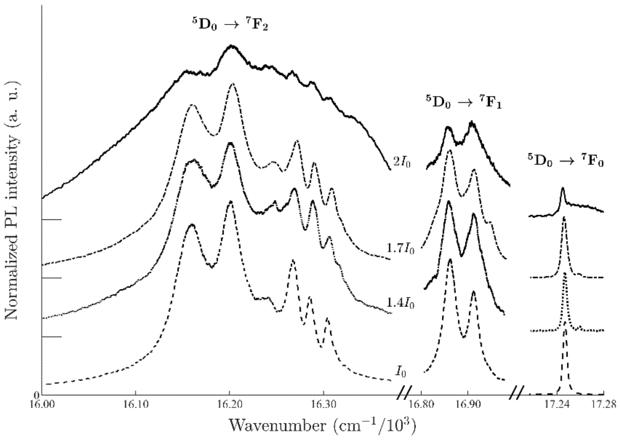

Figure 1: Normalized PL spectra of the $Eu(CH_3COO)_3{\cdot}H_2O$ salt in optical cell under different excitation intensities. The spectra are shifted up on the vertical scale by the same amount relative to each other in order of increasing excitation intensity.

[1] K. Binnemans *et al.*, Coord. Chem. Rev., 295 (2015) 1

POSTER NO. 20

Wenzel-to-Cassie transition on lubricant-impregnated surfaces

D. Tzitzilis[1], I. Ntakoumis[1], C. Tsekeridis[1], and P. Papadopoulos[1]

[1] *University of Ioannina, Ioannina. Greece*

email: `phyuoi7698tzitzilis@gmail.com`

Lubricant impregnated surfaces (LIS) are microstructured surfaces impregnated with a low surface tension lubricant. They have shown great promise in various applications that require non-wettable superhydrophobic surfaces. These surfaces belong to the class of liquid-repellent and non-adhesive surfaces.

The present work aims to investigate the possibility of switching between Wenzel and Cassie states, through the injection of lubricant into microstructured hygrophobic surfaces. The "key" to the transition from Wenzel to Cassie is the change of the microscopic contact angle of the drops, which is due to the change in the environment of the drop, from air to another liquid which acts as a "lubricant". In addition, the role of the morphology of microstructured surfaces, the roughness and the surface tension of the lubricant-drop liquids in the realization or not of the aforementioned transition was studied.

To observe the Wenzel-Cassie transition of droplets on the microstructred we used a homemade laser scanning confocal microscopy (LSCM) in reflection interference mode. To calculate the interfacial surface tensions, we used an optical tensiometer. In this work we make numerical calculations of the shape of the droplet surface to study the geometrical limits within which the Wenzel-Cassie transition occurs. We minimize the Gibbs energy of the drop using the Steepest Descent algorithm and determine the deepest point more accurately than empirical relations.

The results of our measurements and calculations show that the transition of droplets from the Wenzel state to the Cassie state by lubricant injection is feasible and is favored on surfaces with large heights and short interpillar distances.

Poster No. 21

Plasma irradiation: a promising technique for modifying magnetic properties in molecular magnets

D. Czernia[1] and P. Konieczny[1]

[1]*Institute of Nuclear Physics PAN, Cracow, Poland*

email: `dominik.czernia@ifj.edu.pl`

Molecular magnets are a class of metal-organic materials exhibiting unique physical properties sensitive to external stimuli such as temperature, pressure, light, or the presence of guest molecules. Although not in molecular systems yet, it was shown that the plasma treatment can also be used as a stimulus to control the desired parameters of magnetic materials.

Here, we report results obtained for the three-dimensional molecular Nb^{IV}-Mn^{II} ferrimagnet ($\mathbf{NbMn_2}$) subjected to plasma irradiation under various conditions. The long-range ordered state can be observed below $T_C = 47.5$ K, and antiferromagnetic interaction between two magnetic ions was confirmed by the saturation magnetization of 9 Bohr magnetrons per $\mathbf{NbMn_2}$ formula unit, which corresponds to two spins $\mathrm{S} = 1/2$ and one $\mathrm{S} = 5/2$.

The $\mathbf{NbMn_2}$ samples were ground down and scattered on the adhesive tape to ensure a large surface-to-volume ratio of exposed crystallites. Then, the samples were irradiated with plasma made of air, nitrogen, oxygen, and argon with different power and treatment time. After the irradiation, all samples were protected from air and vacuum by an additional layer of adhesive tape put at the top of the samples.

The magnetic properties after plasma treatment show a clear appearance of the second magnetic phase with T_C around 70 K (Fig. 1) for at least medium power and 10 minutes irradiation time, indicating the threshold effects. The influence of heat and ultraviolet light generated during plasma was ruled out with additional measurements. The powder X-ray diffraction measurements show the same diffraction patterns with the shift of diffraction peaks (Fig. 2) for irradiated samples towards higher angles, indicating the decrease of crystal lattice parameters due to the evaporation of the water of crystallization. It is in line with the increase of T_C, suggesting the enhancement of exchange couplings.

We show that although plasma irradiation is not a common approach to modify physical properties in molecular magnets, it indeed offers a promising way of obtaining new magnetic phases.

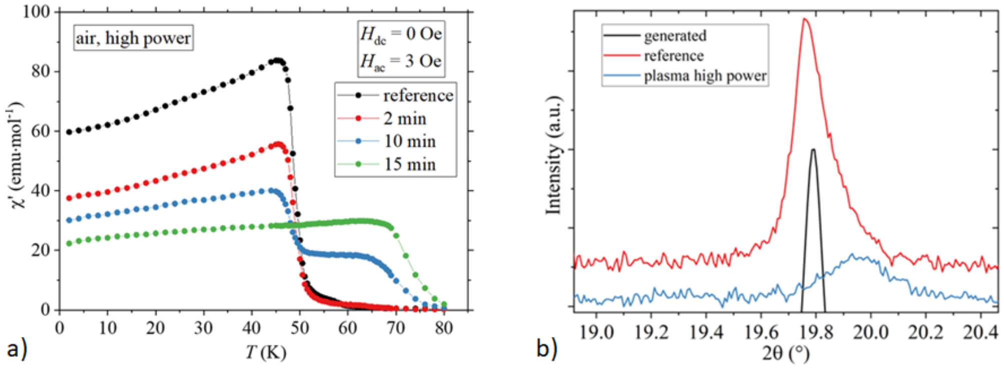

Figure 1: (a) The real part of the AC magnetic susceptibility of $\mathbf{NbMn_2}$ measured for samples irradiated for 10 minutes with high-power air, nitrogen, oxygen, and argon plasma. (b) One of the powder diffraction peaks of $\mathbf{NbMn_2}$ obtained from the structure file (black), the sample before (red), and after 10 minutes high-power air plasma treatment (blue).

Acknowledgements: This work was supported by the Polish Minister of Education and Science (grant No.: DI2017 006047).

Poster No. 22

Twist bend nematic phase in mixtures of cyanobiphenyls with CB7CB

B. Klucznik[1] and M. Tykarska[1]

[1] *Military University of Technology, Warsaw, Poland*

email: `mailto:barbara.klucznik@wat.edu.pl`

Twist bend nematic phase (N_{TB}) is known since about 20 years [1], but it is still intensively examined by scientists. Many papers have been written about finding new mesogens forming this phase [2, 3]. There is only few works concerning results of miscibility studies in binary systems where only one component forms N TB phase [4–6]. Pure compounds forming this phase have high melting points thus N_{TB} phase is usually monotropic. That fact causes problems with examination of this phase. Preparation of mixtures is a way to lower melting temperatures.

The aim of this work is the investigation of temperature and concentration range of N_{TB} phase existence in mixtures formulated by adding different cyanobiphenyls (*n*CB, *n*=3-5,7-12,14) to CB7CB compounds (see structures of compounds in Fig.1). Low N_{TB}-N transition temperature (6,2°C) was received in mixture containing 0.7 mole ratio of 9CB. Mixtures in this system do not crystallize at room temperature.

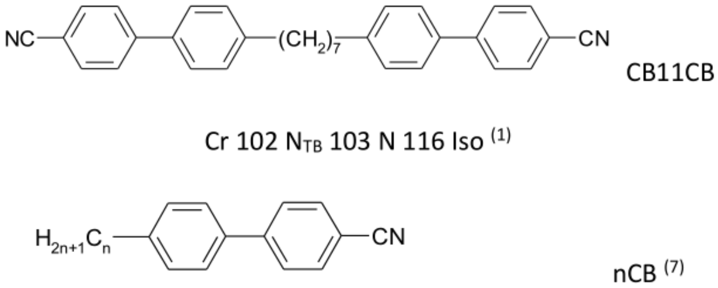

CB11CB

Cr 102 N_{TB} 103 N 116 Iso (1)

nCB (7)

Figure 1: Structure tested compounds

[1] M. Cestari *et al.*, Phys. Rev E, 84 (2011), 031704
[2] R.J. Mandle *et al.*, Liq. Cryst., 42 (2015), 688
[3] R. J. Mandle *et al.*, Soft Matt., 12 (2016), 7883
[4] Z. Lu *et al.*, Liq. Cryst., 41 (2014), 471
[5] P. Oswald, A. Dequidt, Phys. Rev. E, 105 (2022), 024707
[6] M.R. Tuchband *et al.*, arXiv:1511.07523
[7] G.W. Gray *et al.*, Liq. Cryst. Ordered Fluids, 2 (1973), 617

Poster No. 23

Electronic transport properties of an electromagnetically driven Weyl and multi Weyl semimetals under the presence of Magnetic fields

S. Yadav[1]

[1]*Institute of Nuclear Physics PAN, Cracow, Poland*

email: `shivam.yadav@ifj.edu.pl`

Weyl and multi Weyl semimetals (WSM/mWSM) have captured a lot of attention due to their unusual electronic transport properties. In this poster we will describe the Magneto-optical conductivity of a single node of WSM and mWSM for both type I and type II cases using the Kubo formalism. We will also learn how a periodically driven WSM/mWSM can be analyzed using the Floquet formalism in the large frequency regime. We will finally calculate the Planar Hall conductivity and Planar thermo-electric coefficient for single node of WSM/mWSM.

[1] S. Yadav *et al.*, Phys. E: Low-dim. Sys. Nanostruc., 144 (2022), 115444
[2] S. Yadav *et al.*, Phys. B: Con. Matt., 656 (2023), 414765